

HE  
18.5  
.A37  
no.  
DOT-  
TSC-  
UMTA-  
80-17  
v.3

IT NO. UMTA-MA-06-0025-80-3

# INCREASED RAIL TRANSIT VEHICLE CRASHWORTHINESS IN HEAD-ON COLLISIONS

## Volume III - Guidelines for Evaluation and Development of New Railcar Designs

Arne H. Wiedermann  
Anatole Longinow  
Edward E. Hahn

IIT RESEARCH INSTITUTE  
10 West 35th Street  
Chicago IL 60616



JUNE 1980  
FINAL REPORT



DOCUMENT IS AVAILABLE TO THE PUBLIC  
THROUGH THE NATIONAL TECHNICAL  
INFORMATION SERVICE, SPRINGFIELD,  
VIRGINIA 22161

Prepared by  
U.S. DEPARTMENT OF TRANSPORTATION  
URBAN MASS TRANSPORTATION ADMINISTRATION  
Office of Technology Development and Deployment  
Washington DC 20590

#### NOTICE

This document is disseminated under the sponsorship of the Department of Transportation in the interest of information exchange. The United States Government assumes no liability for its contents or use thereof.

#### NOTICE

The United States Government does not endorse products or manufacturers. Trade or manufacturers' names appear herein solely because they are considered essential to the object of this report.

HE  
18,5  
A37  
no.

DOT-TSC-UMTA-80-17, III

Technical Report Documentation Page

1. Report No. UMTA-MA-06-0025-80-3	2. Government Accession No.	3. Recipient's Catalog No.
4. Title and Subtitle INCREASED RAIL TRANSIT VEHICLE CRASHWORTHINESS IN HEAD-ON COLLISIONS - Volume III - Guidelines for Evaluation and Development of New Raicar Designs		5. Report Date June 1980
		6. Performing Organization Code
7. Author(s) Arne H. Wiedermann, Anatole Longinow, Edward E. Hahn		8. Performing Organization Report No. DOT-TSC-UMTA-80-17,III
9. Performing Organization Name and Address IIT Research Institute * 10 West 35th Street Chicago IL 60616		10. Work Unit No. (TRAIS) UM904/R0734
		11. Contract or Grant No. DOT-TSC-1052-3
12. Sponsoring Agency Name and Address U.S. Department of Transportation Urban Mass Transportation Administration Office of Technology Development and Deployment Washington DC 20590		13. Type of Report and Period Covered Final Report June 1975 to June 1978
		14. Sponsoring Agency Code
15. Supplementary Notes *Under Contract to: U.S. Department of Transportation Research and Special Programs Administration Transportation Systems Center Cambridge MA 02142		
16. Abstract  The nature and severity of potential passenger injury and fatality producing mechanisms due to secondary collisions which occur in intracity train crash environments are assessed. This analytical methodology is used to identify the factors and car design parameters, including car interior components which significantly influence passenger injury and fatality. In this manner meaningful design guidelines are established which will minimize and/or limit the hazard to which the passengers will be exposed in the event of most crash environments.		
<div data-bbox="662 1389 964 1645" data-label="Image"></div>		
17. Key Words Passenger injury, head-on collisions, railway car crashworthiness, train crashes, transportation safety, mass transit, urban rail car, rapid transit car, crashworthiness, commuter rail car		18. Distribution Statement  DOCUMENT IS AVAILABLE TO THE PUBLIC THROUGH THE NATIONAL TECHNICAL INFORMATION SERVICE, SPRINGFIELD, VIRGINIA 22161
19. Security Classif. (of this report) UNCLASSIFIED	20. Security Classif. (of this page) UNCLASSIFIED	21. No. of Pages 166
		22. Price





1. Report No. UMTA-MA-06-0025-80-3		2. Government Accession No.		3. Recipient's Catalog No.	
4. Title and Subtitle INCREASED RAIL TRANSIT VEHICLE CRASHWORTHINESS IN HEAD-ON COLLISIONS Volume III: GUIDELINES FOR EVALUATION AND DEVELOPMENT OF NEW RAILCAR DESIGNS				5. Report Date June 1980	
				6. Performing Organization Code	
				8. Performing Organization Report No. DOT-TSC-UMTA-80-17,III	
7. Author(s) Arne H. Wiedermann, Anatole Longinow, Edward E. Hahn				10. Work Unit No. (TRAIS) MA-06-0025(UM904/R0734)	
9. Performing Organization Name and Address IIT Research Institute* 10 West 35th Street Chicago, Illinois 60616				11. Contract or Grant No. DOT-TSC-1052-3	
				13. Type of Report and Period Covered Final Report June 1975 - June 1978 Volume III of IV	
				14. Sponsoring Agency Code UTD-30	
12. Sponsoring Agency Name and Address U.S. Department of Transportation Urban Mass Transportation Administration 400 Seventh Street, S.W. Washington, DC 20590					
15. Supplementary Notes *under contract to: U.S. Department of Transportation Research and Special Programs Administration Transportation Systems Center Cambridge, Massachusetts 02142					
16. Abstract As systems manager for the Urban Mass Transportation Administration (UMTA) Rail System Supporting Technology Program, the Transportation Systems Center (TSC) is conducting research and development efforts directed toward the introduction of improved technology in urban rail system applications. As part of this program, TSC is conducting analytical and experimental studies toward improved safety in urban rail systems. A specific goal in this area of safety is to reduce the number of injuries that may result from the collision of two trains.  This report, <u>Volume III</u> , addresses the nature and severity of potential passenger injury and fatality producing mechanisms due to secondary collisions which occur in intracity train crash environments. This analytical methodology is used to identify the factors and car design parameters, including car interior components which significantly influence passenger injury and fatality. In this manner, meaningful design guidelines are established which will minimize and/or limit the hazard to which the passengers will be exposed in the event of most crash environments.  This final report is comprised of three other volumes which are: Volume I: Initial Impact (UMTA-MA-06-0025-80-1); Volume II: Primary Collision (UMTA-MA-06-0025-80-2); and Volume IV: IITRAIN Users' Manual (UMTA-MA-06-0025-80-4).					
17. Key Words Collisions; Commuter Rail Cars; Crashworthiness; Evaluation; Guidelines; Head-On Collisions; Impacts; Models; Railcar Crashworthiness; Train Crashes; Transportation Safety; Urban Railcars				18. Distribution Statement  Available to the public through the National Technical Information Service, Springfield, Virginia 22161.	
19. Security Classif. (of this report) Unclassified		20. Security Classif. (of this page) Unclassified		21. No. of Pages 22. Price	



## PREFACE

As systems manager for the Urban Mass Transportation Administration (UMTA) Rail System Supporting Technology Program, the Transportation Systems Center (TSC) is conducting research and development efforts directed toward the introduction of improved technology in urban rail system applications. As part of this program, TSC is conducting analytical and experimental studies toward improved safety in urban rail systems. A specific goal in this area of safety is to reduce the number of injuries that may result from the collision of two trains.

On 30 June 1975, TSC contracted with IIT Research Institute (IITRI) to perform this study to develop engineering methods and data pertaining to improved technology in urban rail systems which will lead to increased rail transit vehicle crashworthiness and passenger injury minimization. This final report is submitted in four volumes. Part 1 describes the results of Task 1 which is concerned with the initial impact of two transit cars. The results of Task 2 which is concerned with the primary collision of two impacting transit car consists are described in Part 2. Part 3 describes the results of Tasks 3 and 4 of this study which are concerned with prediction of passenger injury and guidelines for evaluation of railcar designs. The final volume is a manual containing a description of the organization and use of the IITRAIN computer code which was developed as a tool to help meet the goals of this contract.

Major IITRI contributors to the work covered in this report include Edward E. Hahn, Arne H. Wiedermann, Anatole Longinow, Robert W. Bruce and Steven C. Walgrave. The author takes this opportunity to acknowledge the contributions to this report made by Dr. A. Robert Raab, Mr. Samuel Polcari, Dr. Ming Chen, Mr. George Neat and Mr. Ronald Madigan of the U.S. Department of Transportation, TSC, Cambridge, Massachusetts.

# METRIC CONVERSION FACTORS

Approximate Conversions to Metric Measures				Approximate Conversions from Metric Measures			
Symbol	When You Know	Multiply by	To Find	Symbol	When You Know	Multiply by	To Find
<b>LENGTH</b>				<b>LENGTH</b>			
in	inches	2.5	centimeters	mm	millimeters	0.04	inches
ft	feet	30	centimeters	cm	centimeters	0.4	inches
yd	yards	0.9	meters	m	meters	3.3	feet
mi	miles	1.6	kilometers	km	kilometers	0.6	miles
<b>AREA</b>				<b>AREA</b>			
m <sup>2</sup>	square inches	6.5	square centimeters	cm <sup>2</sup>	square centimeters	0.16	square inches
ft <sup>2</sup>	square feet	0.09	square meters	m <sup>2</sup>	square meters	1.2	square yards
yd <sup>2</sup>	square yards	0.8	square meters	km <sup>2</sup>	square kilometers	0.4	square miles
mi <sup>2</sup>	square miles	2.6	square kilometers	ha	hectares (10,000 m <sup>2</sup> )	2.5	acres
<b>MASS (weight)</b>				<b>MASS (weight)</b>			
oz	ounces	28	grams	g	grams	0.035	ounces
lb	pounds (16 oz)	0.45	kilograms	kg	kilograms	2.2	pounds
	(2000 lb)	0.5	tonnes	t	tonnes (1000 kg)	1.1	short tons
<b>VOLUME</b>				<b>VOLUME</b>			
teaspoon	teaspoons	5	milliliters	ml	milliliters	0.03	fluid ounces
tablespoon	tablespoons	15	milliliters	ml	liters	2.1	pints
fluid ounce	fluid ounces	30	milliliters	ml	liters	1.06	quarts
cup	cup	0.24	liters	l	liters	0.26	gallons
pint	pints	0.47	liters	l	cubic meters	35	cubic feet
quart	quarts	0.96	liters	m <sup>3</sup>	cubic meters	1.3	cubic yards
gallon	gallons	3.8	liters	m <sup>3</sup>			
qt	quarts	0.95	liters				
gal	gallons	3.8	liters				
ft <sup>3</sup>	cubic feet	0.03	cubic meters				
yd <sup>3</sup>	cubic yards	0.76	cubic meters				
<b>TEMPERATURE (exact)</b>				<b>TEMPERATURE (exact)</b>			
F	Fahrenheit temperature	5/9 (after subtracting 32)	C	C	Celsius temperature	9/5 (then add 32)	F

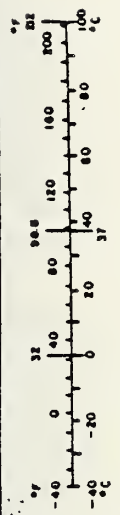




# TABLE OF CONTENTS

	<u>Page</u>
1. INTRODUCTION	1
1.1 Program Objectives	1
1.2 Passenger Survivability Considerations	4
1.3 Passenger Configurations	7
2. BIOMECHANICAL RESPONSE TO IMPACT	9
2.1 Basic Considerations	9
2.2 Injury-Fatality Criteria	11
3. IMPACTED SURFACE/STRUCTURE EFFECTIVENESS	14
3.1 Basic Considerations	14
3.2 Perfect Absorber	18
3.3 Elastic Response	19
3.4 Inelastic Response	21
3.5 Sensitivity Evaluation	23
3.6 Composite Systems	28
3.7 Typical Results	31
3.8 Nomenclature	31
4. PASSENGER MOTION	34
4.1 Acceleration Pulse Shape Characteristics	34
4.2 "Lumped Mass" Translation Behavior	41
4.3 Passenger Characteristics - Anthropometric Data	52
4.4 Standing Passenger	57
4.5 Forward Facing Seated Passenger	64
4.5.1 Hip Loft Model	64
4.5.2 Pinned Hip Model	80
4.5.3 Influence of Slip	82
4.5.4 Variability of Impact Conditions	89
4.5.5 Influence of Pulse Shape	91
4.6 Backward Facing Seated Passenger	95
4.7 Sideward Facing Seated Passenger	101
4.8 Multiple Passenger Interactions	108
4.9 Nomenclature	110
5. PASSENGER INJURY PREDICTION METHODOLOGY	114
5.1 General Approach	114
5.2 Standing Passenger	121
5.3 Forward Facing Seated Passenger	125
5.4 Sideward Facing Seated Passenger	130
5.5 Backward Facing Seated Passenger	133
5.6 Typical Results	133
APPENDIX: COMPUTER CODE DESCRIPTION	143

## LIST OF ILLUSTRATIONS

	<u>Page</u>
1. Onboard Accident Scenario for Current Transit Bus Operations	6
2. Passenger Configurations	8
3. Injury Scale for Impact of Body Components	12
4. Potential Load-Deflection Relationship	16
5. Selected Resistance Functions	17
6. Severity Index Function $f(v)$	24
7. Influence Coefficients for Severity Index	26
8. Influence Coefficients for $a_o^*$	27
9. Local Stiffness for Composite Beam/Support System	29
10. Influence of Yield Stress on Severity Index - Perfect Absorber	30
11. Influence of Spring Constant on Severity Index - Elastic Behavior	32
12. Acceleration Pulse Classification	35
13. Characteristics of Trapezoidal Acceleration Pulse	38
14. Pulse Characteristics for the Double Step Pulse	40
15. Solution Diagram for Step Pulse	42
16. Solution Diagram for Triangular Pulse	43
17. Path Diagram for Passenger/Bulkhead Interaction	44
18. Impact Environment - Large $\zeta^*$	47
19. Impact Environment - Step Pulse	48
20. Impact Environment - Triangular Pulse	50
21. Influence of $\alpha$ on Impact Velocity	51
22. Height/Weight Data Summary	54
23. Tumbling Passenger Trajectories	59
24. Velocity Perturbation - Tumbling Passenger	60
25. Velocity Increment Variations with Velocity and Acceleration for the Adult Female Standing Passenger	62
26. Velocity Increment Variation for Standing Passenger	63
27. Critical Stiffness for Floor Systems	65
28. Hip*Loft Model for Forward Facing Seated Passenger	67
29. Angular Velocity - Rotation Relationship for Hip Loft Model, $\alpha = 0.126$	70
30. Angular Velocity - Rotation Relationship for Hip Loft Model, $\alpha = 0.3$	71

# LIST OF ILLUSTRATIONS (continued)

	<u>Page</u>
31. Rotation History for Hip Loft Model	74
32. Center of Gravity Velocity for Hip Loft Model	75
33. Center of Gravity Velocity History for Hip Loft Model	76
34. Impact Details for Hip Loft Model	77
35. Influence of Acceleration on Velocity Components	79
36. Angular Velocity - Rotation Relationship for Pinned Hip Model	81
37. Time Function	83
38. Rotation History for Pinned Hip Model	84
39. Center of Gravity Velocity Components for Pinned Hip Model	85
40. Hip Slip Characteristics for Pinned Hip Model	87
41. Influence of Slip on Angular Velocity - Pinned Hip Model	89
42. Influence of Slip on Center of Gravity Velocity Components - Pinned Hip Model	90
43. Vector Diagrams for Impact Velocities of Seated Passenger Facing Forward	92
44. Impact Velocity Dependence on Model	93
45. Impact Velocity Dependence on Slip - Pinned Hip Model	94
46. Influence of Pulse Shape upon Angular Velocity Pinned Hip Model for Forward Facing Seated Passenger	96
47. Influence of Pulse Shape on Impact Velocity	97
48. Flexion Response Envelopes for 50th Percentile Adult Male	98
49. Angular Velocity History for Neck Model	102
50. Response Characteristics of Neck Model	103
51. Safe Region in Train Crash Domain For Backward Facing Seated Passenger	104
52. Pinned Hip Model for Sideward Facing Seated Passenger	105
53. Angular Velocity for Sideward Seated Passenger	106
54. Impact Velocity for Sideward Seated Passenger	107
55. Path Diagrams for Multiple Impact Evaluation	109
56. Passenger Injury Prediction Methodology	115

## LIST OF ILLUSTRATIONS (concluded)

	<u>Page</u>
57. Normal Distribution Function	118
58. Distribution Factor for Population Groups	119
59. Velocity Increment for Standing Passenger	123
60. Program Details for Standing Passenger	124
61. Mean Impact Velocity Function for Forward Facing Seated Passenger	127
62. Program Details for Forward Facing Seated Passenger	128
63. Distribution of Body Component Involved in Impact	129
64. Mean Impact Velocity Function for Sideward Facing Seated Passenger	131
65. Program Details for Sideward and Backward Facing Seated Passenger	132

## LIST OF TABLES

1. Summary of Influence Coefficients	25
2. Height/Weight Characteristics	53
3. Anthropometric Data for Seated Passengers	57
4. Floor Impact Velocity	61
A-1 Input Format	144



## 1. INTRODUCTION

The collision of two consists of transit cars can be broken into three separate, but interdependent, phenomena: initial impact, primary collision, and secondary collision. Initial impact is concerned with the mechanics of the initial impact of the leading cars of two consists. The interaction of all of the cars and car components of two impacting consists comprise the primary collision. Secondary collisions include the interaction of passengers with the car components, passengers with passengers and passengers with other loose objects. This final report, submitted in four volumes, describes the results of the IIT Research Institute (IITRI) program which is concerned with the collision of transit car consists on straight level track. Part 1 of the final report is concerned with the initial impact of the leading cars of two consists. The results of the study of the primary collision of two impacting consists are given in Part 2, and Part 3 is concerned with secondary collisions including the prediction of passenger injury and guidelines for evaluation of new railcar designs. The final volume is a manual containing a description of the organization and use of the IITRAIN computer code which was developed as a tool to help meet the goals of this contract.

### 1.1 Program Objectives

The program objectives, as taken from the contract, are restated here.

Item 1a: Formulate an analytical model in two dimensions, longitudinal and vertical, of the leading cars of two impacting consists in sufficient detail to examine the mechanics of head-on initial impact on straight track. This model will include the distribution of mass in the cars as well as the nonlinear force-deformation relationships existing among major structural subassemblages. Consideration will be given to the shapes and configurations of the impacting surfaces and to the forces generated by



the impact. The model shall be capable of establishing the critical parameters which govern whether the cars crush, displace vertically and override, or crush with subsequent override.

Item 1b: Utilize the above analytical model of initial impact to assess impact controlling devices currently in service, such as anticlimbers, couplers and draft gears of various designs. This assessment shall uncover the critical parameters of such devices which govern whether the cars crush, displace vertically and override or crush with subsequent override. The contractor shall develop recommendations concerning future directions of effort in design of impact controlling devices which would be particularly pertinent to crashworthiness goals.

Item 1c: Develop an experimental test plan for the evaluation of the strength and effectiveness of future designs for impact controlling devices. These tests are to assure that the forces generated during impact do not produce structural failure of the impact controlling device or vertical misalignment and override of the car body. The test plan is to be sufficiently detailed so that all equipment, fixtures, instrumentation and procedures are completely described.

Item 2a: Develop an analytical model in two dimensions, longitudinal and vertical, of the primary collision of two impacting consists of urban railcars of similar and different configurations. This model will include the formulation of the leading cars developed in Part 1 of this program, as well as the distributions of mass and nonlinear force-deformation relationships existing among major structural subassemblages. This model shall be capable of determining the extent of crushing and/or override suffered by the individual cars in the consists, as well as the time histories of displacement, velocity, and acceleration in both the longitudinal and vertical directions.

Item 2b: Develop methods for generating the dynamic force-deformation relationships for structural subassemblages comprising the critical modules of railcars. These methods shall include

finite-element analysis, scale modeling and full-scale testing procedures including specifications for required testing equipment and instrumentation. Utilize the finite-element analytical method to generate the nonlinear force-deformation relationships among major components of a typical urban railcar.

Item 3: Develop the analytical methodology of passenger injury due to secondary collision to include modes of injury due to longitudinal, vertical, and pitching motions of the vehicles after impact. This methodology shall be capable of considering the location of the passenger prior to impact, his orientation (seated, standing, facing forward, facing sideways, facing rearward), the configuration of interior features of the cars, passengers density, and passenger restraint. This methodology shall also be capable of determining the severity of the injury sustained by the passenger.

Item 4: Utilize the results of Items 1 through 3 to develop guidelines for the evaluation of proposed railcar designs, and guidelines for the development of new railcars. These guidelines are to be developed in parametric form, so that individual parameters may be considered and the effects of specific values assigned or computed for these parameters may be assessed. These parameters are to include:

- a - the number of cars in the consist
- b - operational velocity ranges
- c - dimensions and weights of each car
- d - placement and dimensions of windows and doors
- e - placement and weights of mechanical/electrical equipment
- f - interior configurations of passenger compartment
- g - carbody force-deformation relationships between major structural subassemblages
- h - locations of carbody centers of gravity (c.g.)

## 1.2 Passenger Survivability Considerations

The objective of the task reported in this volume was to assess the nature and severity of potential passenger injury and fatality producing mechanisms due to secondary collisions which occur in intracity train crash environments and to use this analytical methodology to identify the factors and car design parameters, including car interior components which significantly influence these events. In this manner, meaningful design guidelines can be established which will minimize and/or limit the hazard to which the passengers will be exposed in the event of most crash environments.

The overall problem is very complex; however, a rational examination of the many aspects of the phenomena involved should provide an insight into the establishment of practical steps which can be taken to mitigate the most undesirable events. The train crash conditions of interest may also be varied, but clearly the major change in motion is colinear, corresponding to main frame decelerations (or accelerations for certain cases in a consist-consist collision) resulting in a specified change in gross velocity. Since only secondary collisions are of interest for this task any "crushing" environments involving passengers are not considered. The injury producing mechanisms of concern are those resulting from the relative motion of the car or car component and the passenger or passengers and their subsequent interactions. The interior configurations of the cars which comprise the seats, seat arrangements, stanchions, etc., represent rather complex and sometimes relatively rigid boundaries or surfaces at which many severe interactions will occur. The motion of the passenger will be as varied as the range of passenger positions, orientations, passenger alertness, etc. The details of a passenger-structure interaction, including the structural response of the local car component and the biomechanical and related physiological response of the body or body component, will define the nature and severity of any secondary collision induced injury. Thus the approach selected was to establish injury and/or fatality criteria for a



variety of body component categories, to examine the response characteristics for a class of both simple and complex structural systems common to train cars, and to determine the motion details of both passenger and car components for the spectrum of crash conditions of general interest. These three basic elements were assembled into a computer code with which to evaluate injury profiles for specific train crash environments (established from consist crash analysis such as IITRAIN), passenger distributions, passenger density, interior car component properties, and interior configurations. Statistical anthropometric data were used along with other uncertainty factors to yield results which reflect real world variances which are expected to be present in an actual crash situation.

The multiplicity of situations which can occur is so great that if one is to proceed in an effective manner it is essential to identify the more common and more hazardous ones and to concentrate the available resources in these areas. An onboard accident scenario for intracity train crashes was not established; however, some insight into such a scenario may be obtained by examining a somewhat related scenario for transit bus operations.<sup>1</sup> Such a scenario is presented in Figure 1. The bus motions which produce, by far, the most onboard accidents are those relating to decelerations and accelerations and thus correspond to the general type of vehicle motion expected from consist-consist or consist-abutment collisions. To a certain extent this similarity justifies the use of the entire bus scenario for the intracity train crash situation. Clearly the most vulnerable passengers are those which are standing in a relatively open area. Furthermore, the standing passenger very likely will not make use of any assist devices and an injury, if it does occur, is likely to be the result of falling to the floor of the train car. Note that the categories "female", age group "over 50", and especially "over 65", are by far the most common,

---

<sup>1</sup> Mateyka, J. A., "Safety Considerations in Design of New Transit Bus Seats", Proceedings of the Eighteenth Stapp Car Crash Conference, p 71, Society of Automotive Engineers, 1974.

# BUS MOTION AT TIME OF ACCIDENT

- 56% Decelerating
- 21% Normal Operation
- 16% Accelerating
- 7% Turning

# PASSENGER LOCATION

- 39% Forward of First Cross Seat
- 32% First Cross Seat to Rear Door
- 25% Behind Rear Door

# PASSENGER AT TIME OF ACCIDENT

- 46% Standing
- 30% Sitting
- 17% Walking
- 7% Unknown

# WAS PASSENGER CARRYING OBJECT?

- 54% Yes
- 46% No

# PASSENGER USE OF ASSIST DEVICES

- 28% Yes
- 72% No

# WHAT WAS OBJECT BEING CARRIED?

- 47% Package
- 33% Purse
- 14% Umbrella
- 6% Child

# WHICH DEVICE USED?

- 34% Stanchion
- 51% Seat Handle
- 5% Overhead Bar

# SEX OF INJURED PASSENGER

- 82% Female
- 18% Male

# HOW INJURED?

- 61% Fell to Floor
- 17% Hit Seat
- 12% Hit Stanchion
- 9% Hit Farebox
- 3% Hit Driver Partition

# AGE GROUP OF INJURED PASSENGER

- 53% Over 50
- 47% Under 50
- 18% Over 65

FIGURE 1. ONBOARD ACCIDENT SCENARIO FOR CURRENT  
BUS OPERATIONS From Mateyka (Ref. 1)

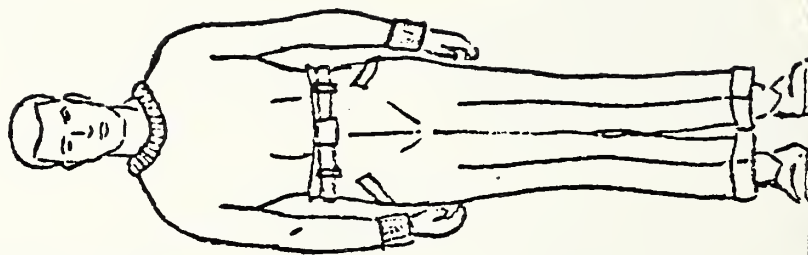
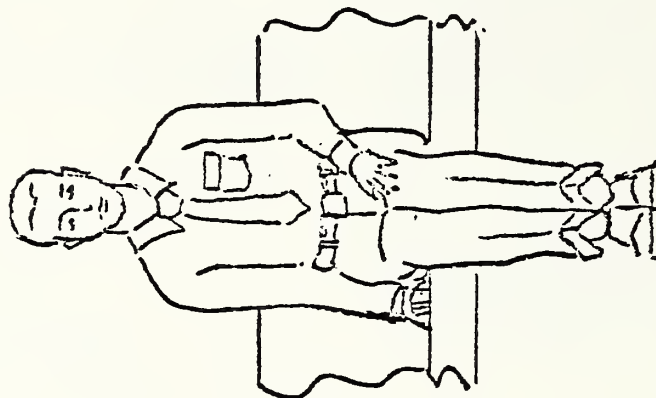


suggesting that physical alertness or responsiveness are important factors in the occurrence of injury or fatalities in typical train crash environments.

### 1.3 Passenger Configurations

Clearly the standing passenger should be given special attention in any meaningful methodology development effort. In addition, the passenger configurations of forward facing seated passenger, backward facing seated passenger, and sideward facing seated passenger are of great interest and have been included in the current methodology. These four basic passenger configurations are illustrated in Figure 2. The difference between the forward facing and the backward facing seated passenger is the direction in which the precrash velocity changes. The forward facing seated passengers will be thrown forward tending to leave the seats whereas the backward facing seated passengers will be pressed back into their seats.

(c) Sideward Facing Seated Passenger



- (a) Forward Facing Seated Passenger
- (b) Backward Facing Seated Passenger

(d) Standing Passenger

FIGURE 2. PASSENGER CONFIGURATIONS

## 2. BIOMECHANICAL RESPONSE TO IMPACT

### 2.1 Basic Considerations

Data for injuries resulting from falls, automotive accidents, and other related secondary collision accidents have been collected and analyzed for many years<sup>2</sup>. In addition, human tolerance experiments to various motion excitations have been conducted. Thus, a vast body of data exists upon which to estimate the nature and degree of an injury produced by a given impact stimulus. Unfortunately, in the case of actual injuries, the preconditions of the events, such as the impact velocity, are frequently poorly defined.

It is clear that the physical condition of the individual involved in an accident as influenced by age, diet, etc., has a significant relationship upon the details and consequences of the event. Thus data acquired with the use of cadavers are in many instances biased in some manner. This general data base has been examined where relevant and used in the subsequent methodology.

A number of injury criteria, actual injury-fatality criteria, have been established which can be used to define the nature and degree of injury to whole body, head or other body components due to impact with blunt objects or surfaces, i.e., under nonpenetrating conditions. While these criteria are relatively crude and somewhat uncertain, they represent the current state of the art in injury criteria and are probably adequate for the initial development of an injury prediction methodology.

The most sophisticated and documented impact severity criteria is the Gadd Severity Index (SI) or variants thereof. This index is defined as

$$SI = \int_0^{t_d} [a(t)]^n dt \quad (1)$$

---

<sup>2</sup>Cassidy, R. J. and Romeo, D. J., "Assessment of Crashworthiness of Existing Urban Rail Vehicles", Calspan Corporation Final Report ZL-5368-K-1, June 1975.

where

- $t$  = time (in sec)
- $a(t)$  = the acceleration history of the body or body component (measured in g units)
- $n$  = an exponent which depends upon body component
- $t_d$  = duration of the acceleration pulse.

Note that the change in velocity of the body or body component,  $V_o$ , due to the acceleration pulse is

$$V_o = \int_0^{t_d} a(t) dt \quad (2)$$

Thus when  $n=1$  and there is no rebound, the severity index is proportional to the incident velocity. The acceleration pulse  $a(t)$  is a relatively strong vector function of position on the body (component) and thus a specific location should be considered to make the above definition of a severity index meaningful. Such refinements have not been accomplished to date! The exponent  $n$  has been evaluated<sup>3</sup> for frontal head impact conditions and a value of 2.5 best fits the limited set of data. This value suggests the increased importance of the peak or the near peak value of the acceleration in contributing to the severity of a head impact event.

It has also been determined that the duration of the acceleration pulse may define, in addition to the value of the severity index, the nature of the injury, such as skull fracture versus a concussion for some head impact situations. Peak accelerations have also been correlated<sup>3</sup> to some injury data. The value of  $n$  for use in evaluating the severity index for other body components has been attempted but these are estimates and a few firm data are available with which to support the estimates.

The response of some body components to severe motion stimuli, such as the thorax and neck, have been made but they are of rather limited value. The data for the flexion (dorsal) response of the neck were used in a limited manner and proved to be quite useful (see Section 4.7).

---

<sup>3</sup>Snyder, R. G., "Human Impact Tolerance", Highway Safety Research Institute, The University of Michigan, SAE Preprint 700398, 1970.



## 2.2 Injury-Fatality Criteria

The goal of the injury prediction methodology is to predict the number, nature, and severity of injuries which occur in a given intracity train crash situation. The severity of an injury can be expressed in terms of an injury scale ranging from "minor" to "critical" and being bounded externally by the categories "no injury" and "fatal". These categories are listed in Figure 3. Their definitions, at least for single injuries, are generally accepted within the medical community. The precision with which a given severity index can be related for this injury scale is generally poor. It appears reasonable to use this many levels on the injury scale as a means of obtaining a more detailed description of the outcome of a postulated train crash such that at least the relative influence of certain car design features can be evaluated. The problem then is to select one or more injury-fatality criteria relationships applicable to a given impact/body component mode and to relate it to the injury scale. This step has been accomplished and these relationships are presented in Figure 3. They have been used in the injury prediction methodology. It is clear that these specifics are not well founded in facts; nonetheless, they are the best available (or at least, they are what is needed). Hopefully these specifics are reasonably accurate in a few instances, and an attempt was made to make them relatively consistent. When better data become available these criteria can be updated.

A severity index value of 1000 sec for a frontal head impact generally corresponds to an injury in the minor-to-moderate range whereas a value of 2000 sec suggests a critical-to-fatal injury level. These two points were used to establish the criteria curve for a head impact and related to a Gadd Severity Index for the condition of  $n=2.5$ . Since the value of  $n$  for the other body components or impact locations such as the face are not well defined, a value of  $n=2.5$  was selected. In this manner, the calculation procedure used in the methodology would be simplified. It would appear that the general trend implicit in the Gadd Severity Index



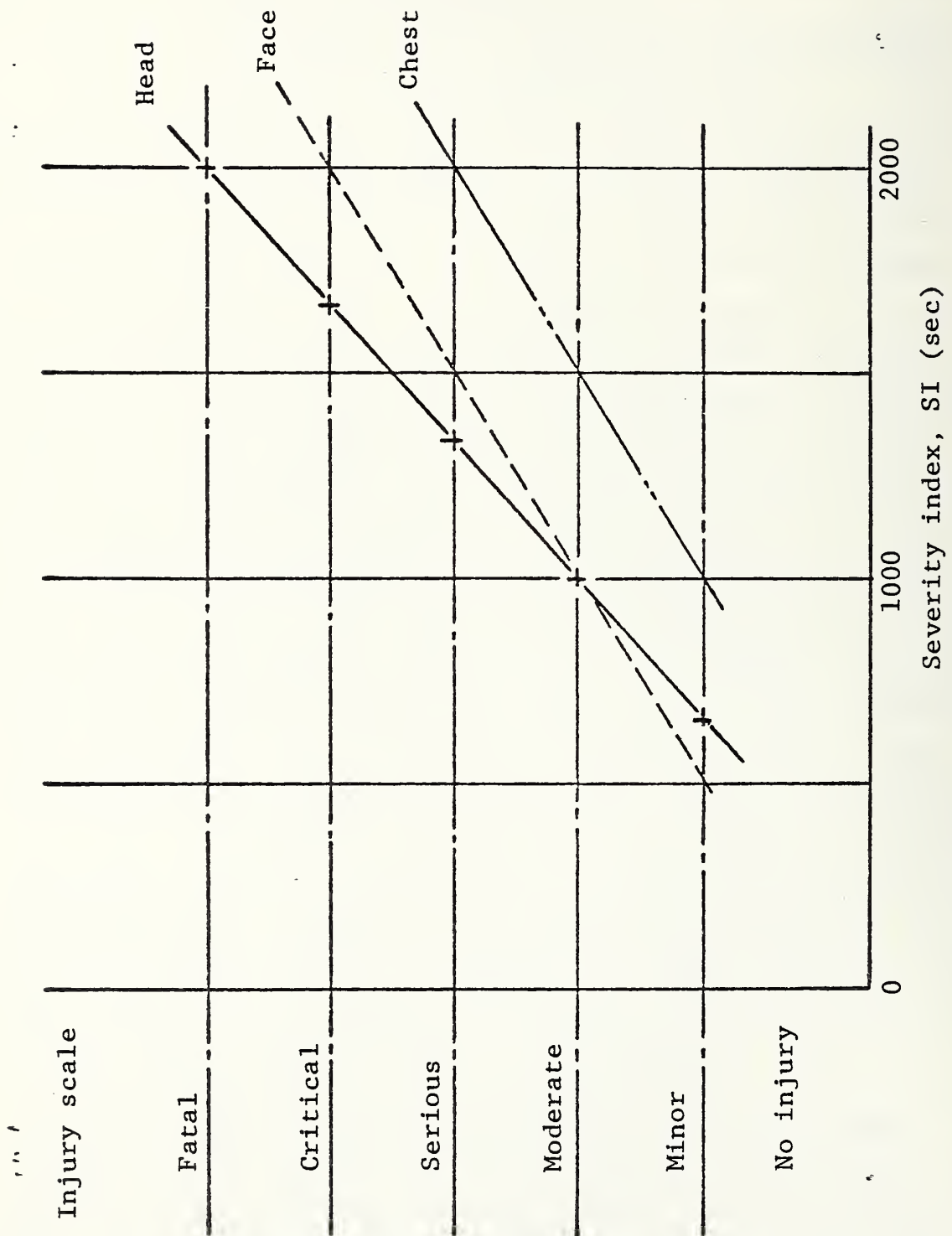


FIGURE 3. INJURY SCALE FOR IMPACT OF BODY COMPONENTS

form is reasonable and that  $n$  would certainly be greater than unity (a simple velocity dependence). Other body components, such as the chest, are most likely not quite as sensitive to acceleration peaks as the head would be, hence the value of  $n$  is probably somewhat less than 2.5. Nonetheless, such a value was used throughout. The criteria for the face were selected on the basis that at low levels of excitation, more damage would occur to the face than to the head. The opposite behavior was believed to be true at high levels of excitation. The face structure is thus envisioned as an energy absorbing system which starts to crush at low stress levels and isolates the sensitive brain at higher stress levels. The curve for the chest was placed well below that for the face in view of its (apparent) stronger structural characteristics.

It should be obvious that the injury criteria currently available greatly limit the accuracy that any injury prediction methodology can make. This aspect of the overall, rather complex problem is perhaps the most limiting factor encountered in the development of the methodology.

### 3. IMPACTED SURFACE/STRUCTURE EFFECTIVENESS

#### 3.1 Basic Considerations

It has been established that the level of injury that a body component sustains upon impact with a relatively rigid object can be characterized by some aspect of the "lumped mass" acceleration details experienced by the body component or parts thereof during the impact process. It is clear that the acceleration details and therefore the injury level will be influenced, perhaps significantly, by the nature and responsiveness of the object (i.e., the surface and/or structure), especially at the contact point. The response of car interior components, such as a seatback, will depend upon the totality of imposed loads, their points of application, their time phasing, and the displacement histories of the attachment points of the structural component. Thus the influence of the response characteristic of the impacted surface/structure upon the injury level may be quite complex.

A series of mechanical response functions was selected to represent simple yet typical impact/surface responses, and the acceleration histories for a simple lumped mass impact situation were evaluated. These acceleration histories were then used to determine the corresponding injury-criteria (index) dependence and sensitivity on the structural and impact parameter values. The sensitivity analysis is presented in terms of influence coefficients and demonstrates that the response function examined, the incident or impact velocity of the passenger or body component is a relatively influential variable. It suggests that significant reduction in injury can be achieved by retarding the relative motion between the passenger and the train component prior to the local impact. A brief examination of a two-component structural system was performed to illustrate the significant role that attachment stiffness can play in the design of car interior substructures or components.

A potential load-deflection relationship is illustrated in Figure 4 for the local deformation at the impact point of a body component of weight,  $W_0$ . The impact is assumed to be normal to the surface and the relative incident or impact velocity is  $V_0$ . The soft surface layer of the body component and/or the existence of a thin layer of padding on the surface will, in this analysis, provide for a somewhat distributed contact or application area,  $A_0$ . The initial resistance after the body component and surface are effectively mated will, most likely, be a relatively stiff and elastic resistance. If sufficient energy (i.e., kinetic energy of the body component) is available then the structure may yield in some fashion, more probably with some strain hardening effect until all of the incident energy is absorbed by the surface/structure. At this point the body component motion will be fully arrested and some bounce or throwback effect will subsequently occur as the load drops during the elastic unloading phase. Finally, the pad or surface layer will unload. The area under the load deflection curve represents the energy absorbed by the surface/structure.

Four idealized resistance functions were selected for analysis to represent the primary resistance features illustrated in Figure 4. In each case no inertial effect of the surface/structure was included. The four idealized resistance functions are illustrated in Figure 5. They include the perfect absorber which is characterized by a constant resistance force. Note that very few structures of this nature will exist and care must be used to ensure that adequate displacement capacity ( $x_0$ ) is available so that the system will not "bottom out". The second case is the "classical" elastic case. The third and fourth cases treat the assumed to be more common cases of strain hardening yielding structures. In the latter case an initial threshold force level exists.

An analysis of the response of each of the resistance functions can now be performed to determine the acceleration history of the body component during the impact process. This acceleration history can then be used to evaluate an appropriate injury index

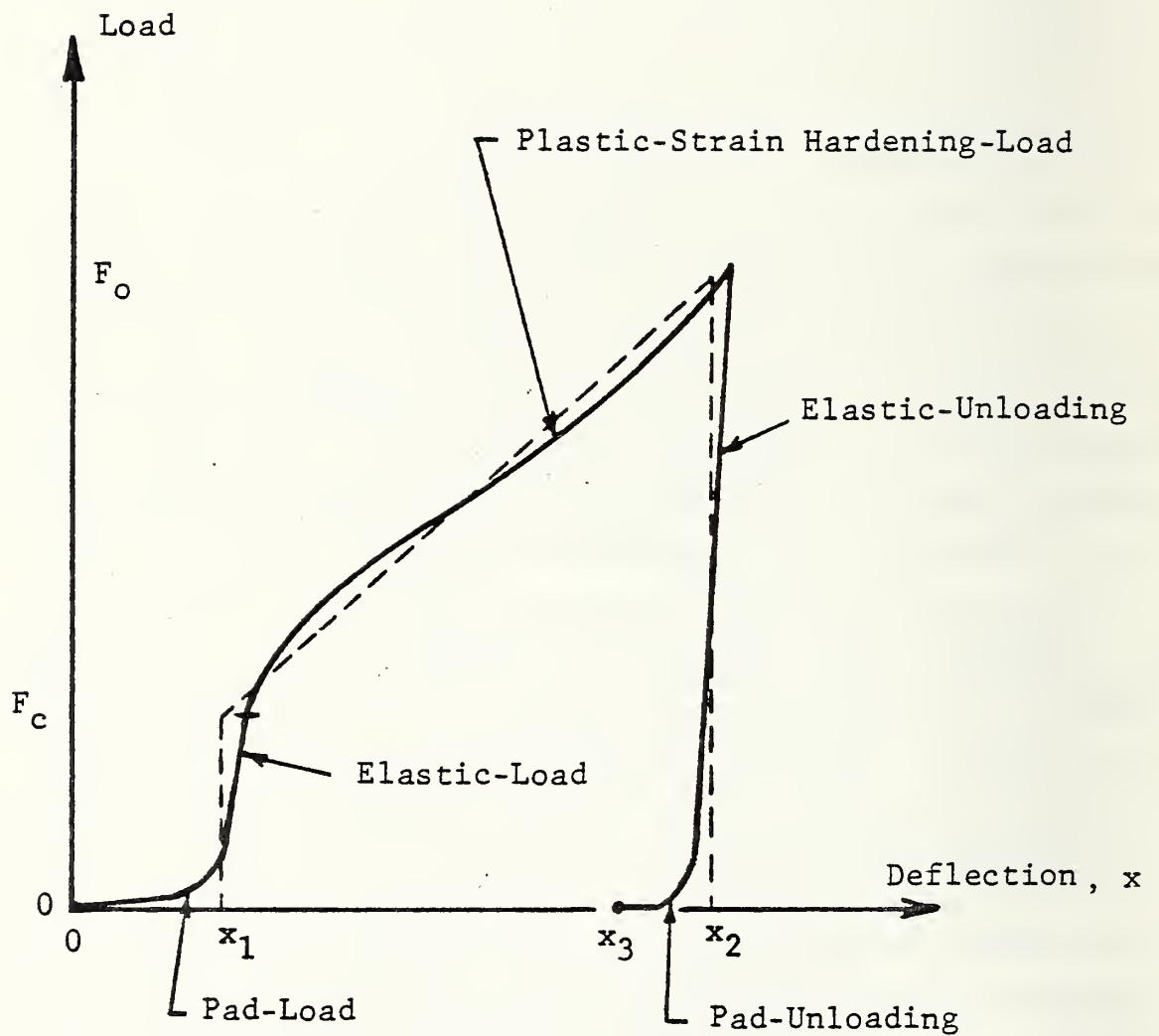
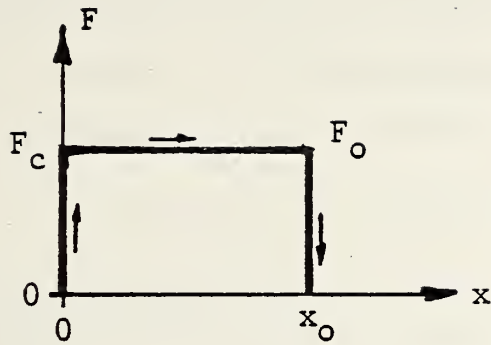


FIGURE 4. POTENTIAL LOAD-DEFLECTION RELATIONSHIP

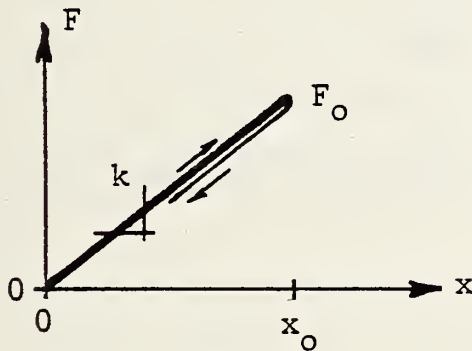


Case A



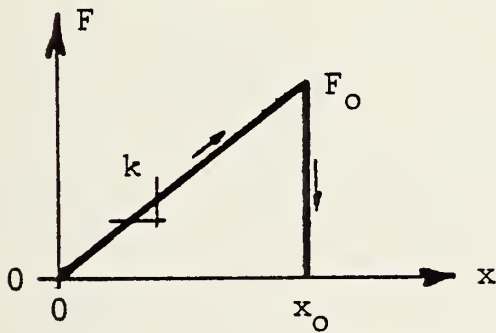
Perfect Absorber

Case B



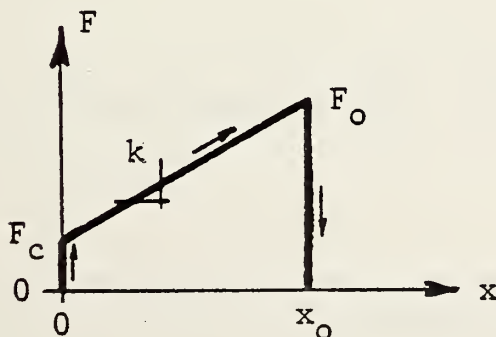
Elastic

Case C



Strain Hardening

Case D



Yield Limiting  
with Strain Hardening

FIGURE 5. SELECTED RESISTANCE FUNCTIONS

such as the severity index, SI, or the peak acceleration,  $a_o^*$ . For the former, the load application time  $t_d$  is also a factor both with respect to evaluating the magnitude of the severity and perhaps in defining the nature of the injury.

### 3.2 Perfect Absorber

The perfect absorber, case A, is characterized by a constant resistance force,  $F_c$ . This force is derived from the product of the application area,  $A_c$ , and the yield stress,  $\sigma_y$ , which is a property of the material involved. Thus

$$F_c = A_c \sigma_y \quad (3)$$

The equation of motion for the impacting body component of weight,  $W_c$ , is

$$\frac{dV}{dt} = - \frac{F}{W_c} \quad (4)$$

where

$V$  = velocity

$t$  = time

$F$  = force =  $F_c$

Subject to the initial condition

$$V(0) = V_o$$

and

$$x(0) = 0$$

where  $x$  is the displacement associated with the contact point. Integration yields

$$V = V_o - a_o t \quad (6)$$

where  $a_o = F_c/W_c$  is the deceleration (a constant). The body component comes to rest (i.e.,  $V=0$ ) at

$$t = t_o = V_o/a_o \quad (7)$$

The displacement is given by the differential equation

$$\frac{dx}{dt} = v \quad (8)$$

which when integrated yields

$$x = v_0 t - a_0 t^2/2 \quad (9)$$

The maximum displacement,  $x_0$ , is

$$x_0 = 1/2 v_0 t_0 \quad (10)$$

The motion is fully arrested at this point and all of the energy inherent in the incident body component is totally dissipated. The duration of the load,  $t_d$ , is thus equal to

$$t_d = \frac{v_0 W_c}{A_c \sigma_y} \quad (11)$$

Finally, the severity index (SI) from its basic definition (see equation (1)) is

$$SI = (a_0)^{1.5} v_0 = \left[ \left( \frac{A_c}{W_c} \right) \sigma_y \right]^{1.5} v_0 \quad (12)$$

If the peak acceleration  $a_0^*$  is used as a measure of injury then for the perfect absorber

$$a_0^* = a_0 = \frac{A_c \sigma_y}{W_c} \quad (13)$$

### 3.3 Elastic Response

The elastic response surface, case B, is characterized by a resistance force which is proportional to the contact point displacement, that is

$$F = kx \quad (14)$$

where  $k$  is the so-called spring constant. The above resistance form is absolute and independent of the direction of the movement (i.e., loading versus unloading phase). The solution for this

resistance case, for the above cited boundary conditions, is classic and given for the velocity as

$$V(t) = V_o \cos(\omega t) \quad (15)$$

where

$$\omega = \sqrt{\frac{k}{W_c}}$$

The acceleration and displacement histories are given as

$$a = \omega V_o \sin(\omega t)$$

and

$$x = x_o \sin(\omega t)$$

(16)

where the maximum displacement is

$$x_o = \frac{V_o}{\omega} \quad (17)$$

The time at which the maximum displacement is achieved is

$$t_o = \frac{\pi}{2\omega} = \frac{\pi}{2} \sqrt{\frac{W_c}{k}} \quad (18)$$

Due to the conservative nature of an elastic system the energy inherent in the motion of the body component is transferred without loss into potential energy of deformation of the elastic system and this energy is readily available to accelerate the body component back in the direction from which it came. This response feature results in further acceleration of the body component until such a time that it loses contact with the surface. The above response equations apply and the load duration  $t_d$  is simply

$$t_d = 2 t_o = \pi \sqrt{\frac{W_d}{k}} \quad (19)$$

The severity index for this case is

$$SI = 2B_o \left( \frac{k}{W_c} \right)^{0.75} V_o^{2.5}$$



where

(20)

$$B_0 = \int_0^{\pi/2} \sin^{2.5} \alpha d\alpha = 0.71.$$

The peak acceleration is

$$a_0^* = \sqrt{\frac{k}{W_c}} v_0. \quad (21)$$

### 3.4 Inelastic Response

The inelastic response surface, cases C and D, are characterized by a response force which is similar in form to that of the elastic case (equation (14)) except that all of the transferred energy is lost due to plastic deformation of the surface (structure) and thus no rebound can occur. Equation (14) only applies for the loading phase.

Case C, the strain hardening case, corresponds identically to the resistance function form of the elastic response surface and the motion solution equations (15) and (16) apply. However, the body component comes to rest at the point of maximum displacement, hence the duration of the load is

$$t_d = t_0 = \frac{\pi}{2} \sqrt{\frac{W_c}{k}}, \quad (22)$$

All of the other motion results apply directly.

The severity index for case C is thus

$$SI = B_0 \left[ \frac{k}{W_c} \right]^{0.75} v_0^{2.5}. \quad (23)$$

The peak acceleration is given by equation (21).

Case D is the more general case and includes case A as one limiting case and case C as the other limiting case. The resistance for case D includes an initial resistance  $F_c$  at zero displacement, thus the resistance is

$$F = F_c + kX. \quad (24)$$

The corresponding motion solutions are

$$\begin{aligned} V &= V_o \cos(\omega t) - \frac{\omega F_c}{k} \sin(\omega t) \\ a &= -\omega V_o \sin(\omega t) - \omega^2 \frac{F_c}{k} \cos(\omega t) \end{aligned} \quad (25)$$

and

$$x = \frac{V_o}{\omega} \sin(\omega t) + \frac{F_c}{k} \cos(\omega t) - \frac{F_c}{k}.$$

The maximum deflection and the load duration can be readily evaluated by considering the general case to be composed of two similar cases of the form of case C that is, the difference of two triangular resistance functions. A hypothetical preload deformation  $x_c$  is used such that

$$x_c = \frac{F_c}{k}, \quad (26)$$

The initial velocity for the preload contribution must be correspondingly increased such that when  $x=0$  (and  $F=F_c$ ),  $V=V_o$ .

The load duration is

$$t_d = t_o = \frac{1}{\omega} \arctan \left[ \frac{V_o}{x_c \omega} \right] = \sqrt{\frac{W_c}{k}} \arctan \left[ \sqrt{\frac{W_c}{k}} \cdot \frac{V_o}{F_c} \right]. \quad (27)$$

and the maximum displacement is

$$x_o = \frac{V_o}{\omega} \sin(\omega t_o) + x_c \cos(\omega t_o) - x_c, \quad (28)$$

The severity index (SI) is

$$SI = f(v) \left[ \frac{k}{W_c} \right]^{0.75} V_o^{2.5} \quad (29)$$

where

$$f(v) = \frac{B(\beta)}{(\cos \beta)^{2.5}}$$

$$B(\beta) = \int_{\beta}^{\pi/2} \sin^{2.5} \alpha d\alpha$$

$$\beta = \arctan v$$

$$v = \frac{F_c}{V_o \sqrt{kW_c}}$$

The function  $f(v)$  has been evaluated and is presented in Figure 6. In the limit for large values of  $v$

$$f(v) = v^{1.5}. \quad (30)$$

The peak acceleration is given as

$$a_o^* = \sqrt{\frac{kV_o^2}{W_c} + \left(\frac{F_c}{W_c}\right)^2}. \quad (31)$$

### 3.5 Sensitivity Evaluation

An examination of the dependence of the severity index and the peak acceleration on the parameters involved will be of interest inasmuch as such a sensitivity evaluation will indicate which of the parameters are most significant in this injury analysis. In this manner appropriate attention can be given to those parameters in the analyses presented in the subsequent chapters of this report and in the allocation of resources for further research.

The parameters which are involved, although not necessarily in all cases, are the impact velocity,  $V_o$ , the critical force,  $F_c$ , the spring constant,  $k$ , and the weight of the body component,  $W_c$ . The severity index (SI) equations can be expressed in a logarithmic differential form as

$$\frac{d(SI)}{SI} = C_V \frac{dV_o}{V_o} + C_F \frac{dF_c}{F_c} + C_k \frac{dk}{k} + C_W \frac{dW_c}{W_c} \quad (32)$$

where the coefficients  $C_i$  are defined as influence coefficients and correspond to the contribution that a percentage change in the  $i$ th parameter makes to the percentage change in the severity index. Appropriate differentiation of the severity index equations

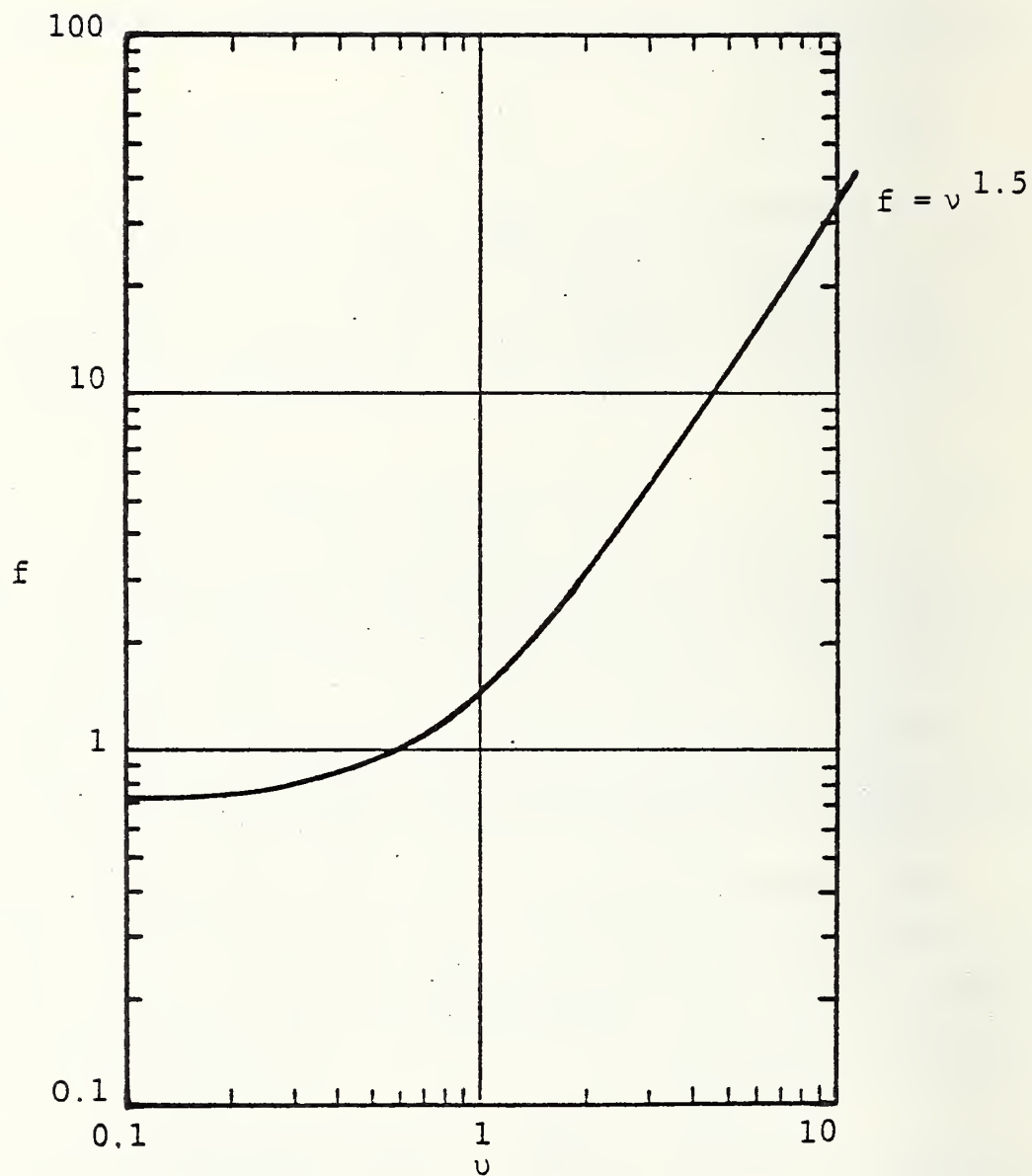


FIGURE 6. SEVERITY INDEX FUNCTION  $f(v)$



presented above provide the values of these coefficients for each of the four response cases treated. A similar treatment was applied to the peak acceleration solutions to yield corresponding influence coefficients  $K_i$ , that is

$$\frac{d(a_o^*)}{a_o^*} = K_V \frac{dV_o}{V_o} + K_F \frac{dF_c}{F_c} + K_k \frac{dk}{V} + K_W \frac{dW_c}{W_c}, \quad (33)$$

The values of the influence coefficients are summarized in Table 1. For the general case, case D, the coefficients are functions of the parameter  $v$  and must be treated as infinitesimal influence coefficients. For this general case the values of the influence coefficients for the severity index and peak acceleration are presented in Figures 7 and 8 respectively.

TABLE 1.-SUMMARY OF INFLUENCE COEFFICIENTS

Case	(SI)				$a_o^*$			
	$C_V$	$C_F$	$C_k$	$C_W$	$K_V$	$K_F$	$K_k$	$K_W$
A	1.0	1.5	0	-1.5	0	1.0	0	-1.0
B	2.5	0	0.75	-0.75	1.0	0	0.5	-0.5
C	2.5	0	0.75	-0.75	1.0	0	0.5	-0.5
D*	functions of $v$				functions of $v$			

\* see Figure 7 and 8

An examination of the absolute values of the influence coefficients indicates that the single most important parameter is the impact velocity,  $V_o$ . Clearly, then the analysis of the motion of passengers in the various passenger configurations must be designed to evaluate the impact velocity accurately and to identify the factors which influence its value. The weight of the body component,  $W_c$ , is moderately important but it does not represent a parameter which could be controlled by car interior component considerations.

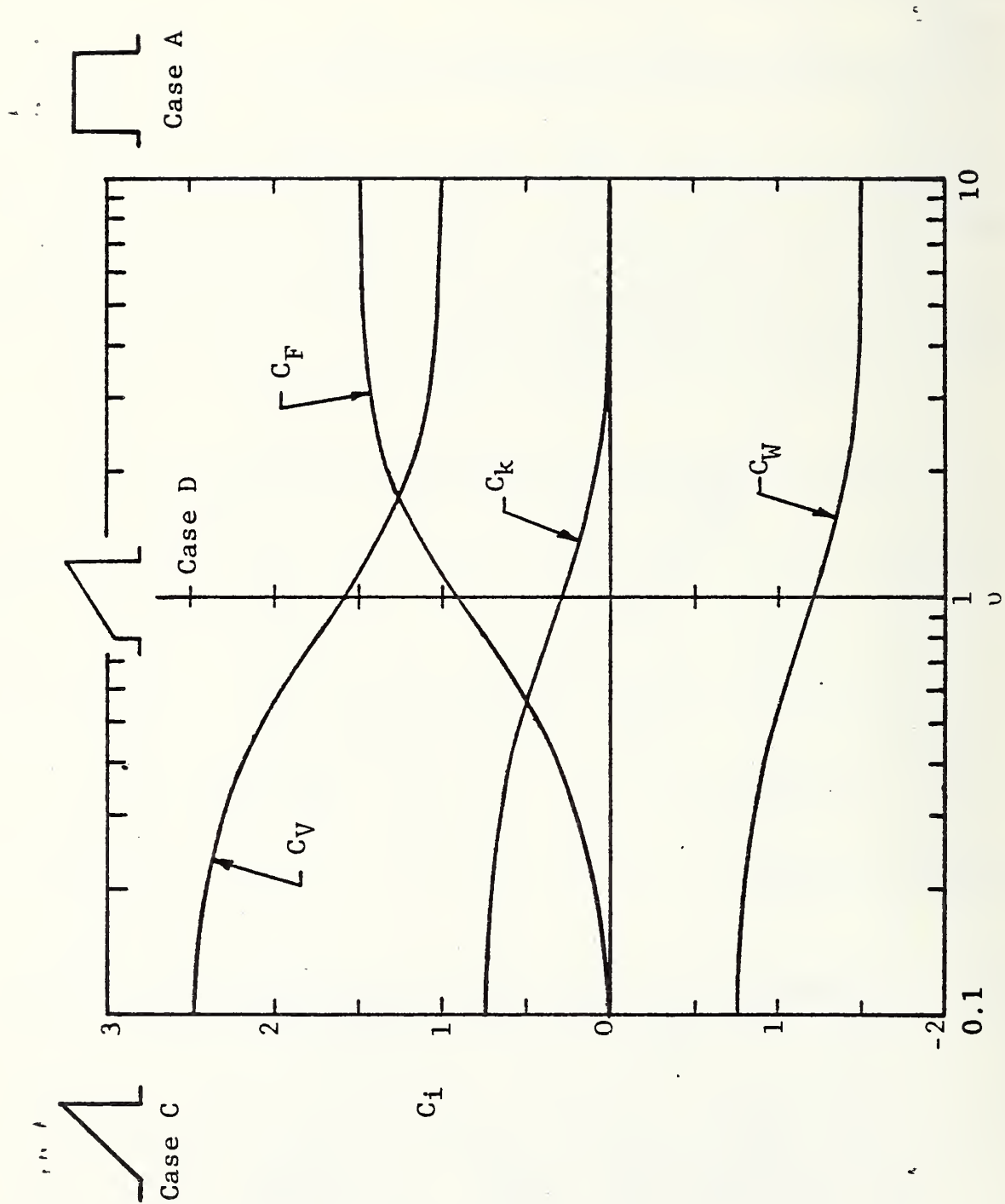


FIGURE 7. INFLUENCE COEFFICIENTS FOR SEVERITY INDEX

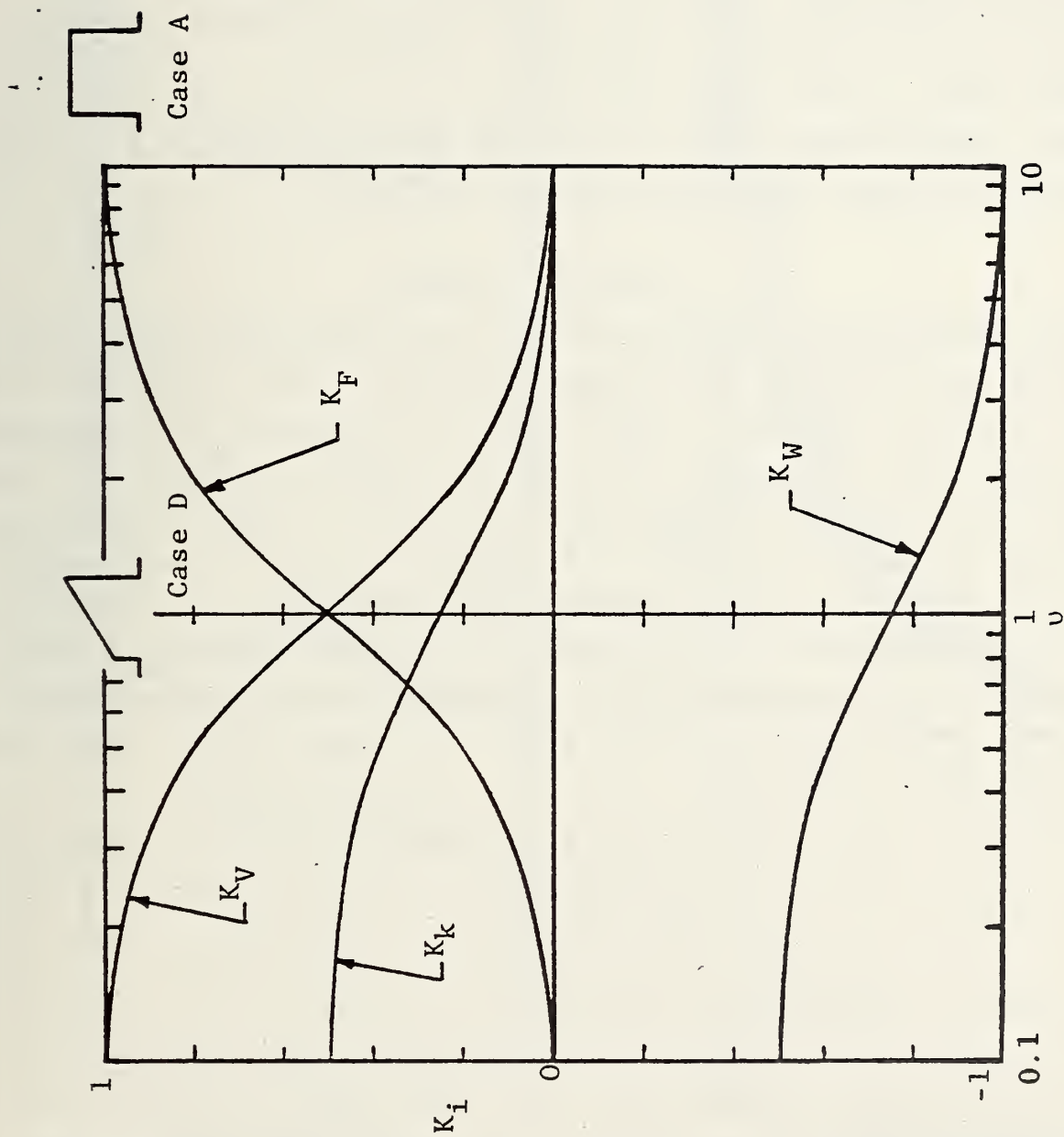


FIGURE 8. INFLUENCE COEFFICIENTS FOR  $a_0^*$

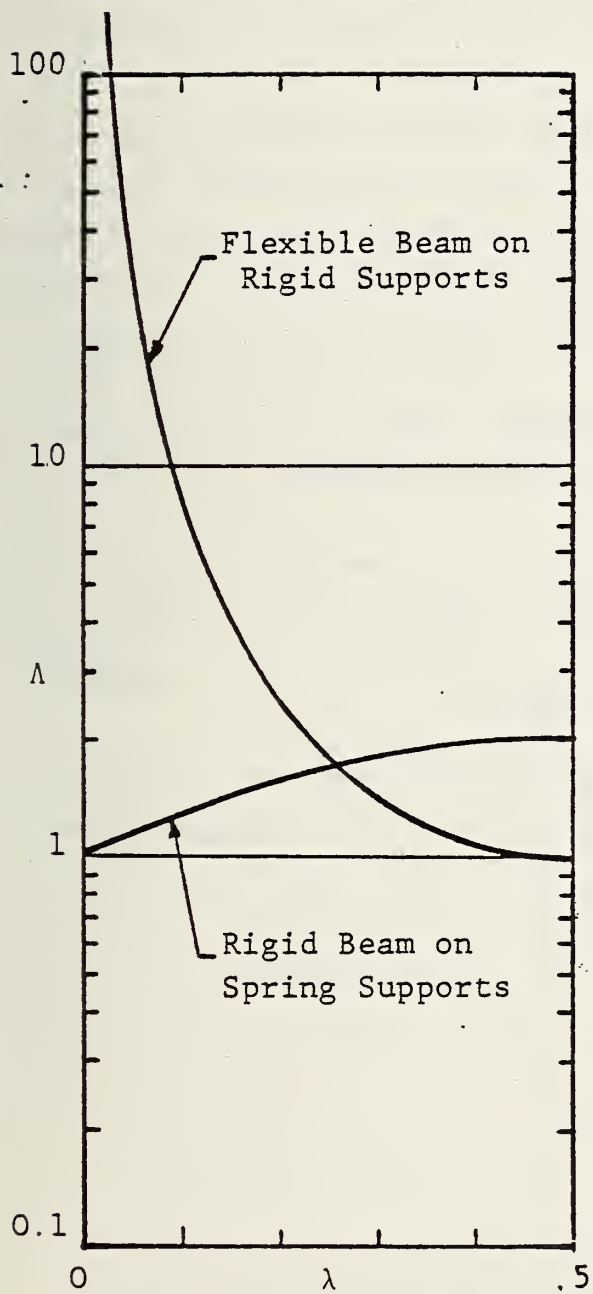
Similarly, the application area,  $A_c$ , is largely a "people" parameter. Since the force, for case A, is proportional to the yield stress the influence coefficient for the stress,  $\sigma_y$ , is essentially equal to that of the force. The value of the influence coefficient for force is moderate. The least significant parameter appears to be the spring constant or stiffness parameter. Although this parameter may be the least influential it is one with which the greatest improvements may be achieved by design because of the greater percentage change that may be available.

### 3.6 Composite Systems

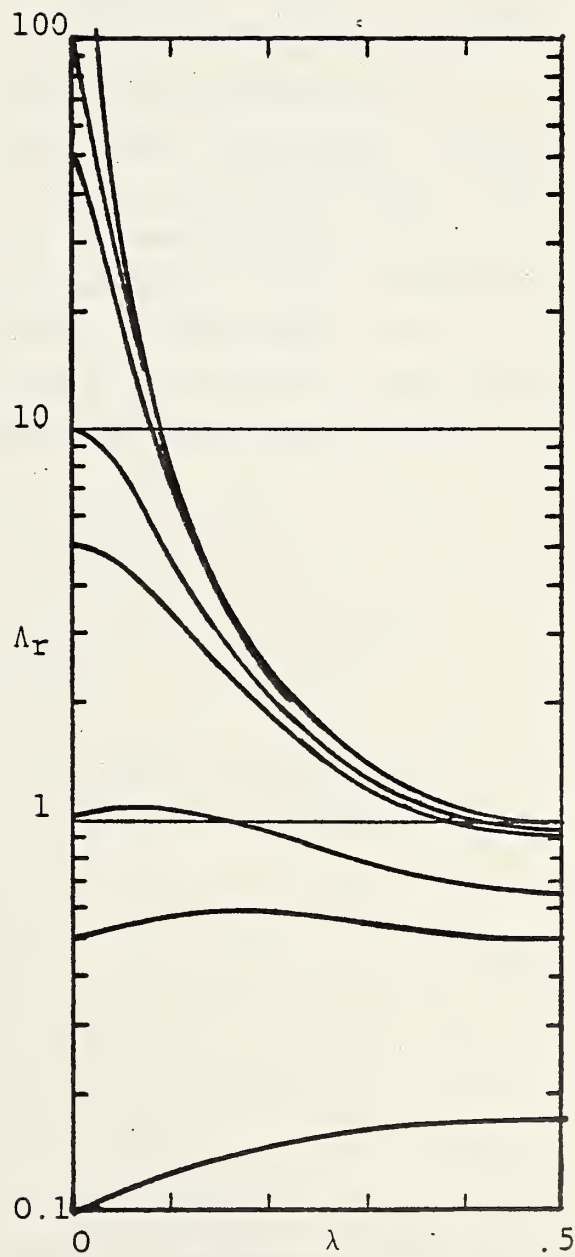
The examined resistance functions were quite simple and do not represent real systems with great precision. The resistance of real structural systems to local impact will be much more complex and depend upon the point of impact, inertial effects of the surface or structure, and many other factors. In this section the variation of the stiffness of a simple composite beam/support system is examined. Such a system could approximate some typical car interior components such as partitions, stanchions, and perhaps to a lesser degree some seatbacks. The beam/support system considered here is a uniform simply supported beam mounted upon two identical spring supports.

Consider first the two limiting cases of a flexible beam on rigid supports and that of a rigid beam on flexible supports. The spring constants  $\Lambda$  for a load applied at a position  $\lambda$  along the beam ( $\lambda = 0$  corresponds to the support position and  $\lambda = 0.5$  corresponds to the midspan position) is presented in a normalized form in Figure 9(a). The spring constant has been normalized by the minimum values respectively for each case. The stiffness variation for different application points is reasonably constant for the rigid beam on spring supports with a maximum variation of a factor of two. On the other hand, the system of the flexible beam on rigid support results in a very large variation for different application points.





(a) Limiting Cases



(b) Flexible Beam on Spring Supports

FIGURE 9. LOCAL STIFFNESS FOR COMPOSITE BEAM/SUPPORT SYSTEM

In particular, the system becomes very stiff near the support positions. Approximately 20 percent of the possible impact positions result in local stiffnesses which are at least 10 times greater than the minimum stiffness.

The design of the overall system can be improved with respect to body component impact considerations by distributing the stiffness between the two components of the system. The local stiffness for this general case is presented in Figure 9(b). This system stiffness  $\Lambda_r$  is normalized by the minimum or midpoint stiffness of the beam component. A much more balanced design can thus be achieved. In particular, the extremely high local stiffness near the support position can be significantly reduced.

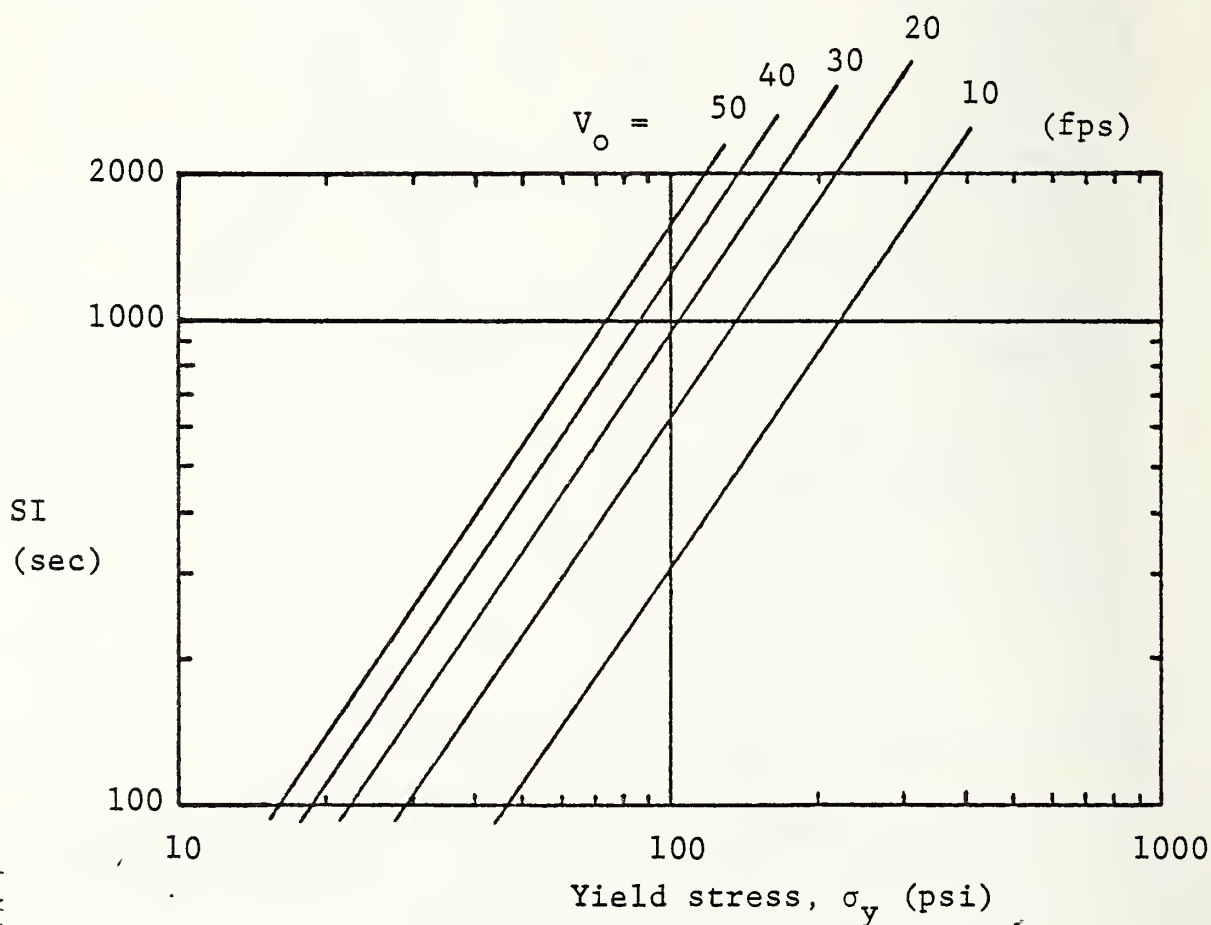


FIGURE 10. INFLUENCE OF YIELD STRESS ON SEVERITY INDEX - PERFECT ABSORBER

### 3.7 Typical Results

The severity index was evaluated for the case of a perfect absorber and the case of an elastic response. Recall that the latter case also corresponds to case C by reducing the severity index by a factor of two. The head impact situation was selected for this evaluation and nominal values for the body component weight and application area of 10 lb and 10 sq inches were selected. The results cover the impact velocity range of from 10 to 50 fps. The results for the perfect absorber are presented in Figure 10 and suggest that a yield stress in the range of from 80 to 200 psi would produce a moderate injury for the velocity range cited. The results for the elastic response case are presented in Figure 11 and illustrate the large role that the impact velocity plays in this system. A value of a spring constant of 1000 lb/inch can produce rather severe injuries at all but the very low velocity levels.

### 3.8 Nomenclature

Symbols and definitions used in Section 3:

a	acceleration
$a_o$	specific acceleration
$a_o^*$	peak acceleration
$A_c$	application area
B	a function
$B_o$	a constant
$C_i$	ith influence coefficient for severity index
$C_F$	severity index influence coefficient for force
$C_k$	severity index influence coefficient for spring constant
$C_v$	severity index influence coefficient for velocity
$C_w$	severity index influence coefficient for weight
f	a function
F	force

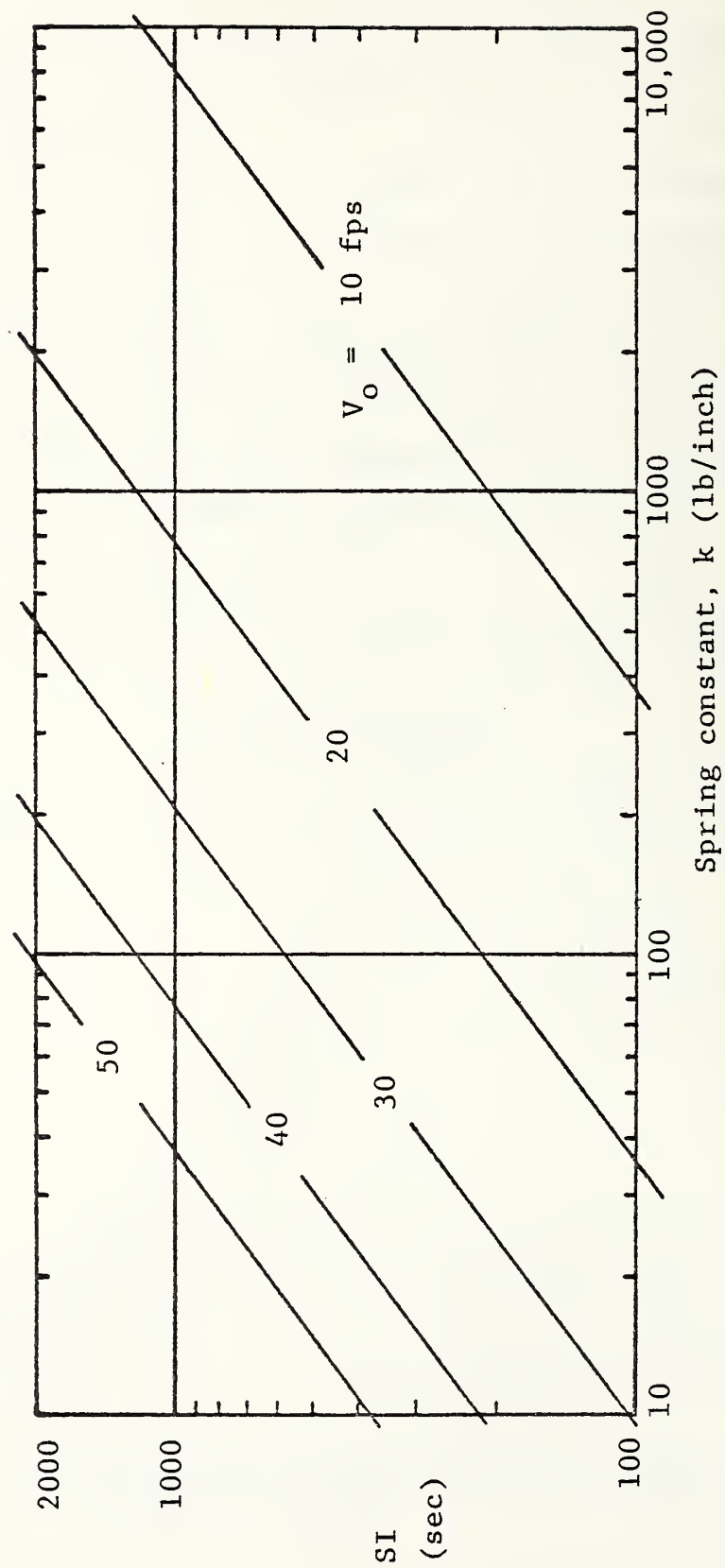


FIGURE 11. INFLUENCE OF SPRING CONSTANT ON SEVERITY INDEX - ELASTIC BEHAVIOR



$F_c$	critical force
$F_o$	maximum force
$k$	spring constant
$K_i$	$i$ th influence coefficient for peak acceleration
$K_F$	peak acceleration influence coefficient for force
$K_k$	peak acceleration influence coefficient for spring constant
$K_V$	peak acceleration influence coefficient for velocity
$K_W$	peak acceleration influence coefficient for weight
SI	severity index
$t$	time
$t_d$	load duration
$t_o$	time of maximum displacement
$V$	velocity
$V_o$	incident velocity
$x$	displacement
$x_c$	hypothetical displacement
$x_o$	maximum displacement
$x_1$	generic displacement
$x_2$	generic displacement
$x_3$	generic displacement
$W_c$	body component weight
$\alpha$	dummy variable for integration
$\beta$	dimensionless variable
$\lambda_z$	dimensionless position along beam
$v$	dimensionless variable
$\omega$	frequency
$\Lambda$	normalized stiffness
$\Lambda_r$	relative normalized stiffness

## 4. PASSENGER MOTION

The primary goal in this section is to develop motion details for persons in the four basic passenger configurations, and to identify the nature and magnitude of impact velocities of their equivalence in each of these situations. As a prelude to presenting these results it was desirable to examine a class of train car acceleration pulses to establish their characteristics and ultimately to unify these pulses by developing equivalence parameters. A simple lumped mass translation behavior analysis was then performed to obtain an insight into potential motion environment. Finally a brief summary of anthropometric data is presented to establish some of the needed passenger characteristics.

At this point the specific motion details of passengers in the standing, forward facing seated, backward facing seated, and side-ward facing seated passenger configurations are presented. The section ends with a brief and somewhat superficial treatment of multiple passenger interactions. This last effort represents an attempt to "measure" the potential influence of some real world situations.

### 4.1 Acceleration Pulse Shape Characteristics

An examination of some numerical results obtained during the course of the current program dealing with the motion details of railcars during a crash, indicate that the acceleration histories can be idealized with relatively simple pulse shapes. These include the step pulse, a double step pulse, and a triangular pulse shape. Some typical acceleration histories are illustrated in Figure 12(a) and 12(b). It is clear that some fine structure will exist and in addition that some low amplitude details may persist for some time. It appears reasonable to define several idealized acceleration pulse shapes and to attempt to utilize these in the subsequent passenger motion studies.

Two rather general pulse shapes are selected, one is a trapezoidal pulse, the other a double step pulse. These pulse shapes are illustrated in Figures 12(c) and 12(d).

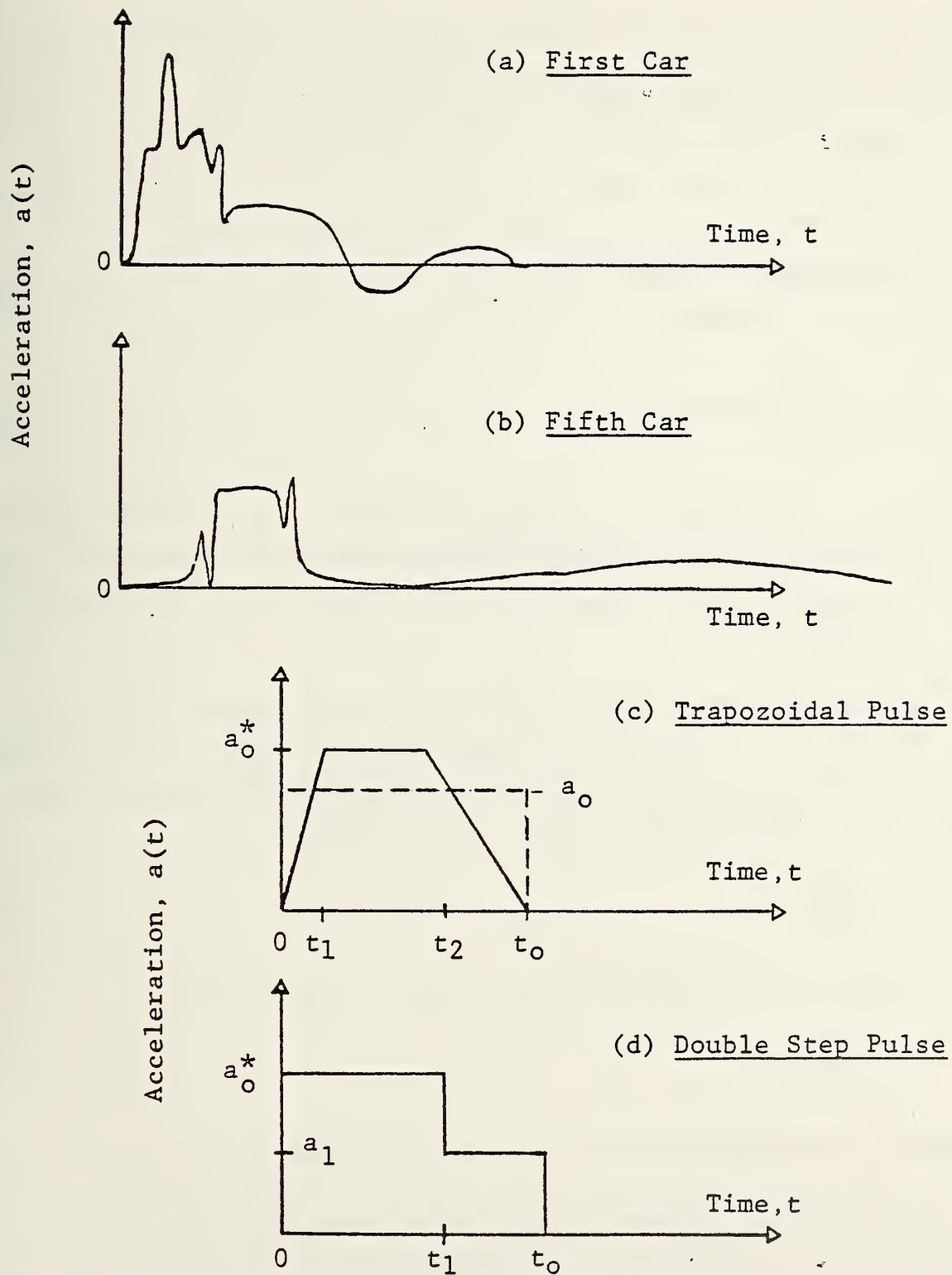


FIGURE 12. ACCELERATION PULSE CLASSIFICATION

The trapezoidal pulse includes within its framework the basic step pulse and the full spectrum of triangular pulses. The double step pulse also includes with its form the basic step pulse. It appears reasonable and practical to refer all pulse shapes to the basic step pulse; a pulse shape which itself is a good approximation to many observed (i.e., calculated) acceleration pulses.

By definition the area under the acceleration pulse  $a(t)$  is equal to the change in velocity  $V_0$  of the train car

$$V_0 = \int_0^{t_0} a(t) dt \quad (34)$$

where  $t$  = time and  $t_0$  = pulse duration. It follows from these definitions that the average acceleration,  $a_0$ , is given as

$$a_0 = \frac{V_0}{t_0} \quad (35)$$

Two parameters have been elected as useful parameters with which to characterize these acceleration pulses. One is an acceleration peaked factor,  $\gamma$ , which is simply the ratio of the peak acceleration  $a_0^*$  to the average acceleration, that is

$$\gamma = \frac{a_0^*}{a_0} \quad (36)$$

The other is a stopping distance factor  $\beta$  defined as

$$\beta = \frac{x_0}{V_0 t_0} \quad (37)$$

where  $x_0$  = stopping distance.

The motion details corresponding to a basic step pulse acceleration, i.e., a constant deceleration level  $a_0$ , are defined by

$$\begin{aligned} a(t) &= a_0 & 0 \leq t \leq t_0 \\ V &= V_0 - a_0 t \end{aligned} \quad (38)$$

$$x = V_0 t - \frac{a_0 t^2}{2}$$



where  $V$  = velocity

$x$  = distance or displacement.

When the train car comes to rest ( $V = 0$ ) and

$$t = t_0$$

$$x = x_0$$

hence one obtains equation (35) from the velocity time relationship and

$$x_0 = 1/2 V_0 t_0 \quad (39)$$

from the displacement relationship. Thus for the basic step pulse

$$\gamma = 1$$

$$\beta = 1/2.$$

These two parameters were evaluated for both the trapezoidal and the double step pulse shape. For the trapezoidal pulse one obtains

$$\gamma = \frac{2}{1 + \tau_2 - \tau_1} \quad (40)$$

and

$$\beta = \frac{(1 - \tau_2)(3 - \tau_2)^2 + \tau_2(3 - \tau_2^2) - 2}{3(1 - \tau_2)(1 + \tau_2 - \tau_1)}$$

where, from Figure 12(c)

$$\tau_1 = \frac{t_1}{t_0} \leq \tau_2$$

and

$$\tau_2 = \frac{t_2}{t_0}.$$

These results are presented in Figure 13. Note that the stopping distance factor,  $\beta$ , only varies from one-third to two-thirds with most of the pulse domain having a value of  $\beta$  of approximately one-half. The acceleration peaked factor,  $\gamma$ , varies from one for the basic step pulse to two for the entire spectrum of triangular pulses.

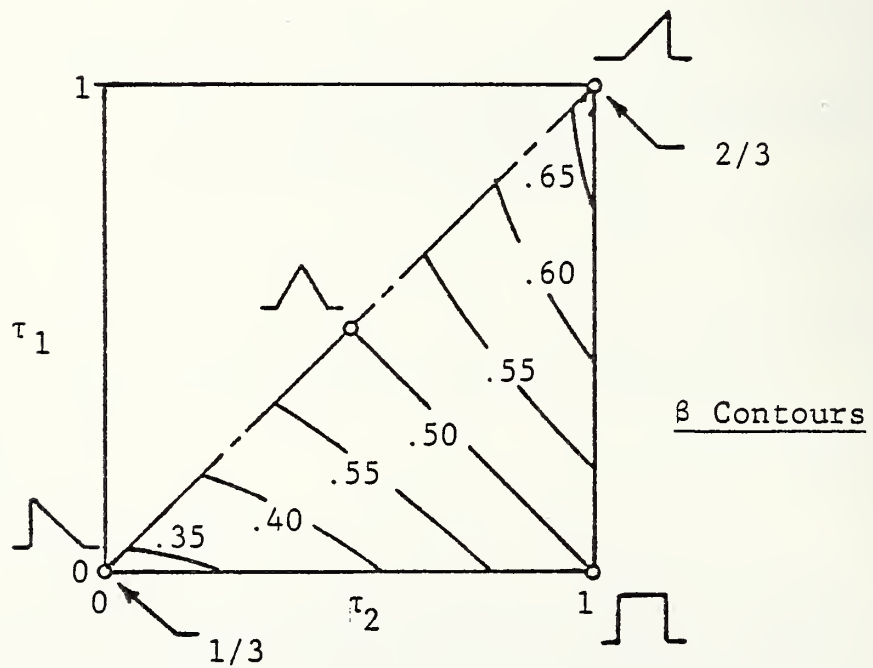
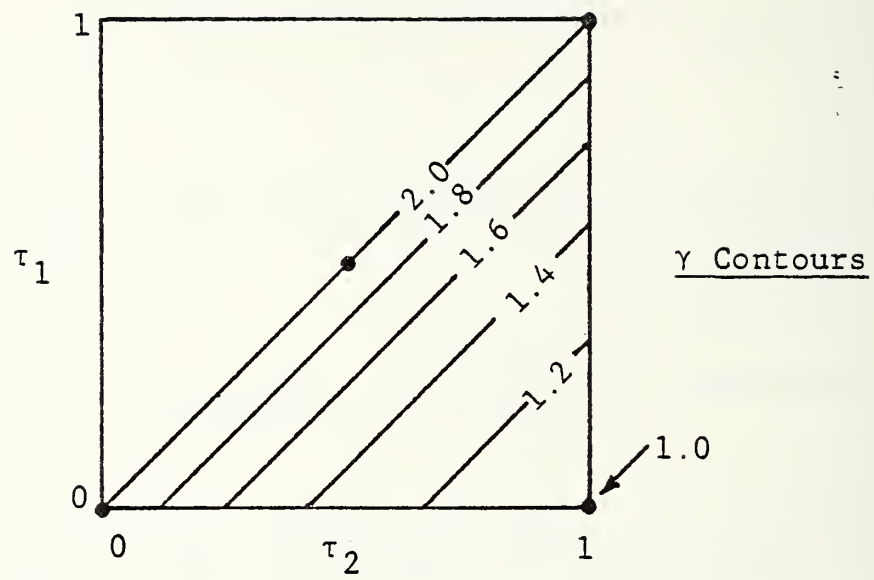


FIGURE 13. CHARACTERISTICS OF TRAPEZOIDAL ACCELERATION PULSE

Similar results were obtained for the double step pulse shape, namely

$$\gamma = \frac{1}{\tau_1 + \delta - \tau_1 \delta} \quad (41)$$

and

$$\beta = \frac{0.5(\delta - \delta \tau_1^2 + \tau_1^2)}{(\tau_1 + \delta - \tau_1 \delta)}$$

where from Figure 12(d)

$$\tau_1 = \frac{t_1}{t_o}$$

and

$$\delta = \frac{a_1}{a_o}^*$$

These results are presented in Figure 14. If one excludes the lower left-hand position of the pulse domain on the basis that any L-shape pulse could be better approximated by a shorter duration basic step pulse then it is clear that the range over which both factors vary is not excessive. This observation suggests that the basic step pulse can be used for analysis purposes in many cases and that adjustment can be made for other pulse shapes by using the above factors in some prescribed manner depending upon the kind of equivalent required. As an example, for energy (or work) equivalence the kinetic energy  $0.5 V_o^2$  would be conserved, that is

$$0.5 V_o^2 = 0.5 \frac{V_o}{t_o} (V_o t_o) = \frac{a_o x_o}{2\beta} = \text{constant}. \quad (42)$$

Thus the proper relationship between the reference and equivalent system requires

$$\left[ \frac{(a_o x_o)}{\beta} \right]_{\text{equiv}} = \left[ \frac{(a_o x_o)}{\beta} \right]_{\text{ref}}. \quad (43)$$

The four motion parameters,  $V_o$ ,  $a_o$ ,  $x_o$  and  $t_o$  are related by two equations (equations (35) and (37) for any given pulse shape). Thus one can conveniently construct a solution diagram for any

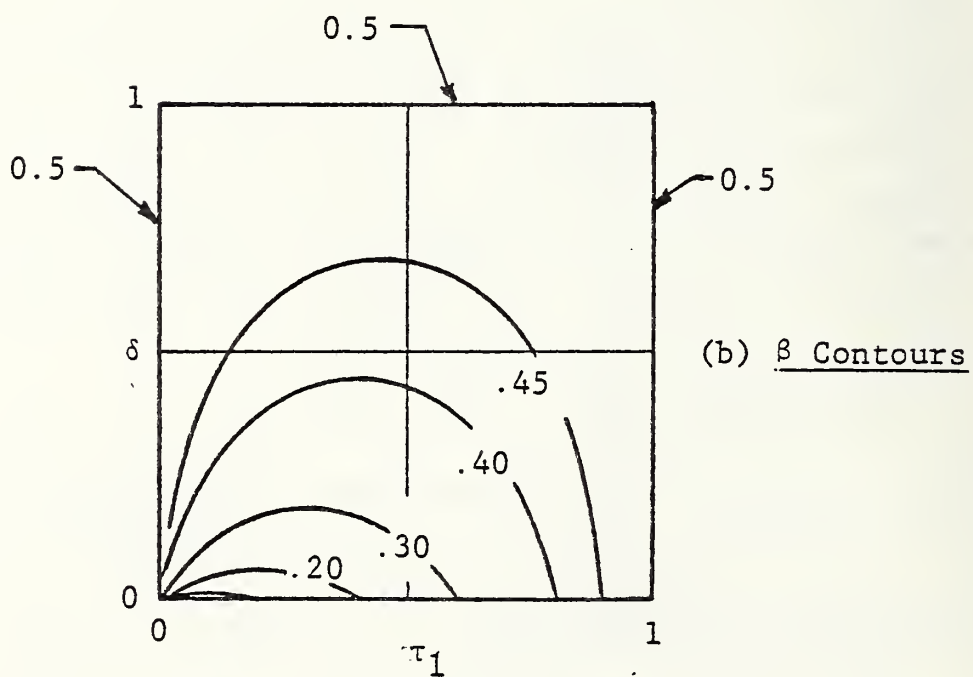
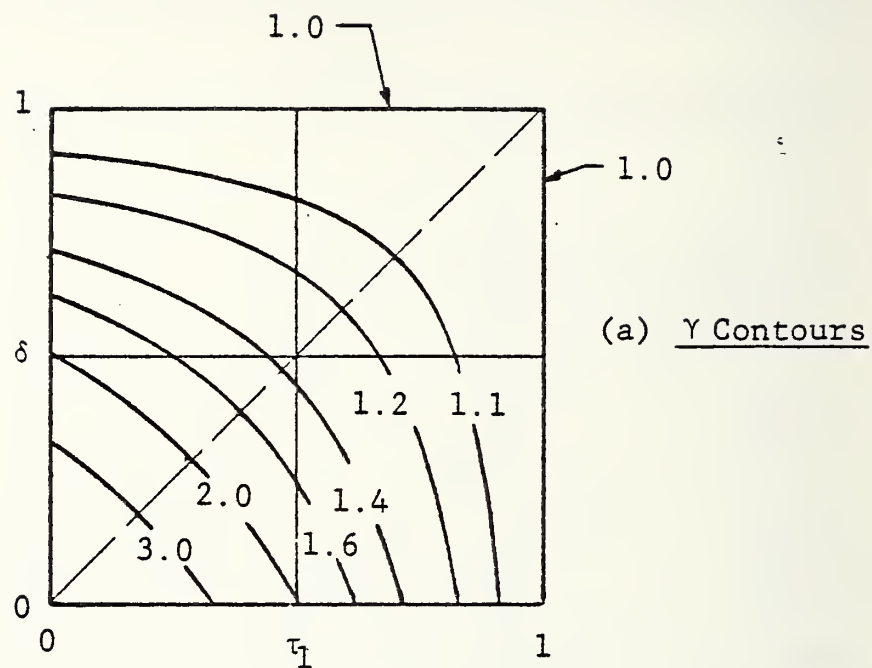


FIGURE 14. PULSE CHARACTERISTICS FOR THE DOUBLE STEP PULSE

pulse shape in which the specification on any two parameters yields the other two. Two such diagrams were constructed and are presented in Figures 15 and 16. The first applies to the step pulse and provides a perspective of the impact domain of general interest to the intracity train crash problem. The second applies to one particular triangular pulse as well as any pulse shape with a stopping distance factor equal to two-thirds.

#### 4.2 "Lumped Mass" Translation Behavior

Perhaps the simplest representation of the motion of a passenger within a compartment of a train which is abruptly decelerated, as in a crash, is that of a lumped mass initially located some distance,  $x^*$ , from an obstacle such as a seatback or bulkhead, fixed to the compartment, and moving with the train. When the crash occurs at zero time ( $t=0$ ) the compartment (i.e., bulkhead) moves in accordance with some prescribed acceleration pulse as previously mentioned. The passenger originally moving at the train velocity,  $V_0$ , continues to move until impact with the bulkhead occurs. The train velocity,  $V_0$ , corresponds to the change in velocity experienced by the car during a crash and may not be equal to the actual velocity of the car. The impact velocity that is the relative velocity between the passenger and the bulkhead is of interest because it is a major parameter in the production of injury mechanisms. It appears reasonable with this simple model to introduce a nominal average force (expressed as a deceleration) as an additional parameter to examine the influence of a variety of possible motion retarding mechanisms, such as seat friction, may have upon the impact velocity.

Representative paths are illustrated in the path diagram of Figure 17. The following analysis is presented in a dimensionless form to facilitate its interpretation and to expand its usefulness. The time scale has been made dimensionless by normalizing time by the crash duration,  $t_0$ . The position scale has been made dimensionless by dividing the absolute position  $x$  by the stopping distance,  $x_0$ , thus



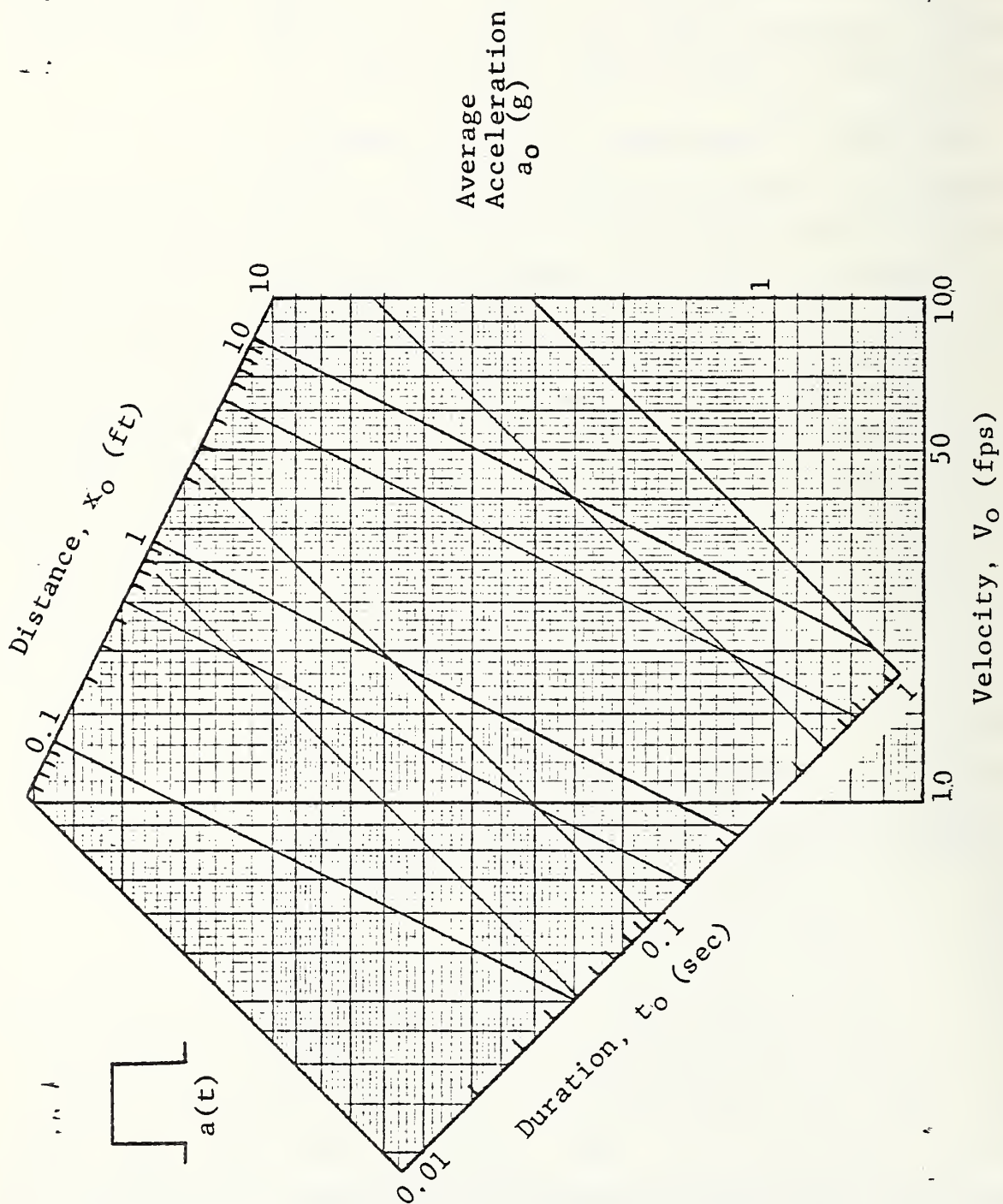


FIGURE 15. SOLUTION DIAGRAM FOR STEP PULSE

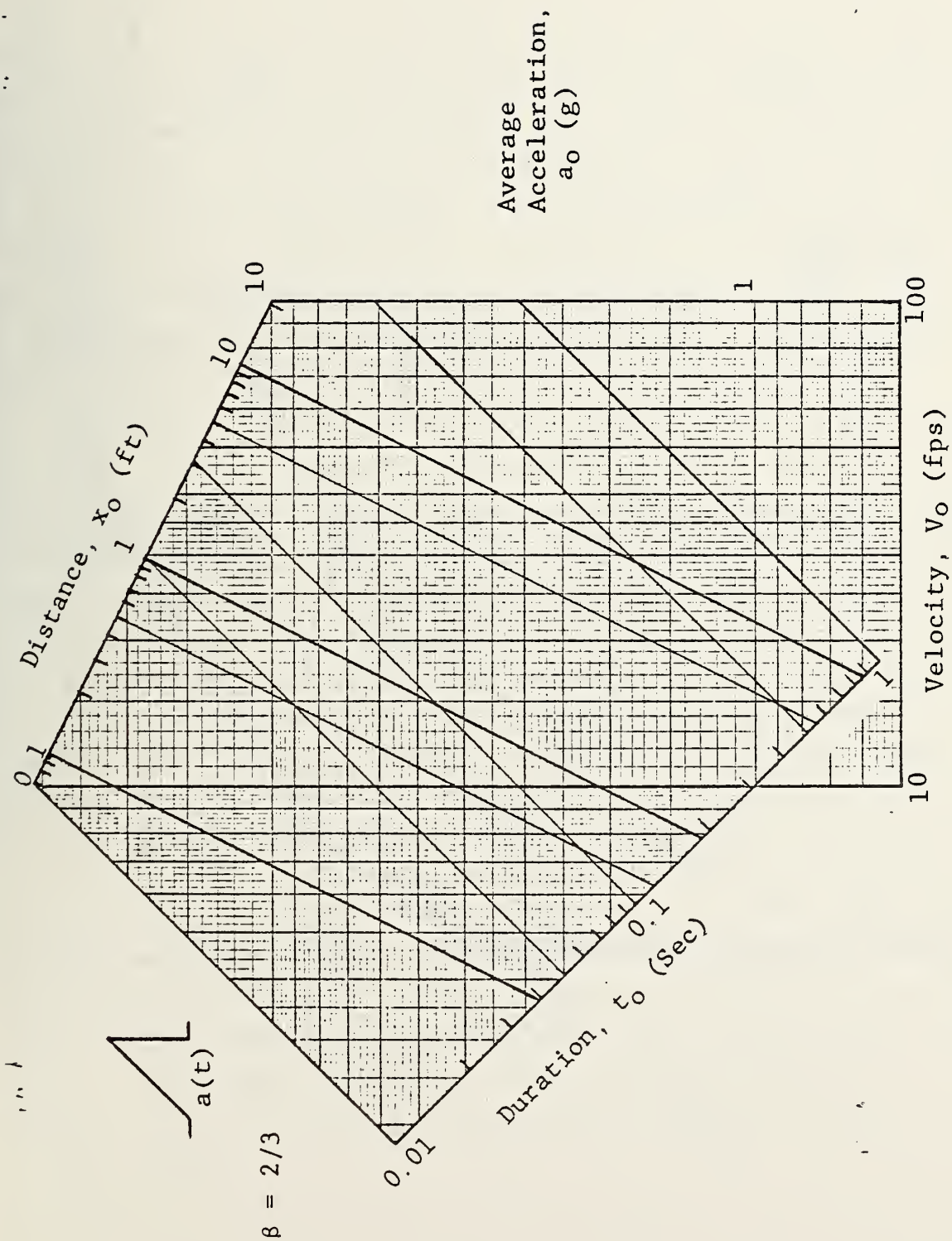


FIGURE 16. SOLUTION DIAGRAM FOR TRIANGULAR PULSE

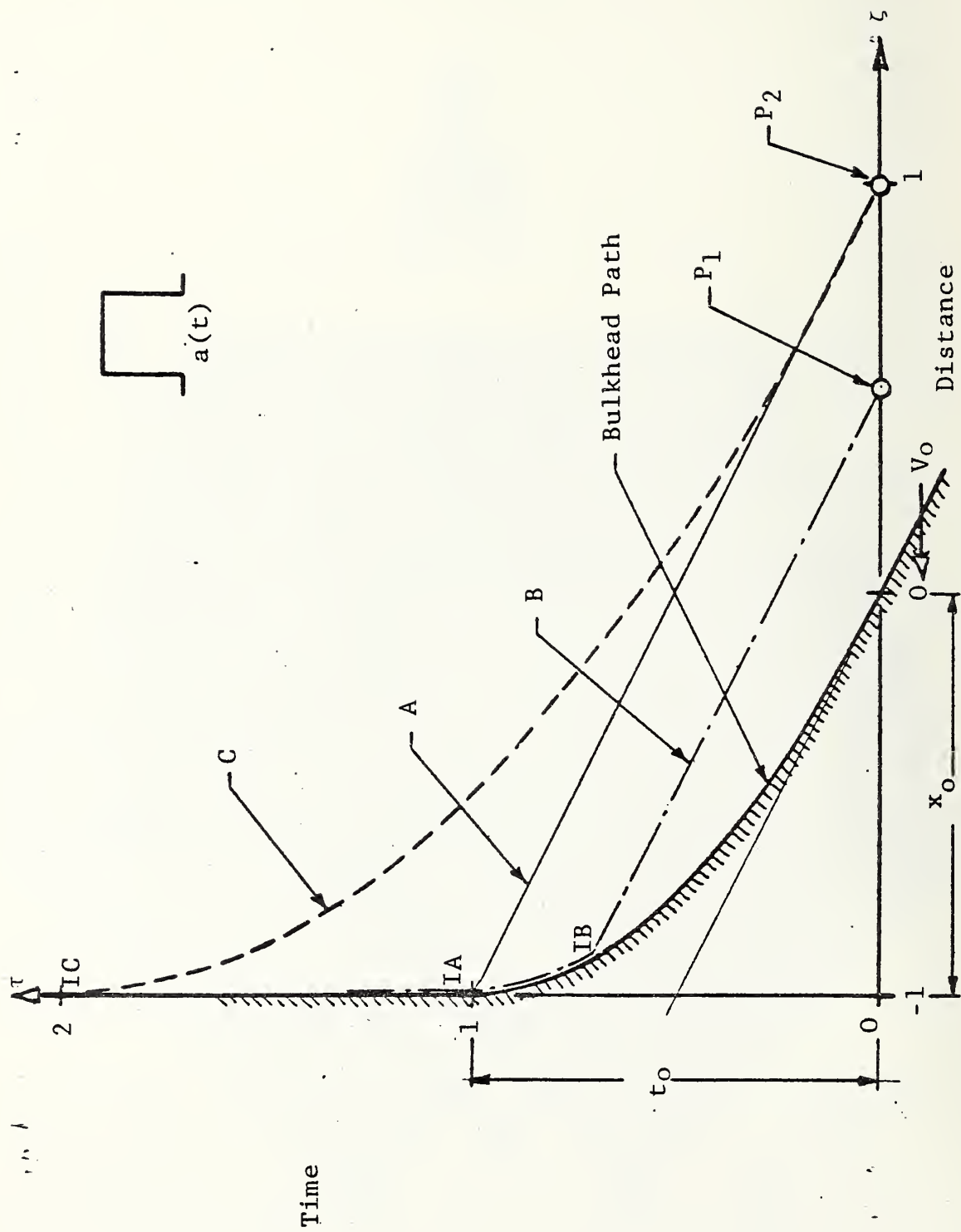


FIGURE 17. PATH DIAGRAM FOR PASSENGER/BULKHEAD INTERACTION

$$\tau = \frac{t}{t_0}$$

and

$$\zeta = \frac{x}{x_0}$$

(44)

Zero time is defined as the start of the crash period. Zero position is defined as the location of the train bulkhead at zero time and positive positions increase in a direction away from the bulkhead. The bulkhead path illustrated in Figure 17 corresponds to a step acceleration pulse. The bulkhead motion vanishes, by definition at  $\zeta = 1$  and  $\tau = 1$ . Thereafter it is motionless. At zero time the bulkhead and all of the passengers ( $P_1$  and  $P_2$ ) move at a velocity  $V_0$  in the negative  $\zeta$  direction. The passenger is initially located at  $\zeta = \zeta^*$  where

$$\zeta^* = \frac{x^*}{x_0} \quad (45)$$

The passenger path in Figure 17 labeled B corresponds to a passenger originally at  $P_1$  who moves unretarded with the velocity  $V_0$  and impact occurs with the bulkhead at point IB. The bulkhead is still in motion hence, the impact velocity  $V_i$  is somewhat less than  $V_0$ . The passenger path labeled A corresponds to a passenger originally at  $P_2$  who also moves in an unretarded fashion. Impact with the bulkhead occurs at point IA at which time the bulkhead velocity is zero. Therefore, the impact velocity is  $V_0$ . Finally, the passenger path labeled C corresponds to the passenger originally located at  $P_2$ , however in this case the passenger motion is retarded such that impact with the bulkhead occurs at point IC. The bulkhead velocity is zero at this time, however, the velocity of passenger is greatly reduced such that the impact velocity is considerably less than  $V_0$ . Recall that the injury level may be proportional to  $V_i^{2.5}$ . The impact velocity,  $V_i$ , is normalized by the initial velocity,  $V_0$ , to provide a dimensionless impact variable, viz.

$$\phi_i = V_i/V_0 \quad (46)$$



and the retarding acceleration  $a'$  is normalized by the average acceleration of the train car,  $a_0$ , to form a dimensionless retarding force, viz.

$$\alpha = \frac{a'}{a_0}. \quad (47)$$

Two impact domains exist; one corresponds to impacts which occur while the bulkhead is still in motion and the other corresponds to impacts which occur after the bulkhead motion stops. This latter domain has been defined as the far field domain. The impact velocity in this domain is

$$\phi_i = \sqrt{1 - 2\alpha\beta(\zeta^* + 1)} \quad (48)$$

and applies to any pulse shape. The parameter  $\beta$  is the stopping distance factor defined in the previous section. The far field results for the step pulse case are presented in Figure 18. Recall that  $\zeta^*$  is the (normalized) location of the passenger at the time of the crash. For this pulse shape  $\beta = 0.5$ , therefore equation (48) becomes

$$\phi_i = \sqrt{1 - \alpha(\zeta^* + 1)}. \quad (49)$$

The results of Figure 18 are generally applicable to other pulse shapes if the value of  $\alpha$  used in this figure is viewed as an equivalent  $\alpha$  equal to the product  $2\alpha\beta$  for other pulse shapes. The region of applicability of this far field relationship depends upon the shape of the acceleration pulse. Thus it will be desirable to examine some near field results.

The near field results for the step pulse are shown in Figure 19. The near field region for this pulse shape is bounded by the curves  $\alpha = 0$  and  $\alpha = \alpha_c$ . The latter is given as

$$\alpha_c = 1 - \zeta^* \quad (50)$$

along which

$$\phi_i = \zeta^*.$$



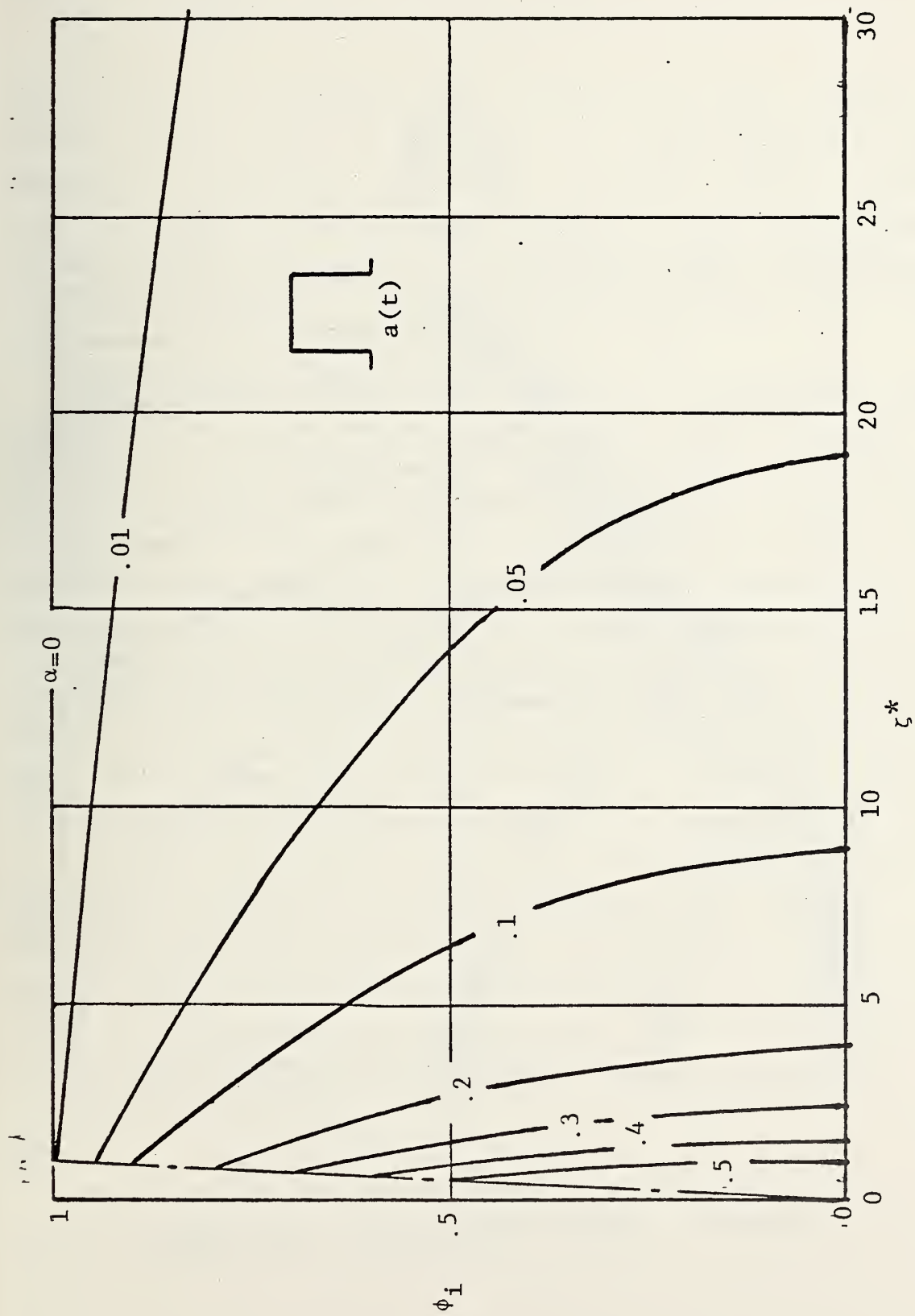


FIGURE 18. IMPACT ENVIRONMENT - LARGE  $\zeta^*$

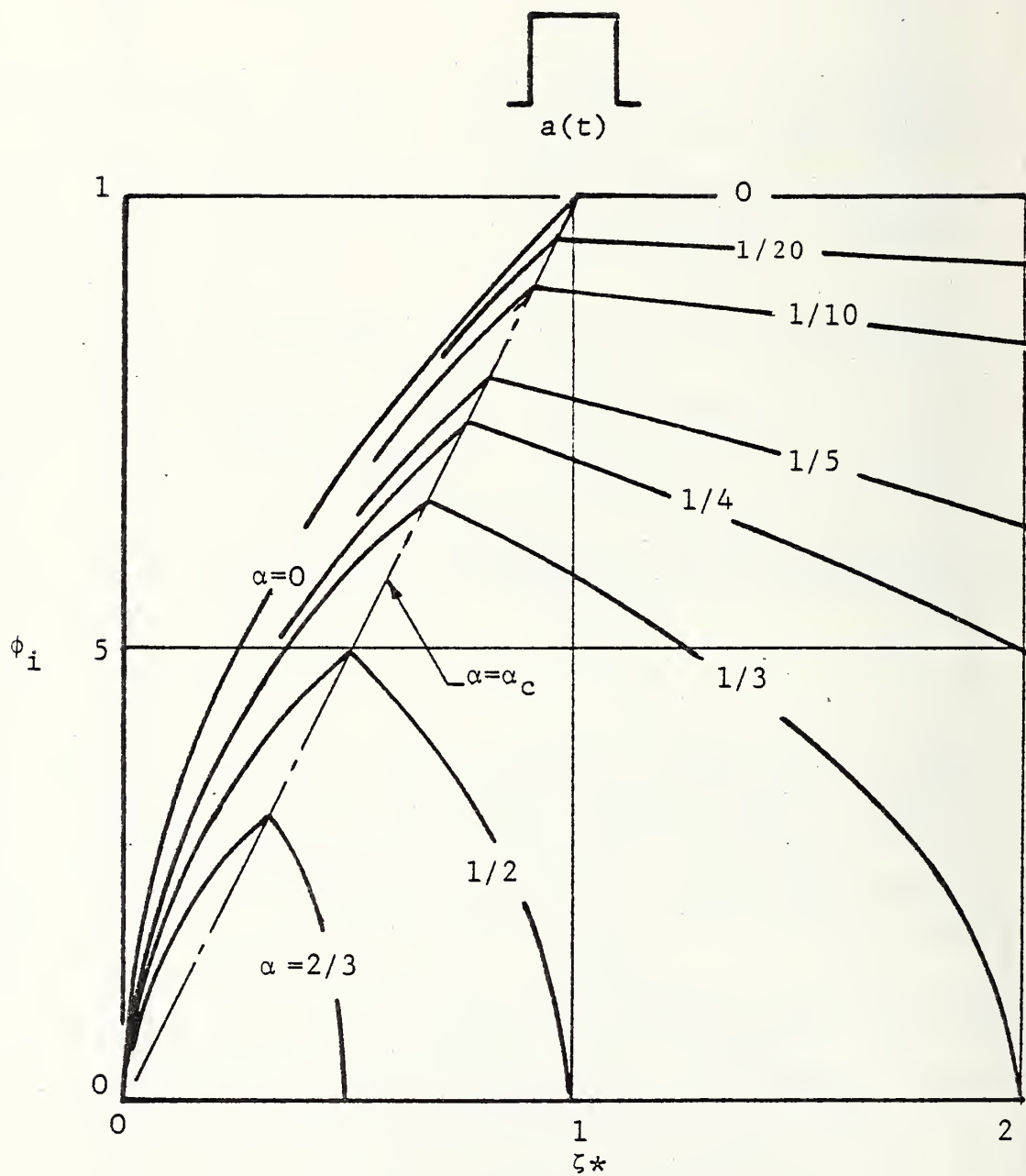


FIGURE 19. IMPACT ENVIRONMENT - STEP PULSE

Along the former

$$\phi_i = \sqrt{\zeta^*}. \quad (51)$$

These results illustrate that in the far field, reductions in impact velocity can be achieved by a combination of increased separation distance and increased retardant force. In the near field the impact velocity can be reduced by reducing the separation distance and/or increasing the retardant force. It appears significant to identify the impact zone which applies, or its approximate equivalence, the stopping distance,  $x_0$ .

The results become more difficult to interpret when one examines other pulse shapes. One of the right triangular pulses was used in a similar analysis. These results are presented in Figure 20. The far field results are unchanged, as was indicated above, however, the domain of application has changed somewhat. The role of the retarding force becomes more obscure. In effect, what can happen is that an increase in the retarding force results in a delay in the impact time and due to larger late time deceleration associated with this particular pulse shape the slightly delayed impact is more severe than an earlier impact would have been. This is seen more clearly in Figure 21 where the influence of  $\alpha$  is presented along lines of constant  $\zeta^*$ , for both pulse shapes.

Other pulse shapes (within the trapezoidal category) were examined and similar apparent anomalies are present. Their exploration at this time will not be particularly productive. It may be useful to define the boundary between the near field and far field for the general trapezoidal pulse shape, that is the  $\alpha = \alpha_c$  path. This is given, in general as

$$\begin{aligned} \alpha_c &= 2 - 2\beta(1 + \zeta^*) \\ \text{and} \\ \phi_i &= 1 - \alpha_c \end{aligned} \quad (52)$$

along this path.

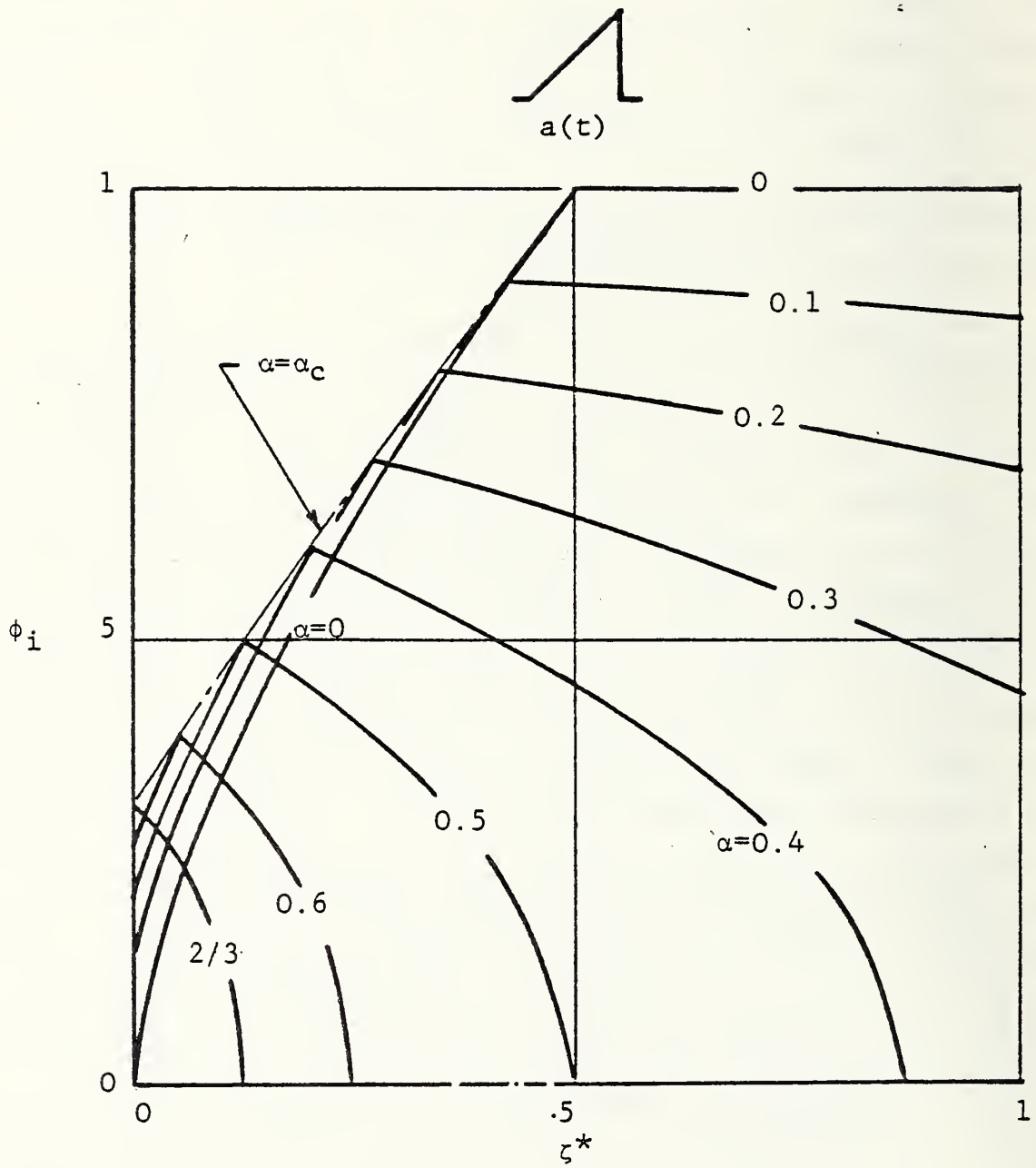
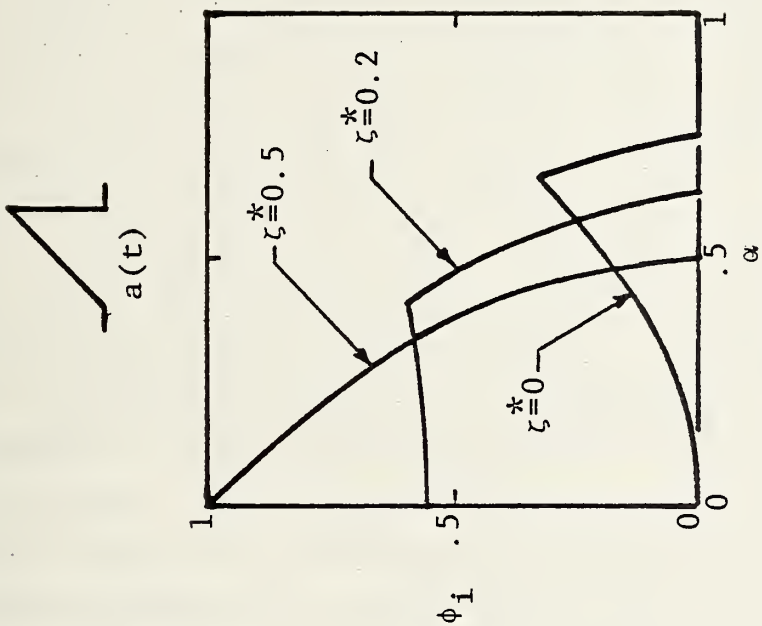
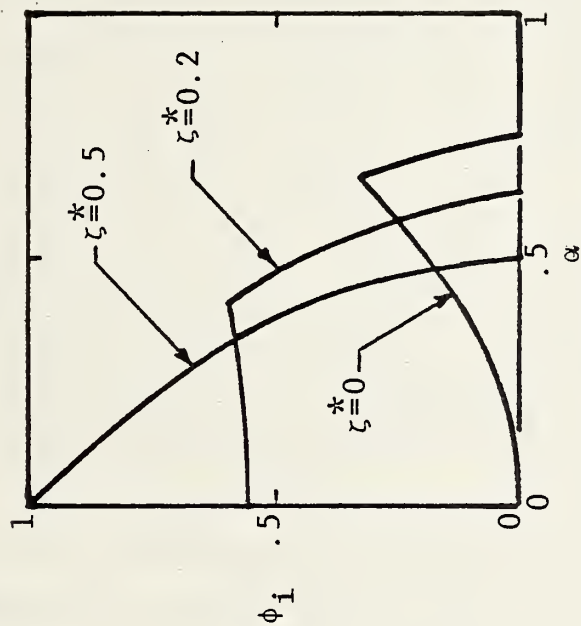


FIGURE 20. IMPACT ENVIRONMENT - TRIANGULAR PULSE



(a) Step Pulse



(b) Triangular Pulse

FIGURE 21. INFLUENCE OF  $\alpha$  ON IMPACT VELOCITY



#### 4.3 Passenger Characteristics - Anthropometric Data

The tumbling motion that a human being experiences from a given motion stimulus will depend, in part, upon various anthropometric parameters. Furthermore, the values of these parameters will generally be statistical in nature, although some parameters may vary in a systematic manner with age, sex, and other classification factors. For the purpose of this study a number of parameter values and their variations must be established or estimated. Damon, et al.,<sup>4</sup> was the source of most anthropometric data used in the subsequent analysis. In some instances simple approximate scaling relations were established to encompass parameter values in a systematic manner for certain population classifications.

The general type of anthropometric data that is required to evaluate tumbling motions of passengers are whole body or body component weight, one or more characteristic lengths such as height and location of the body c.g. relative to some reference point, and the body or body component moment of inertia about some specific axis passing through the appropriate c.g. These data will generally be presented as mean or average values and may be supplemented with some indication of their variance such as their standard deviations. Unfortunately, anthropometric data are quite limited and are frequently biased by the use of rather similar and limited population subgroups, such as young-white-adult-males. Nevertheless, reasonable average values can be estimated together with somewhat less reliable variance estimates. These anthropometric uncertainties must be combined with other types of uncertainties and will result in a statistical smearing of the final results.

---

<sup>4</sup>Damon, A., et al., "The Human Body in Equipment Design", Harvard University Press, 1966.

To demonstrate the general nature of the anthropometric data and to establish scaling relationships for use in the analysis of the motion characteristics of the standing passenger height/weight data are presented in Figure 22. The average adult male weighs 165 lb and is 5.77 ft (5 ft 9.25 inches) tall. Height distribution data suggest limiting values which can be interpreted as "tall" and "short" category classifications. These values are illustrated in Figure 22 and are listed in Table 2, and represent approximately 95 percent of the male adult group. Similarly, but from a smaller data base, the weight variance data permit an estimate of corresponding limiting values for the "thin" and "fat" category classification. These values are also illustrated in Figure 22 and listed in Table 2. The weight variance is referred to herein as a "shape" parameter. Thus eight shape-height categories can be established in addition to the average adult male (now identified by the avg-avg notation). These categories bound the adult male domain as illustrated in Figure 22 and include more than 95 percent of the corresponding population.

TABLE 2.-HEIGHT/WEIGHT CHARACTERISTICS

Category (shape-height)	Weight (lb)	Height (ft)	Moment of Inertia** (lb sec <sup>2</sup> ft)	$\lambda$	$\sigma$
Avg-Avg *	165	5.77	8.58	1.00	1.00
Avg-Short *	124	5.25	5.88	0.91	1.00
Avg-Tall	210	6.25	11.81	1.08	1.00
Thin-Short	90	5.25	5.00	0.91	0.85
Thin-Avg	119	5.77	7.29	1.00	0.85
Thin-Tall	152	6.25	10.04	1.08	0.85
Fat-Short	165	5.25	6.76	0.91	1.15
Fat-Avg	218	5.77	9.87	1.00	1.15
Fat-Tall	278	6.25	13.58	1.08	1.15
10-yr-old child	78	4.50	3.17	0.78	1.00
6-yr-old child	40	3.60	1.30	0.62	1.00

\* Adult female is similar to avg-short.

\*\* Standing

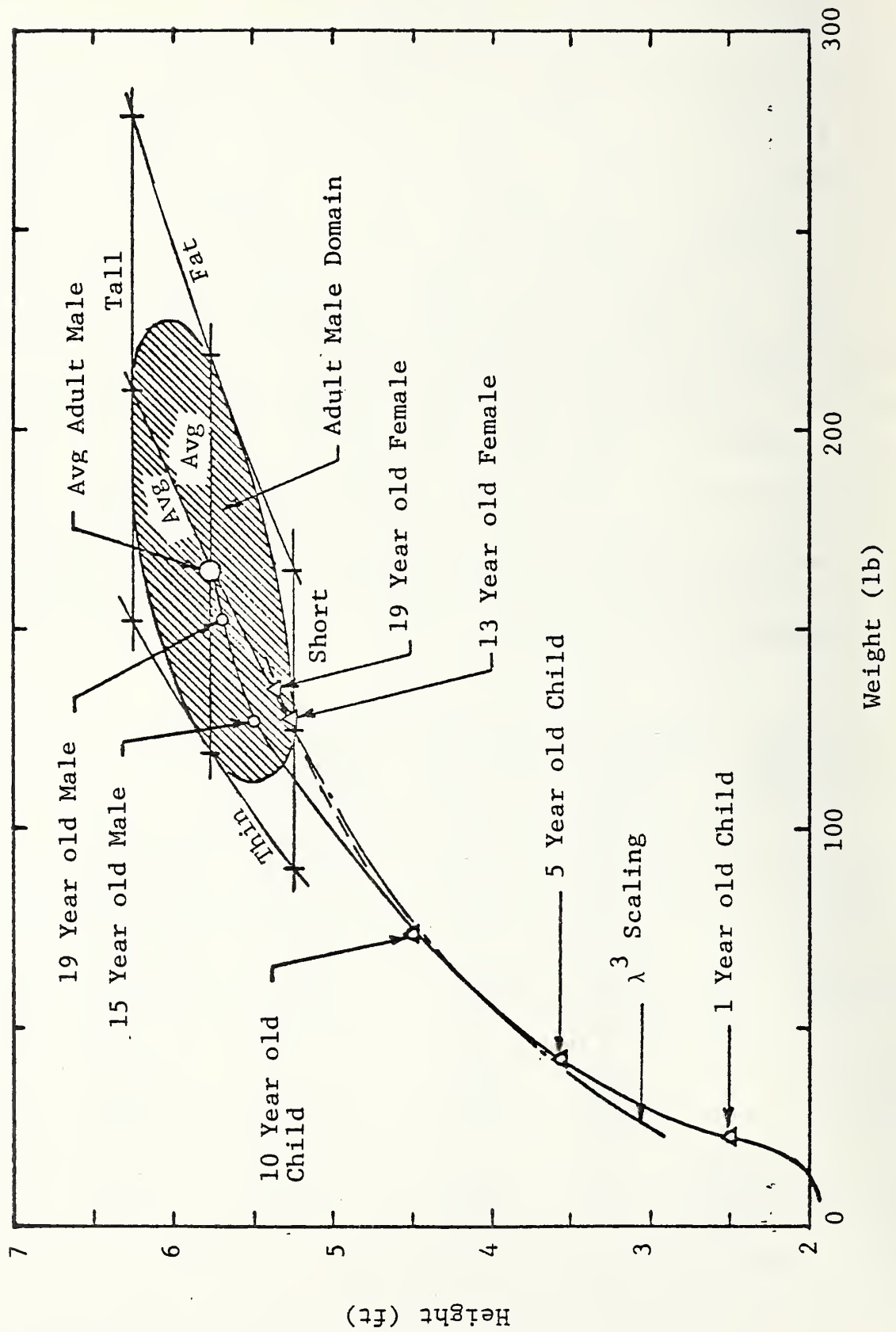


FIGURE 22. HEIGHT/WEIGHT DATA SUMMARY

Height weight data for both males and females of various age groups from birth to age 19 years is shown in summary fashion in Figure 22. These data are consistent with the average adult male data and suggest that the average adult female category may be defined by values corresponding approximately to the avg-short category for adult males. The 5- and 10-year-old child categories were also selected for subsequent analysis and the corresponding height/weight values are illustrated in Figure 22 and represented in Table 2.

Additional body component size, c.g. locations, and moment of inertia data will be needed for the subsequent motion analyses and are generally not available for all of the categories listed in Table 2. Thus several simple scaling laws were developed by assuming that the average body density and internal density distributions were similar to the body shape. Two parameters were then selected to represent the category subgroups. These are the height scale factor  $\lambda$  and the shape scale factor  $\sigma$ . They are defined as

$$\lambda = \frac{H}{\bar{H}}$$

and

(53)

$$\sigma = \frac{w}{\bar{w}}$$

where

$H$  = height

$\bar{H}$  = height of average male adult

$w$  = width

$\bar{w}$  = width of average male adult.

The corresponding values are presented in Table 2. The values of  $\sigma$  were estimated from height-weight data and the appropriate scaling law. The scaling laws are



$$\frac{W}{\bar{W}} = \lambda^3 \sigma^2$$

$$\frac{I}{\bar{I}} = \lambda^4 \sigma$$

$$\frac{L}{\bar{L}} = \lambda$$

$$\frac{S}{\bar{S}} = \sigma \lambda$$

(54)

where

$W$  = body weight

$\bar{W}$  = body weight for average male adult

$I$  = moment of inertia

$\bar{I}$  = moment of inertia for average male adult

$L$  = c.g. location

$\bar{L}$  = c.g. location for average male adult

$S$  = width

$\bar{S}$  = width for average male adult

The  $\lambda^3$  height-weight scaling law is plotted in Figure 22 and illustrates its appropriation for the "average" values from age 5 to adult age. These scaling laws were used to generate, as needed, anthropometric values. Moment of inertia estimates for the standing passenger are listed in Table 2. The size and weight data suggest that the corresponding variances are relatively constant for both males and females and independent of age (above a few years of age).

Anthropometric data are also needed for different body positions, body movements, and body components. These more specific data are rather limited. Estimates were made and are listed in Table 3 for the seated passenger configurations. Variances (standard deviation) of the c.g. location were from 5 to 10 percent, whereas variances of the moment of inertia were 15 to 20 percent. The c.g. location corresponds to the distance between the body component c.g. and the axis of rotation assumed in the



corresponding analysis. The value of the moment of inertia corresponds to rotation about the axis through the body components or components of interest. The characteristic dimension corresponds to the distance between the potential impact location and the axis of rotation used in the corresponding analysis. No specific value is needed for the backward facing passenger since the injury mode is that of whiplash.

TABLE 3.-ANTHROPOMETRIC DATA FOR SEATED PASSENGERS

Body Component	Seated Passenger Facing		
	Forward	Backward	Sideward
	Torso	Head	Whole Body
Body Component Weight (lb)	87.0	10.00	165.00
Moment of Inertia (lb-ft <sup>2</sup> )	27.4	0.27	166.00
Center of Gravity Location (ft)	1.0	0.30	0.27
Characteristic Dimension (ft)	2.5		2.50

#### 4.4 Standing Passenger

The response of a standing passenger to the sudden change in motion of the floor will depend upon many factors, such as the nature and intensity of the change in motion of the floor, the size and orientation of the passenger, and the passenger's alertness and ability to respond to the excitation. If the passenger tumbles or falls the passenger may strike the floor, nearby walls or partitions, or other nearby interior car components. Since any realistic analysis will, of necessity, exclude many of the above factors, the results will have to be interpreted as a nominal, or perhaps upper limit experience of the subject event. It is clear that the passenger's use of his or her arms or hands may mitigate the consequences of the event and thus statistically the consequences of the event should be reduced.

A tumbling man (block) model<sup>5</sup> was selected for the analysis of the standing passenger. Although this is a simple representation of the passenger the use of additional linked elements does not a priori improve the accuracy of the results. Additional, usually unknown or poorly defined parameters are required to properly couple the linked elements such as the head, upper torso, lower torso, arms and legs together. The analysis of three- and seven-element models exposed to explosion effects<sup>5</sup> yielded essentially the same results as did the simple block model.

A series of tumbling block analyses were conducted for the average female subject to several constant deceleration floor environments and velocity changes. One result is illustrated in Figure 23(a). In the absence of any nearby barrier or obstacle the standing passenger rotates (head first) in the direction of motion and a head impact occurs. In the example shown the train car stops in 0.4 sec over a distance of approximately 9 ft. The head impact occurs at 0.66 sec and the impact velocity is approximately 21.8 fps. If a barrier, such as a wall, was located nearby then the passenger head would have impacted at the times and velocities indicated in Figure 23(b) for the barrier distances indicated. If the barrier were located at 21.5 ft for this example, the top of the passenger's head would have impacted the barrier at a velocity of 40.0 fps simultaneously with a floor impact of 21.8 fps. The latter impact involves the side (or front, etc.) of the head. Such multiple impact situations are unlikely and will not be considered in the analyses.

An examination of the motion of the standing passenger revealed the following common behavior. Foot contact with the floor was lost rather early in the process such that the horizontal velocity of the c.g. ( $\dot{x}_{c.g.}$ ) decreased slightly relative to the

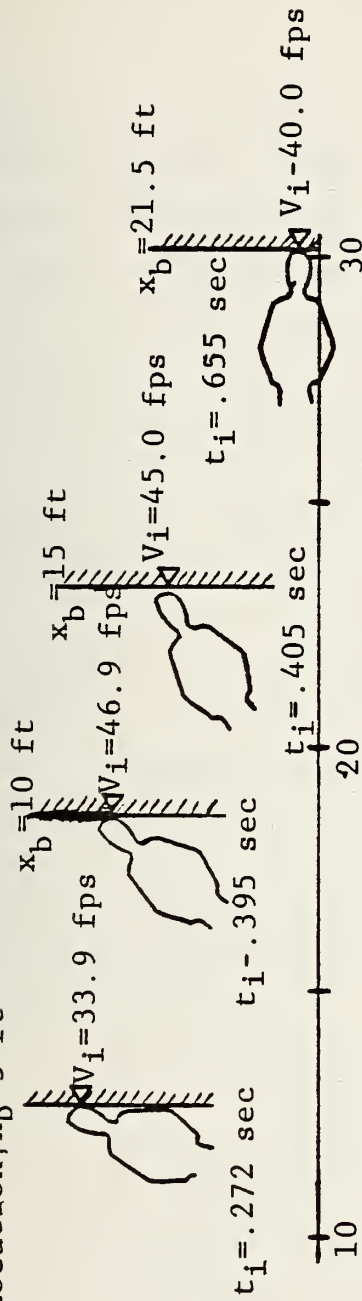
---

<sup>5</sup>Longinow, A., et al, "Debris Motion and Injury Relationships in All Hazard Environments", IIT Research Institute, Final Report J6334, July 1976.

Barrier Location,  $x_b = 5$  ft

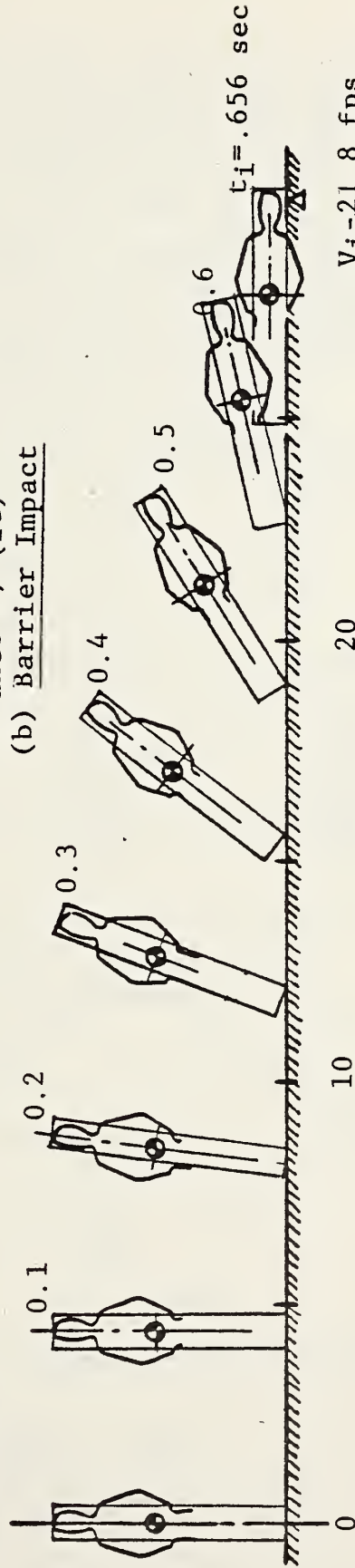
$V_o = 44$  fps

$a_o = 3.5$  g



Time,  $t = 0$  sec

Distance  $x$ , (ft)  
(b) Barrier Impact



Distance  $x$ , (ft)

(a) Floor Impact

$V_i = 21.8$  fps

FIGURE 23. TUMBLING PASSENGER TRAJECTORIES

initial train velocity (i.e., the original velocity of the passenger) and then remained constant at a value of approximately 2 fps less than the initial train velocity. The horizontal velocity of the right side of the head ( $\dot{x}_3$ ) relative to the initial train velocity increased initially, reaching a maximum of 3.6 fps at 0.3 sec and decreasing to a velocity approximately 4 fps less than the initial velocity at 0.66 sec when floor impact occurred. This common behavior is illustrated in Figure 24 together with a list of cases examined. In each of these cases, impact with the floor occurred at 0.66 sec with an impact velocity of approximately 22 fps.

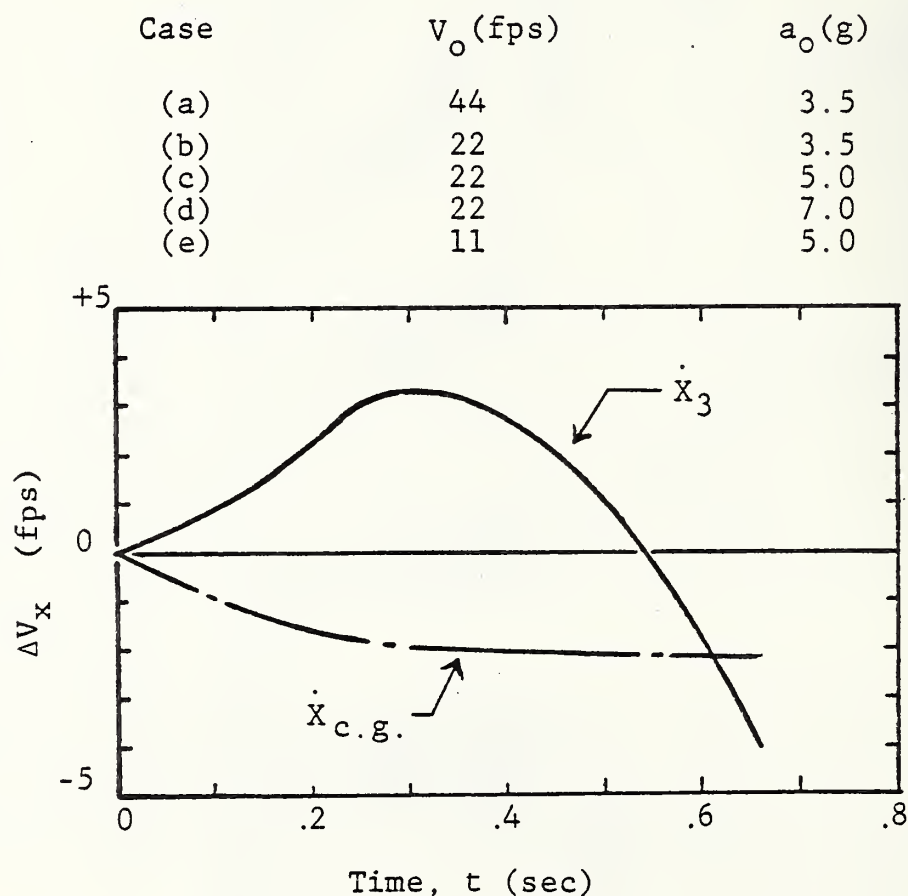


FIGURE 24. VELOCITY PERTURBATION - TUMBLING PASSENGER



For the far field cases where the impact on a barrier occurs after the barrier stops, the time can be approximated by the ratio of the barrier distance,  $x_b$ , to the initial train velocity,  $V_0$ , and the impact velocity would then be equal to the initial train velocity plus the time dependent increment. This formulation is illustrated in Figure 25 for the five cases examined. The curves demonstrate the relative commonalty of the behavior over a range of velocity changes and decelerations of interest.

Additional cases using the anthropometric categories of interest showed that the motion behavior is quite insensitive to the anthropometric categories. Thus a simple impact velocity formulation can be generated to represent all population categories, all deceleration levels and all train speeds of interest. A comparison of the velocity increment variations for the anthropometric categories is illustrated in Figure 26. Table 4 presents the floor impact velocities for these population categories and demonstrates the general insensitivity of this injury producing parameter to the anthropometric variances expected in intracity trains.

TABLE 4.-FLOOR IMPACT VELOCITY

Population Category*		Impact Velocity (fps)
Female	Avg	21.8
Male	Avg	23.1
Male	Tall	24.1
Male	Short	22.0 (23.1)
Male	Thin	23.2
Male	Fat	23.0
Child	10 year old	20.1
Average Adult		(22.4)

\* Adult except as noted.



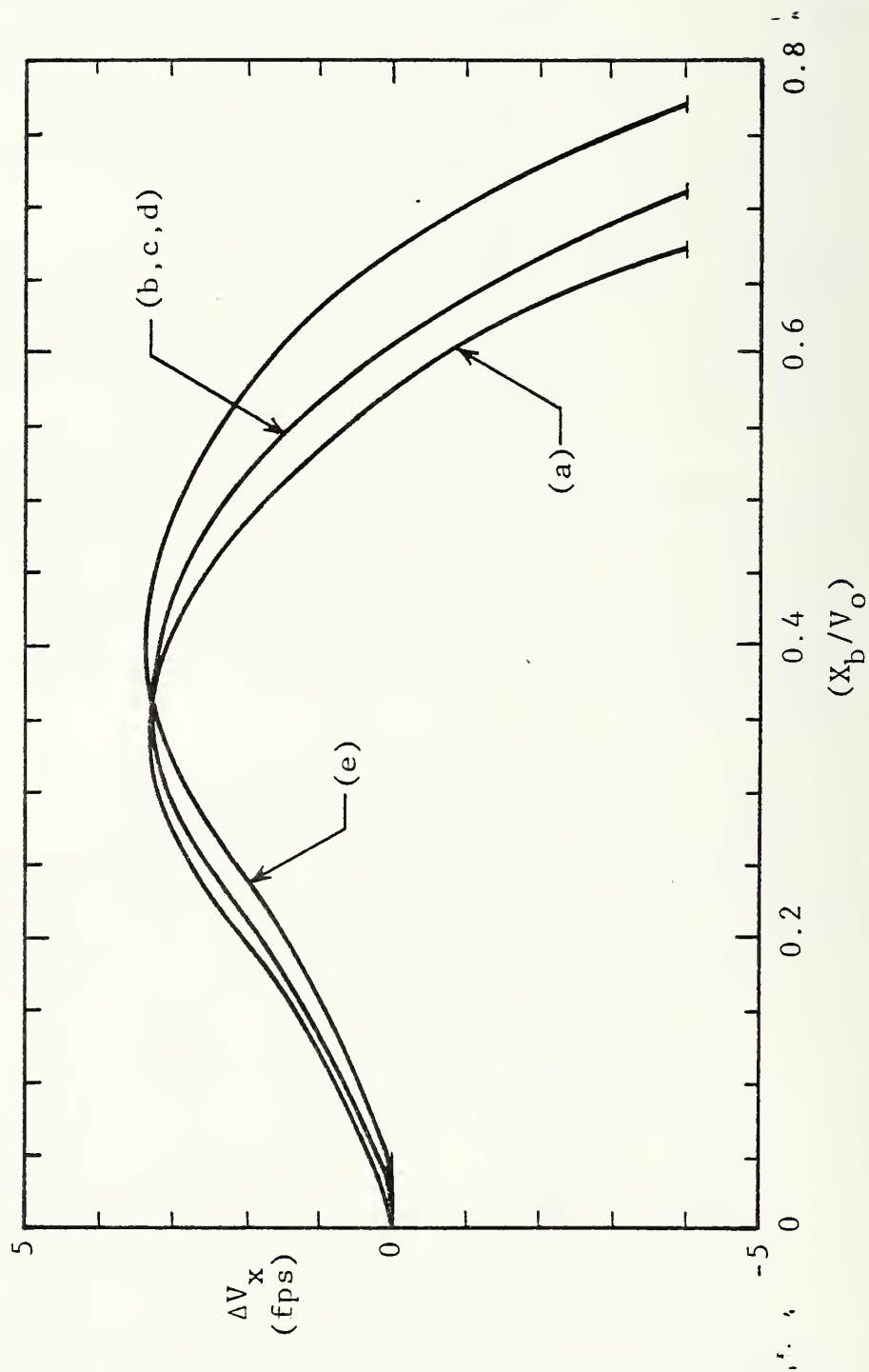


FIGURE 25. VELOCITY INCREMENT VARIATIONS WITH VELOCITY AND ACCELERATION FOR THE ADULT FEMALE STANDING PASSENGER

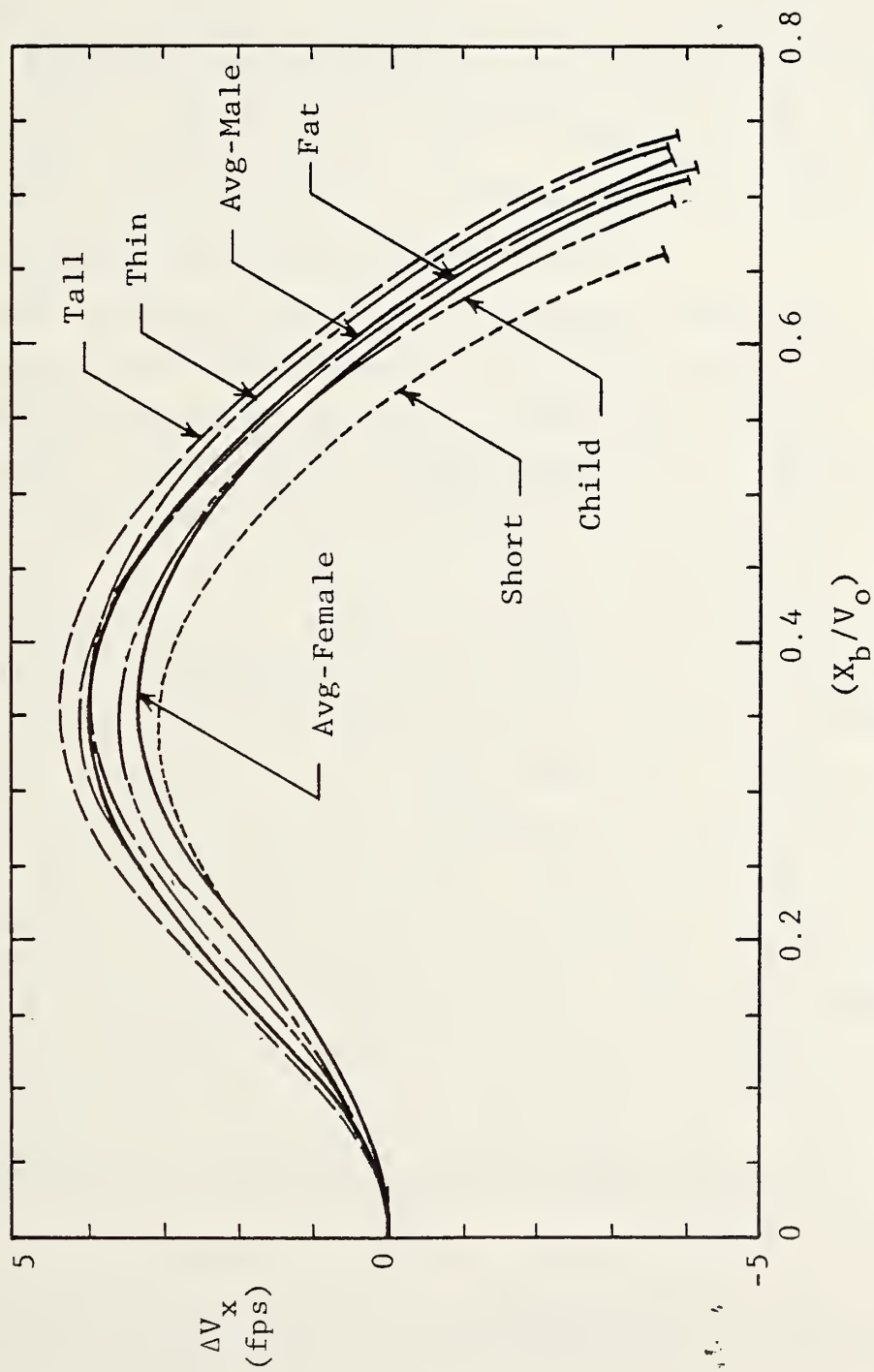


FIGURE 26. VELOCITY INCREMENT VARIATION FOR STANDING PASSENGER

A head impact velocity of 20 fps upon a hard surface, such as a typical train floor, suggests that some injuries could be eliminated or their severity reduced by giving special attention to the design of the floor surface. Figure 27 presents the maximum acceptable stiffness for an elastically behaving floor for various impact velocities using a severity index value of 1000 sec as an arbitrary criteria. The typical impact velocity of 21.8 fps requires a maximum stiffness of approximately 1250 lb/inch.

#### 4.5 Forward Facing Seated Passenger

The term "forward" is not in reference to the direction the train is traveling, but is relative to the direction in which the car velocity decreases. The gross response of the forward facing passenger is a head forward rotation in the passenger facing direction and/or a sliding out of the passenger's seat.

This section treats two limiting models referred to as a hip loft model and a pinned hip model. It is expected that the torso connection to the relatively fixed legs will allow the hips to loft somewhat between the two extremes allowed by the two models. In this manner the actual motion can be bounded. Furthermore, it is expected that the passenger will slide forward before substantial torso rotation occurs. This sliding feature was incorporated into the pinned hip model and the influence of sliding was therefore evaluated in this case. An examination of the variability of the impact conditions on an obstacle (such as a seatback or panel) immediately forward of the passenger provided a rationale for the specification of the impact condition in terms of the variables of interest. This section is concluded by a limited examination of the influence that the train acceleration pulse shape has upon the impact velocity.

4.5.1 Hip Loft Model - The torso of the forward facing seated passenger is represented by a rigid body bar whose lower end (the hip) is constrained to move in the horizontal direction with the motion of the seat (i.e., the train car). The c.g. of the torso is

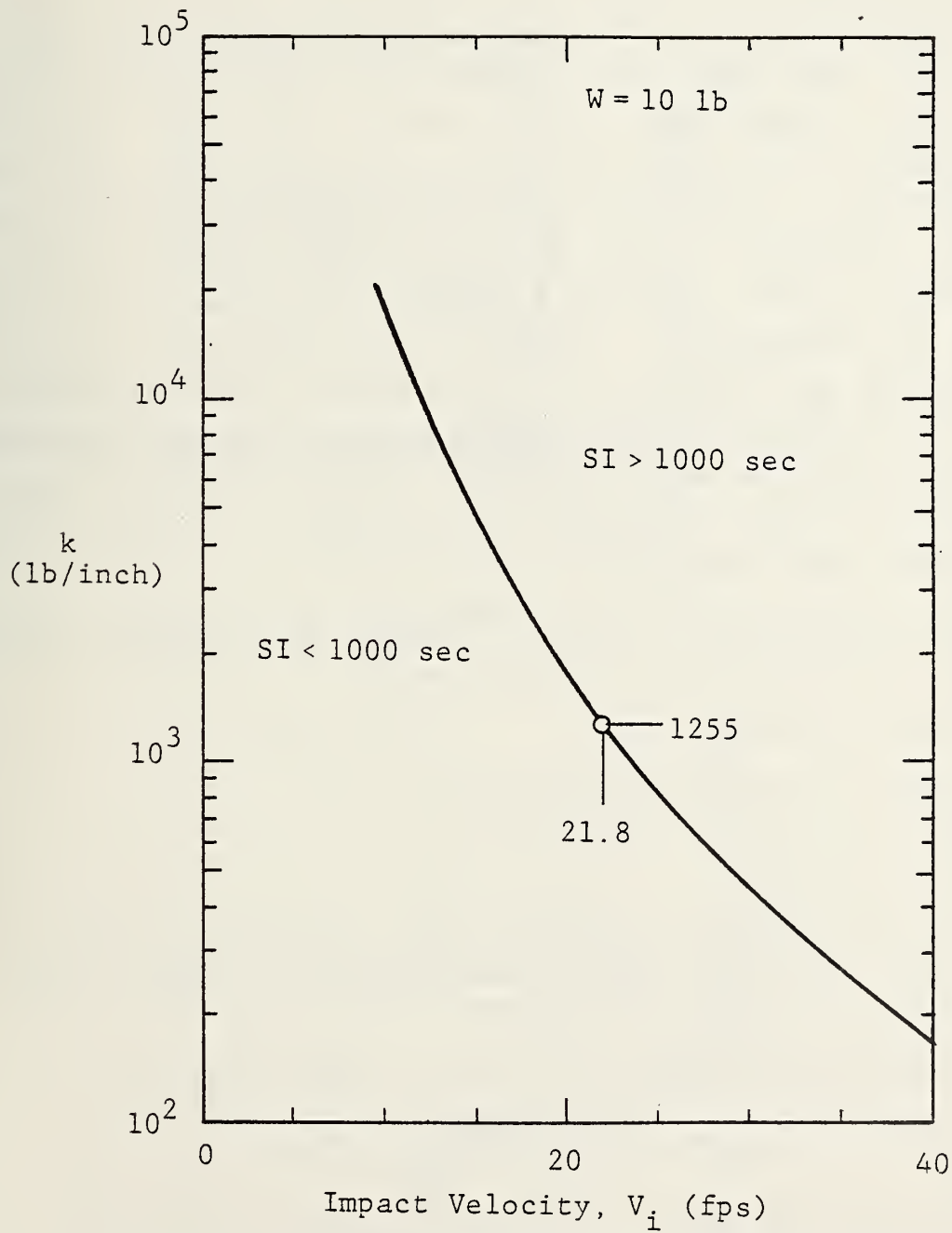


FIGURE 27. CRITICAL STIFFNESS FOR FLOOR SYSTEMS

located a distance  $D$  above the lower end such that when the train car decelerates the body bar rotates forward. This representation is illustrated in Figure 28. The lower end of the body bar is defined as point A, the c.g. as point C and the upper end as point B. The angle of rotation  $\theta$  is positive in the clockwise direction, being zero at the vertical position. This vertical position is the initial position of the body bar. The horizontal displacement of the train car (and hence of point A) is described by the variable  $x$ . The horizontal displacement of the c.g. is described by the variable  $z$ . The displacement of the barrier, which is originally a distance  $S$  from the point ( $x = z = 0$ ) is defined by the variable  $w$ . The location and orientation of the body bar at some preimpact time is shown by the bar A'C'B' while its original position and orientation is shown as ACB in Figure 28(b). The value of  $\theta = \theta_1$  corresponds to the angle of rotation at the time of impact (see Figure 28(a)).

The train motion, which is treated as a constant deceleration motion, is governed by the relationship

$$\begin{aligned}\ddot{x}(t) &= \text{constant} = -a_0 & 0 \leq t \leq t_0 \\ \ddot{x}(t) &= \text{constant} = 0 & t_0 < t \\ x(t_0) &= x_0.\end{aligned}\tag{55}$$

where  $V_0$ ,  $t_0$ ,  $a_0$  and  $x_0$  were defined in Section 4.1 and  $(\dot{\phantom{x}})$  and  $(\ddot{\phantom{x}})$  represent the first and second derivative respectively of the variable with respect to time,  $t$ .

The equations of motion for the c.g., C, are

$$W\ddot{Z} = -F\tag{56}$$

and

$$I\ddot{\theta} = M = FD \cos\theta$$

where

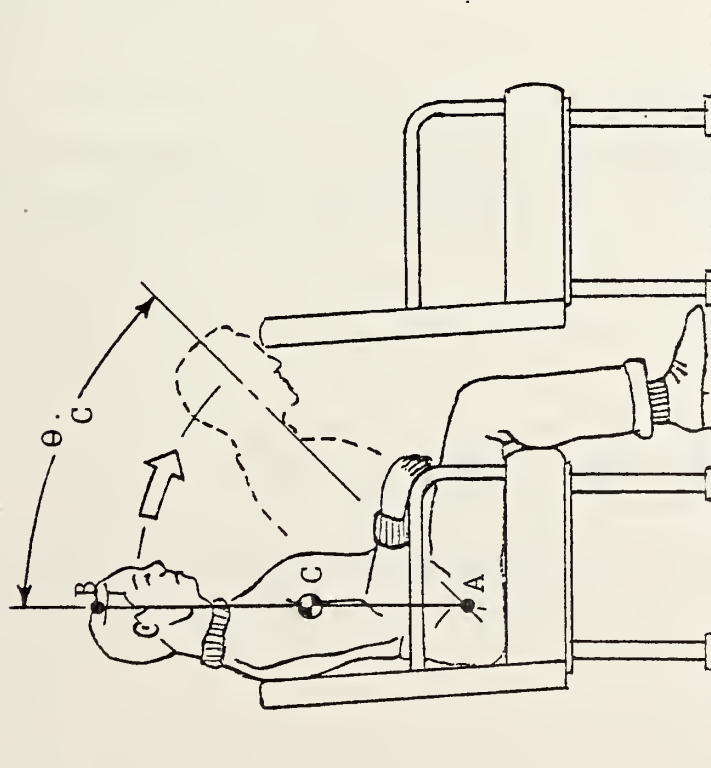
$W$  = weight

$F$  = horizontal reaction force at A

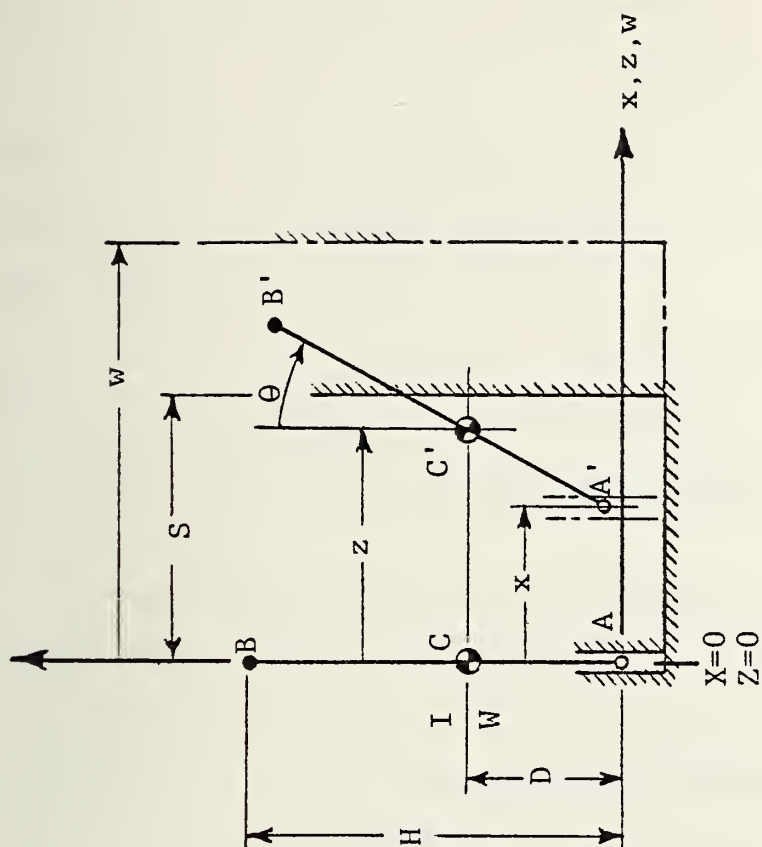
$M$  = moment due to reaction force

$I$  = moment of inertia.





(a) Passenger Configuration



(b) Body Bar Representation

FIGURE 28. HIP LOFT MODEL FOR FORWARD FACING SEATED PASSENGER

Eliminating the force  $F$  yields

$$\ddot{z} = - \frac{I\ddot{\theta}}{WD \cos\theta}, \quad (57)$$

The kinematic constraints of the system require

$$z - x = D \sin\theta \quad (58)$$

which differentiated twice yields

$$\ddot{z} - \ddot{x} = D \cos\theta \ddot{\theta} - D \sin\theta (\dot{\theta})^2. \quad (59)$$

The applicable initial conditions are

$$z(0) = 0$$

$$\dot{z}(0) = V_0$$

$$x(0) = 0$$

$$\theta(0) = 0$$

$$\dot{\theta}(0) = 0.$$

Combining equations (57) and (59) results in

$$\ddot{\theta} \left[ \cos\theta + \frac{\alpha}{\cos\theta} \right] - \sin\theta (\dot{\theta})^2 = - \frac{\ddot{x}}{D} \quad (60)$$

where

$$\alpha = \frac{I}{WD^2}.$$

It will be convenient at this point to eliminate the explicit dependence upon time,  $t$ , by recognizing that the angular velocity,  $\omega$ , is defined as

$$\omega = \dot{\theta} = \frac{d\theta}{dt} \quad (61)$$

so that

$$\ddot{\theta} = \dot{\omega} = \frac{d\omega}{dt} = \frac{d\omega}{d\theta} \cdot \frac{d\theta}{dt} = \omega \frac{d\omega}{d\theta} = 1/2 \frac{d(\omega^2)}{d\theta}. \quad (62)$$

Further simplifications will result if the angular velocity is made dimensionless as

$$\lambda = \frac{\omega D}{V_0} \quad (63)$$

and introducing the following parameter

$$\kappa = \frac{a_o D}{V_o^2}. \quad (64)$$

Equation (60) can be rewritten as

$$\lambda \frac{d\lambda}{d\theta} \left[ \cos\theta + \frac{\alpha}{\cos\theta} \right] - \sin\theta \lambda^2 = \kappa, \quad 0 \leq t \leq t_o \quad (65)$$

and

$$\frac{d\lambda}{d\theta} \left[ \cos\theta + \frac{\alpha}{\cos\theta} \right] - \sin\theta \lambda = 0, \quad t_o \leq t \quad (66)$$

for each of the two constant acceleration phases of the train motion.

A limiting solution corresponding to an instantaneous stopping of the train car ( $\kappa \rightarrow \infty$ ) results in the replacement of equation (65) by a new boundary condition on  $\lambda(o)$ , namely  $\lambda(o) = 1$ , that is the translational momentum is converted instantaneously to rotation momentum as  $D\omega = V_o$ . Thus equation (66) subject to the boundary condition can be integrated to yield

$$\lambda = \sqrt{\frac{1 + \alpha}{\cos^2\theta + \alpha}}. \quad (67)$$

A nominal value of  $\theta_i$  (the angle at which impact occurs) of 45 degrees was selected as being representative of the forward facing seated passenger. Two values of  $\alpha$  were selected as representing the range of interest, these were  $\alpha = 0.126$  and  $\alpha = 0.3$ . The latter value was considered to be the most appropriate. The angular velocity variation with the angle of rotation are shown in Figures 29 and 30 and indicate that for the limiting case as  $\kappa \rightarrow \infty$  the influence of the parameter  $\alpha$  is small.

The time of impact, or the time details of this passenger motion will be of some value, hence it will be convenient to introduce a dimensionless time variable as

$$\tau = \frac{tV_o}{D}, \quad (68)$$

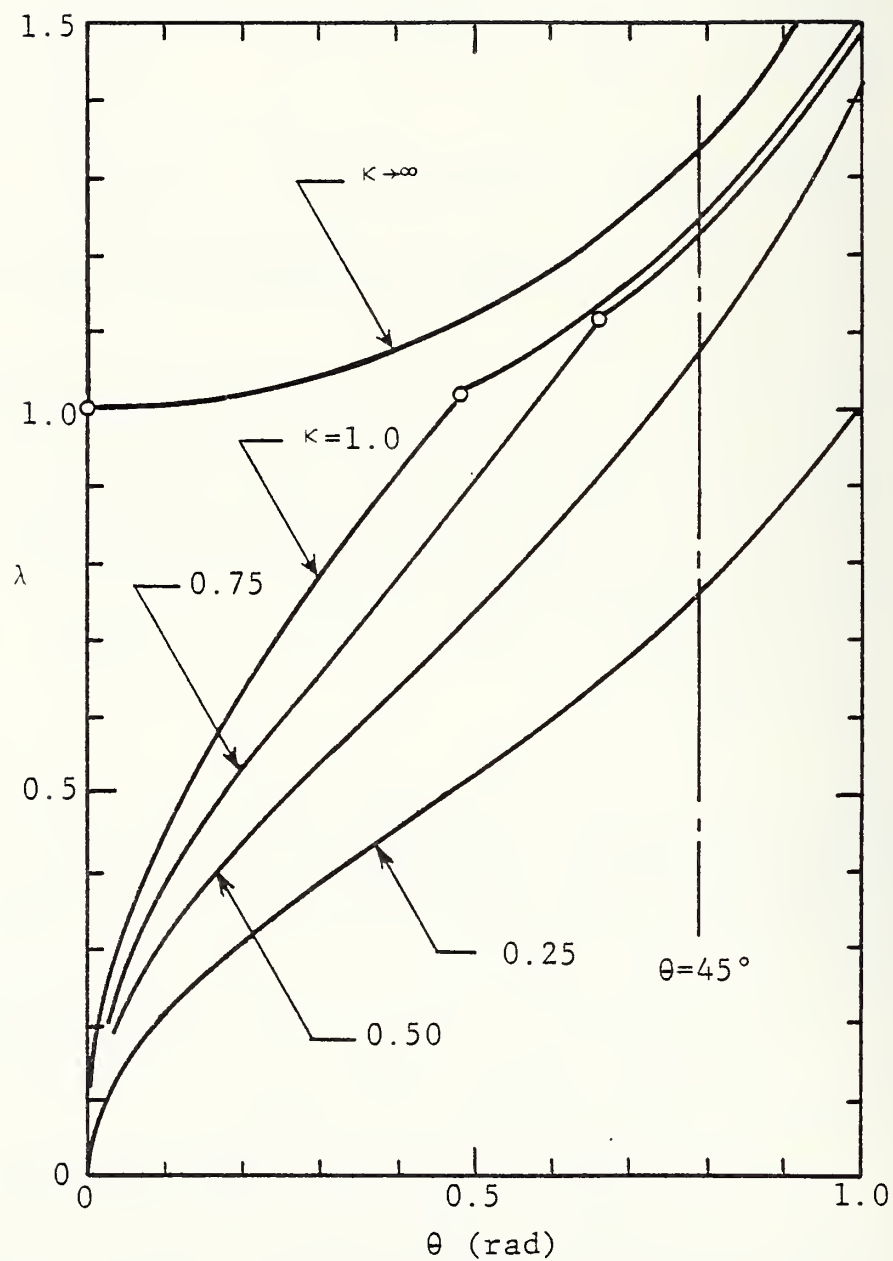


FIGURE 29. ANGULAR VELOCITY - ROTATION RELATIONSHIP  
FOR HIP LOFT MODEL,  $\alpha = 0.126$

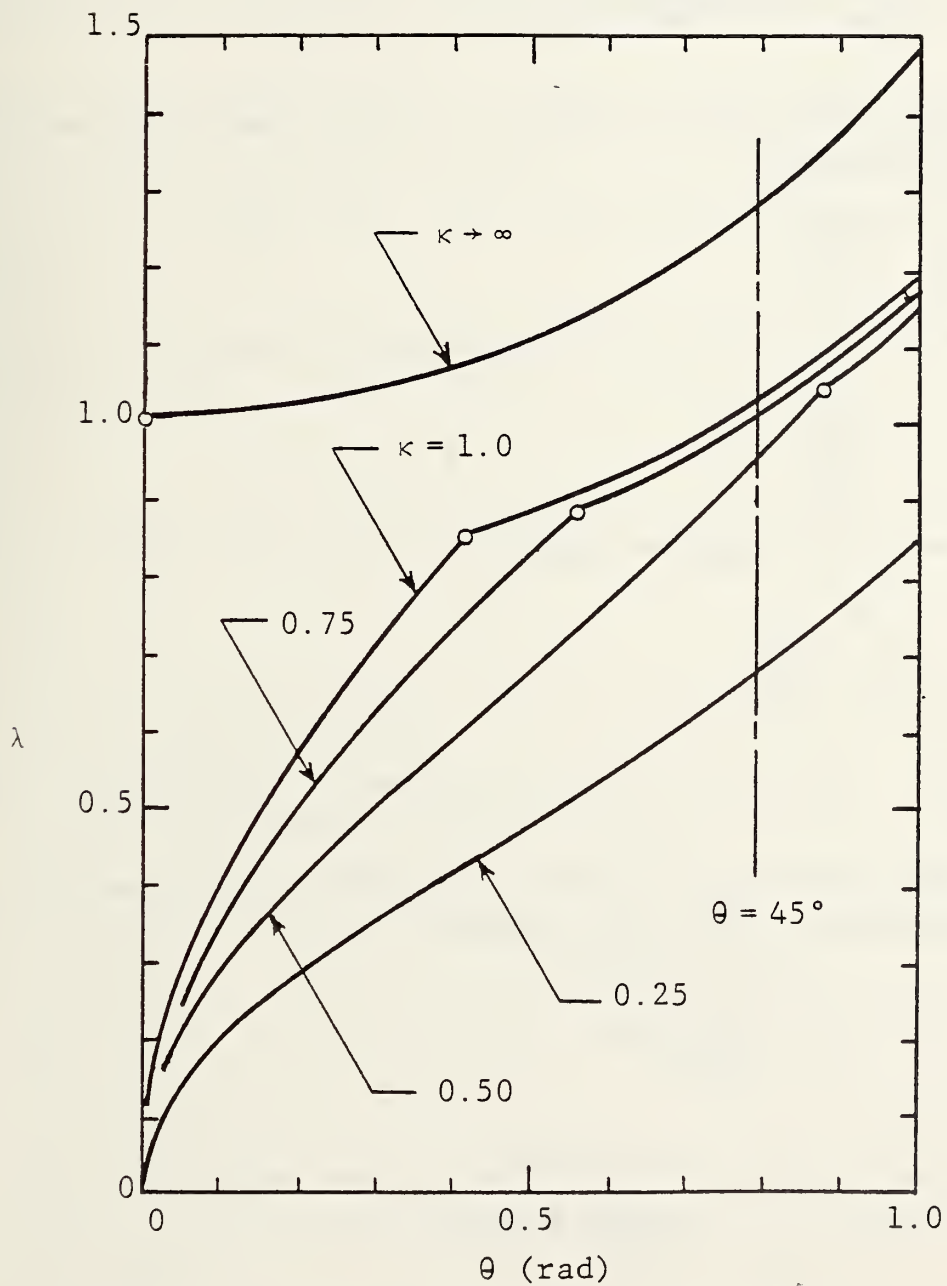


FIGURE 30. ANGULAR VELOCITY - ROTATION RELATIONSHIP  
FOR HIP LOFT MODEL -  $\alpha = 0.3$



Thus the dimensionless form of equation (61) together with equation (67) yields

$$\tau = \int_0^{\theta} \sqrt{\frac{\cos^2 \theta + \alpha}{1 + \alpha}} d\theta. \quad (69)$$

For the general case ( $\kappa < \infty$ ) the deceleration phase of the train ends when

$$\tau_0 = \frac{t_0 V_0}{D} \quad (70)$$

and using the results of Section 4.1 yields

$$\tau_0 = \frac{V_0^2}{a_0 D} = \frac{1}{\kappa}. \quad (71)$$

In general the time is given as

$$\tau = \int_0^{\theta} \frac{d\theta}{\lambda(\theta)}. \quad (72)$$

Equation (65) was solved numerically (subject to the boundary condition  $\lambda(0)=0$ ) together with equation (72) until  $\tau = \tau_0$ . At that time point  $\lambda = \lambda_1$  and  $\theta = \theta_1$  and the solution for the second phase becomes, from equation (66)

$$\lambda = \lambda_1 \sqrt{\frac{\cos^2 \theta_1 + \alpha}{\cos^2 \theta + \alpha}} \quad (73)$$

and

$$\tau = \tau_0 + \int_{\theta_1}^{\theta} \sqrt{\frac{\cos^2 \theta + \alpha}{\cos^2 \theta_1 + \alpha}} d\theta. \quad (74)$$

The time history was obtained by numerical integration of equation (74). The results of these integrations are presented in Figures 29 and 30 for the angular velocity and in Figure 31 for the time details. The time details are only presented for  $\alpha = 0.126$ . Four representative values of  $\kappa$  of 0.25, 0.50, 0.75 and 1.00 were selected.

The above solutions define the motion history of the body bar and can now be used to evaluate the velocity of the potential impact point (point B of Figure 28). The dimensionless velocity of the train case is

$$\chi = \frac{\dot{x}}{V_0} = 1 - \frac{\tau}{\tau_0}, \quad 0 \leq \tau \leq \tau_0$$

(75)

and

$$\chi = 0, \quad \tau_0 \leq \tau$$

Whereas the dimensionless velocity of the c.g. is

$$\phi_z = \frac{\dot{z}}{V_0} \quad (76)$$

and the relative velocity between the c.g. and the barrier is from the derivative of equation (58)

$$\phi_{zr} = \phi_z - \chi = \lambda \cos \theta, \quad (77)$$

The relative velocity dependence on the angle of rotation is presented in Figure 32. The time details of the various velocities are presented (for  $\alpha = 0.126$ ) in Figure 33. It is clear from these results that the horizontal velocity of the c.g. does not change significantly, such that the relative velocity is controlled primarily by the motion of the train car. If the body component impact occurs during the second phase ( $\tau_0 < \tau$ ) of the motion, and it frequently can and does (see Figure 32 for  $\theta = \theta_i$ ), the relative velocities are high.

The details of an impact upon an obstacle located immediately forward of the passenger is illustrated in Figure 34(a). Since there is no vertical force acting upon the c.g. it moves only in the horizontal direction.

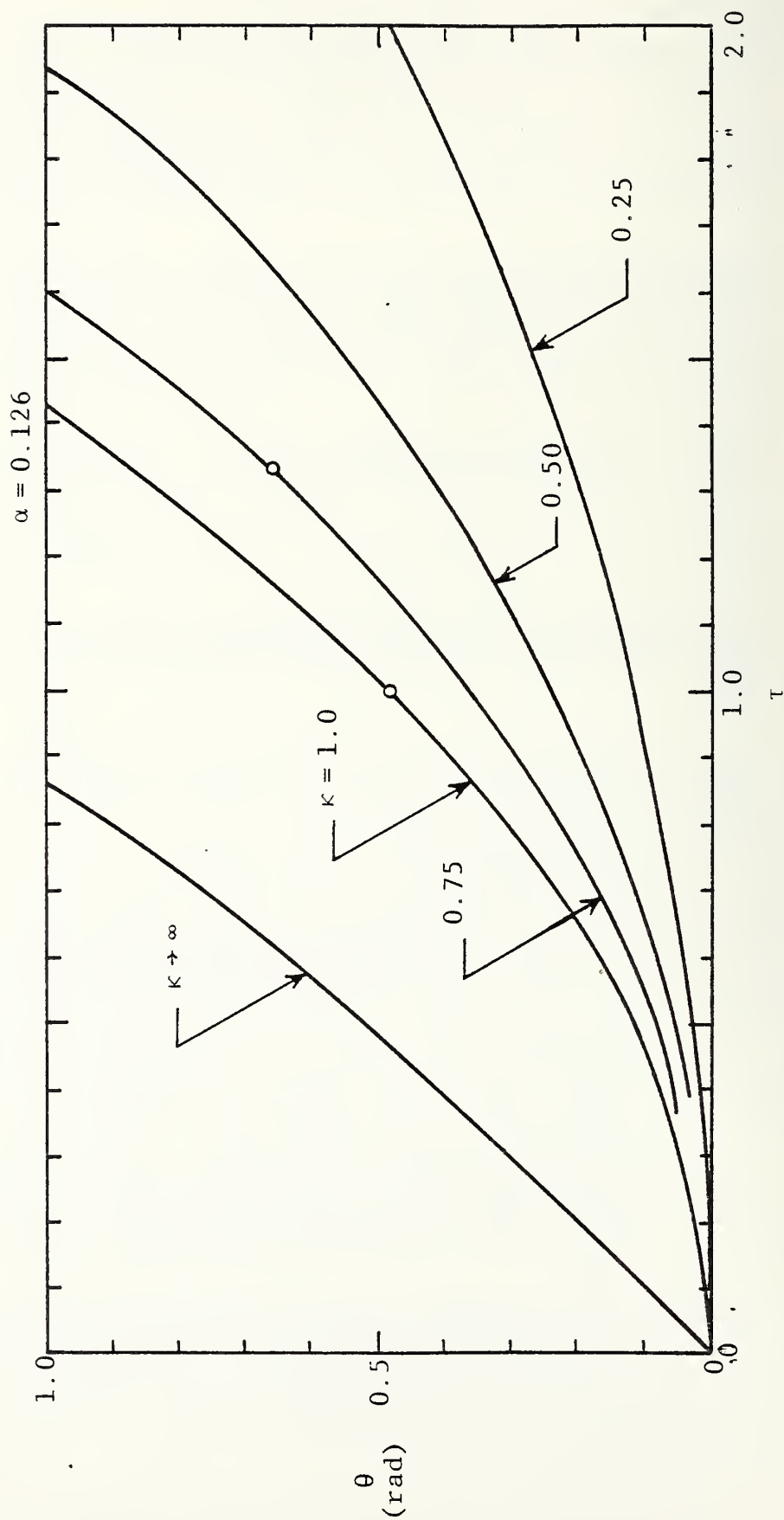


FIGURE 31. ROTATION HISTORY FOR HIP LOFT MODEL

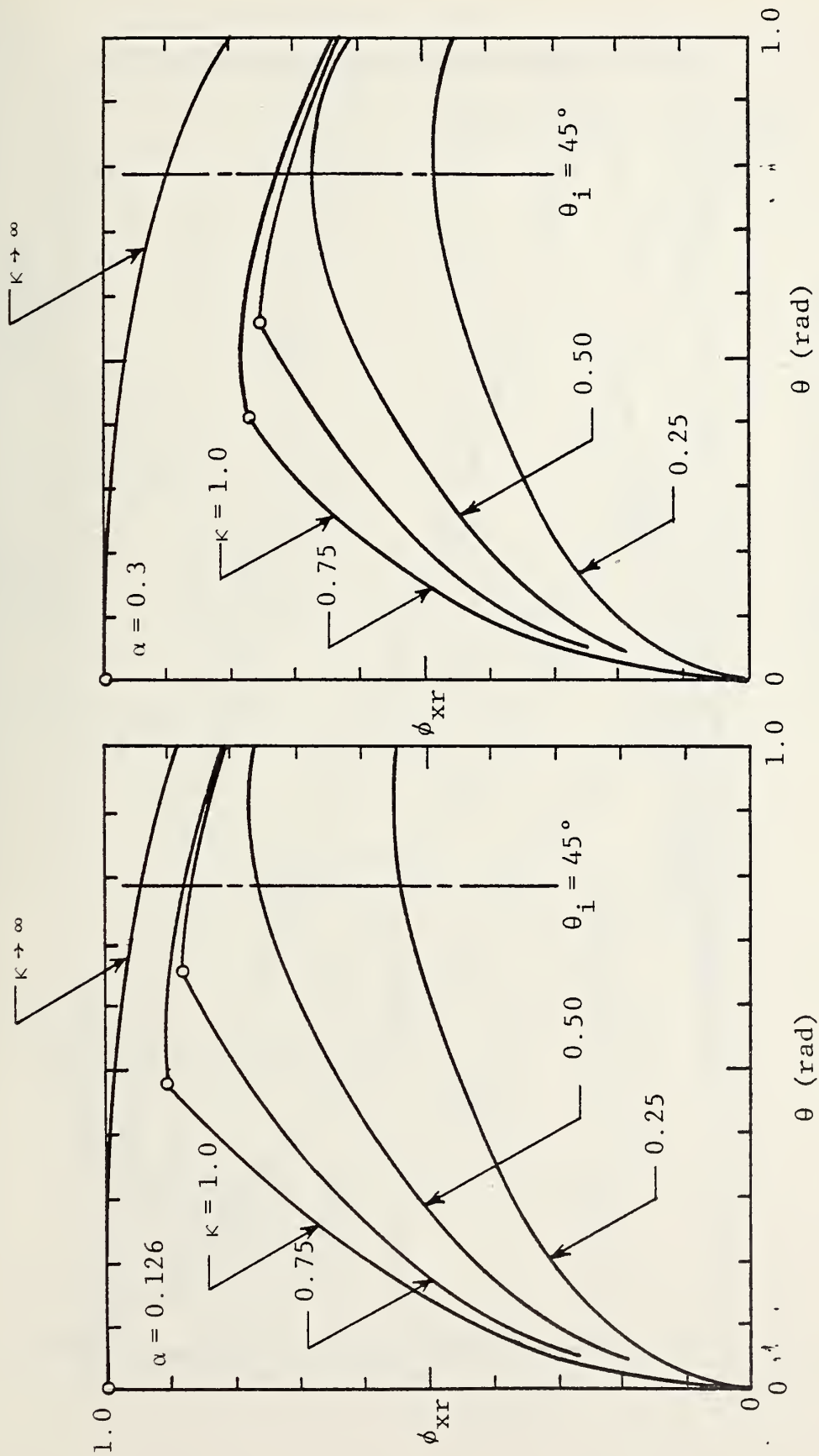


FIGURE 32. CENTER OF GRAVITY VELOCITY FOR HIP LOFT MODEL

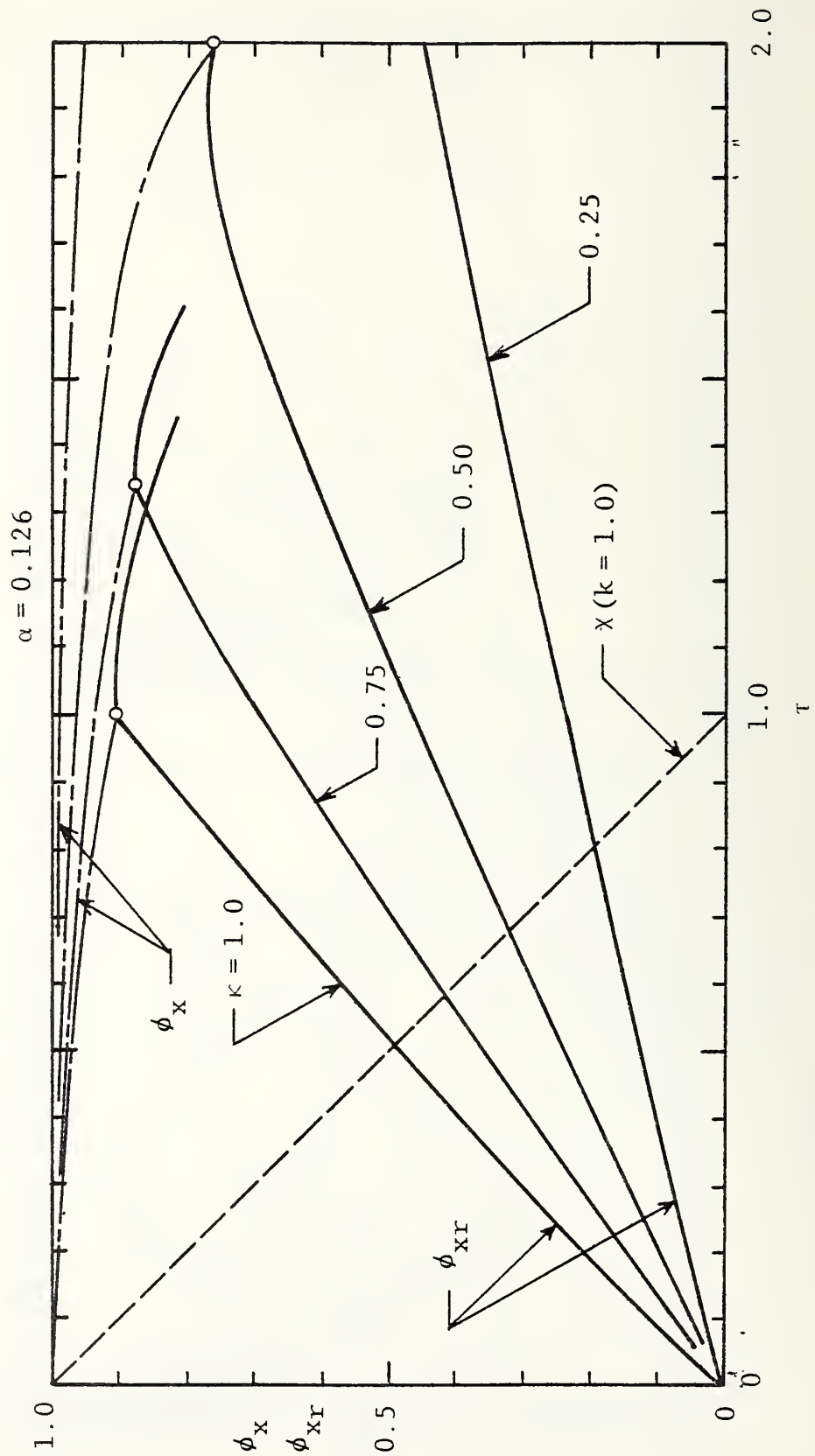
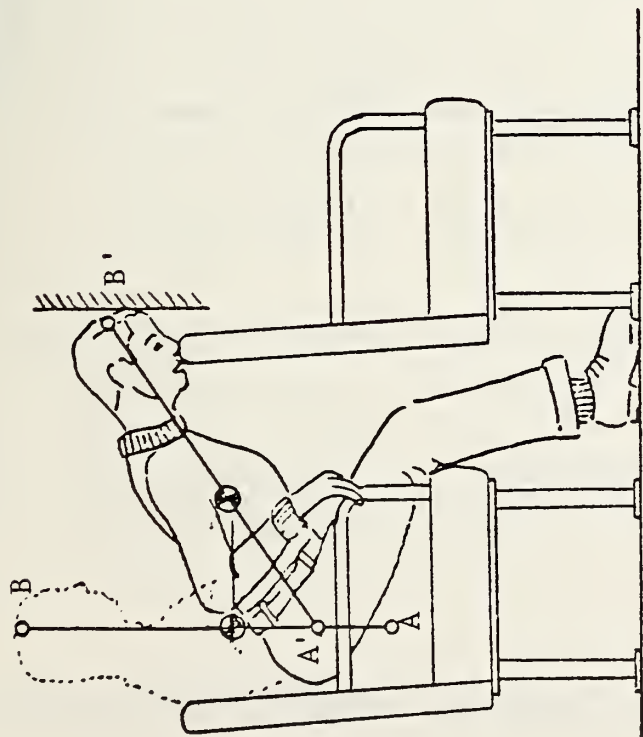
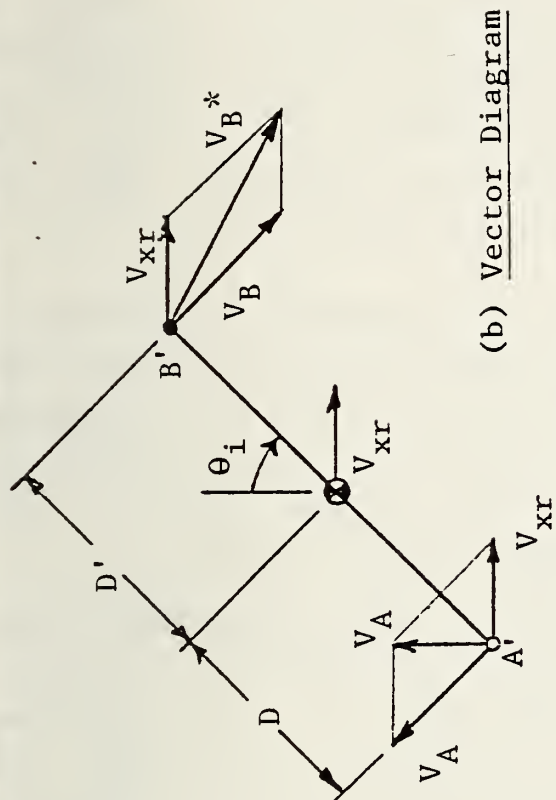


FIGURE 33. CENTER OF GRAVITY VELOCITY HISTORY FOR HIP LOFT MODEL

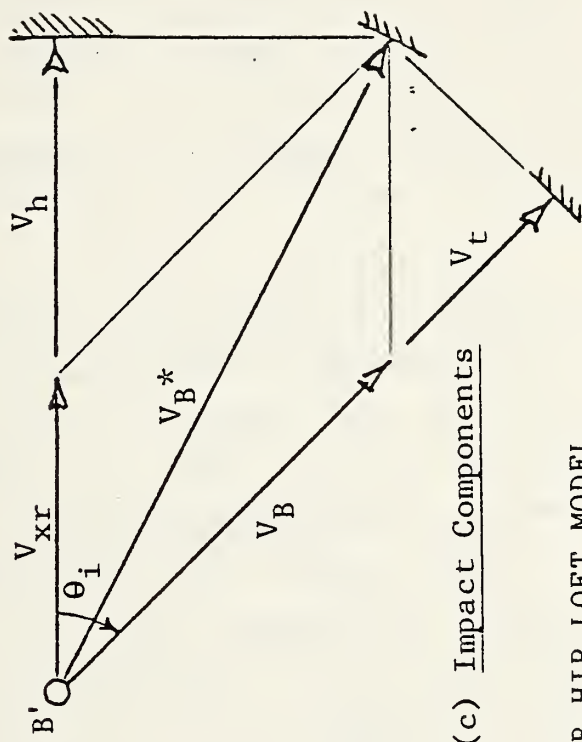




(a) Passenger Configuration at  
Head Impact



(b) Vector Diagram



(c) Impact Components

FIGURE 34. IMPACT DETAILS FOR HIP LOFT MODEL

Thus the hip (point A) moves upward (to position A') during the forward rotating motion. The velocity components of the body bar at the angle of impact ( $\theta_i$ ) are illustrated in Figure 34(b) relative to the car interior. The velocity of the c.g. is  $V_{zr}$ . The velocity of point A' is composed of two components; the c.g. component and the rotational component  $V_A$  where  $V_A = \omega D$ .

The resultant velocity of these two components is  $V_A^*$  which is vertical in accordance to the applied constraint on the lower end of the body bar. The velocity component of point B' (the impact point) is also composed of a c.g. contribution and a rotational contribution,  $V_B$  where  $V_B = \omega D$ . From the definition of the dimension H in Figure 28(b) it is clear that  $H = D + D'$ .

The resultant velocity of point B' is  $V_B^*$ . The normal impact velocity will depend upon the orientation of the impact surface. This feature is illustrated in Figure 34(c) for three surfaces normal respectively to the velocity vectors  $V_{zr}$ ,  $V_B$  and  $V_B^*$ . The corresponding resultant impact velocities,  $V_h$ ,  $V_t$  and  $V_{B^*}$  are all about equal in magnitude hence the well defined value  $V_B$  can be used and the orientation of the surface need not be considered explicitly. The value of  $V_B^*$  in dimensionless terms is

$$\phi_{imax} = \frac{V_B^*}{V_o} = \sqrt{\left[\phi_{zr} + \lambda \frac{D'}{D} \cos \theta_i\right]^2 + \left[\lambda \frac{D'}{D} \sin \theta_2\right]^2}. \quad (78)$$

The dependence of the contributing parameters  $\phi_{zr}$  and  $\lambda$  are presented in Figure 35 for the case  $D' = D$  as a function of  $\kappa$ . The two distinct regions correspond to an impact occurring in each of the two phases of the railcars motion. Furthermore, the parameter  $\kappa$  can be redefined using the results of Section 4.1 as

$$\kappa = \frac{D}{2x_o} \quad (79)$$

and thus is related simply to the car stopping distance  $x_o$ .

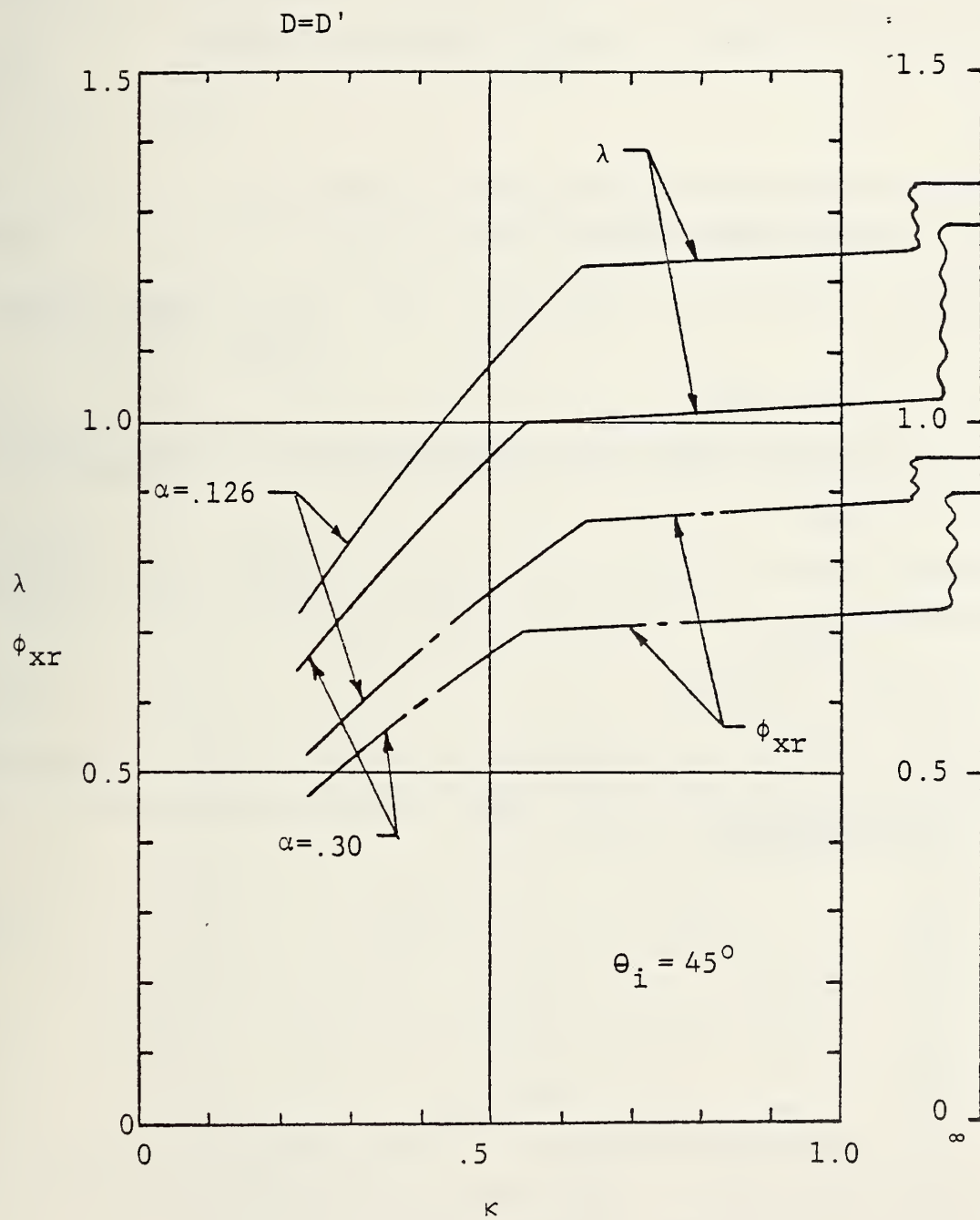


FIGURE 35. INFLUENCE OF ACCELERATION ON VELOCITY COMPONENTS

4.5.2 Pinned Hip Model - The pinned hip model restrains the lower end of the body bar (point A) from moving upward during the rotation of the body bar. Thus an additional equation of motion for the vertical movement of c.g. is required, namely

$$W\ddot{y} = G \quad (80)$$

where

$y$  = the downward displacement of the c.g.

$G$  = the vertical reaction force at A.

The moment equation (in equation 56) must be generalized and rewritten as

$$M = G(z-x) - yF \quad (81)$$

and the kinematic constraints must be expanded to include

$$y = D \cos\theta. \quad (82)$$

Following a similar procedure as before yields the basic differential equation

$$\ddot{\theta} (1+\alpha) = - \frac{\ddot{x}}{D} \cos\theta. \quad (83)$$

When this equation is expressed in terms of the dimensionless variables for each of the two phases of the train car motion, these results are obtained

$$\lambda \frac{d\lambda}{d\theta} (1+\alpha) = \kappa \cos\theta, \quad 0 \leq \tau \leq \tau_0 \quad (84)$$

and

$$\lambda \frac{d\lambda}{d\theta} (1+\alpha) = 0, \quad \tau_0 \leq \tau \quad (85)$$

or

$$\lambda \frac{d\lambda}{d\theta} = 0, \quad \tau_0 \leq \tau. \quad (86)$$

If the limiting solution for  $\kappa \rightarrow \infty$  is sought the initial condition is as before  $\lambda(0) = 1$  and the differential equation (equation (86)) for  $\tau_0 \leq \tau$  applies. Integration yields

$$\lambda = \text{constant} = 1, \quad 0 \leq \tau$$

and from equation (72) further integration yields

$$\theta = \tau.$$

The more general case ( $\kappa < \infty$ ) can also be integrated directly recalling that the boundary condition  $\lambda(0) = 0$  applies for equation (84). Thus

$$\lambda = \lambda^* \sqrt{\sin\theta}, \quad 0 \leq \tau \leq \tau_0 \quad (87)$$

where

$$\lambda^* = \sqrt{\frac{2\kappa}{1+\alpha}} \quad (88)$$

The corresponding results for this phase are presented in Figure 36. The time details are obtained numerically from

$$\tau = \frac{1}{\lambda^*} \int_0^\theta \frac{d\theta}{\sqrt{\sin\theta}}, \quad 0 \leq \tau \leq \tau_0 \quad (89)$$

however, auxiliary solution can be utilized, namely, let

$$T(\theta) = \int_0^\theta \frac{d\theta}{\sqrt{\sin\theta}} = \lambda^* \tau. \quad (90)$$

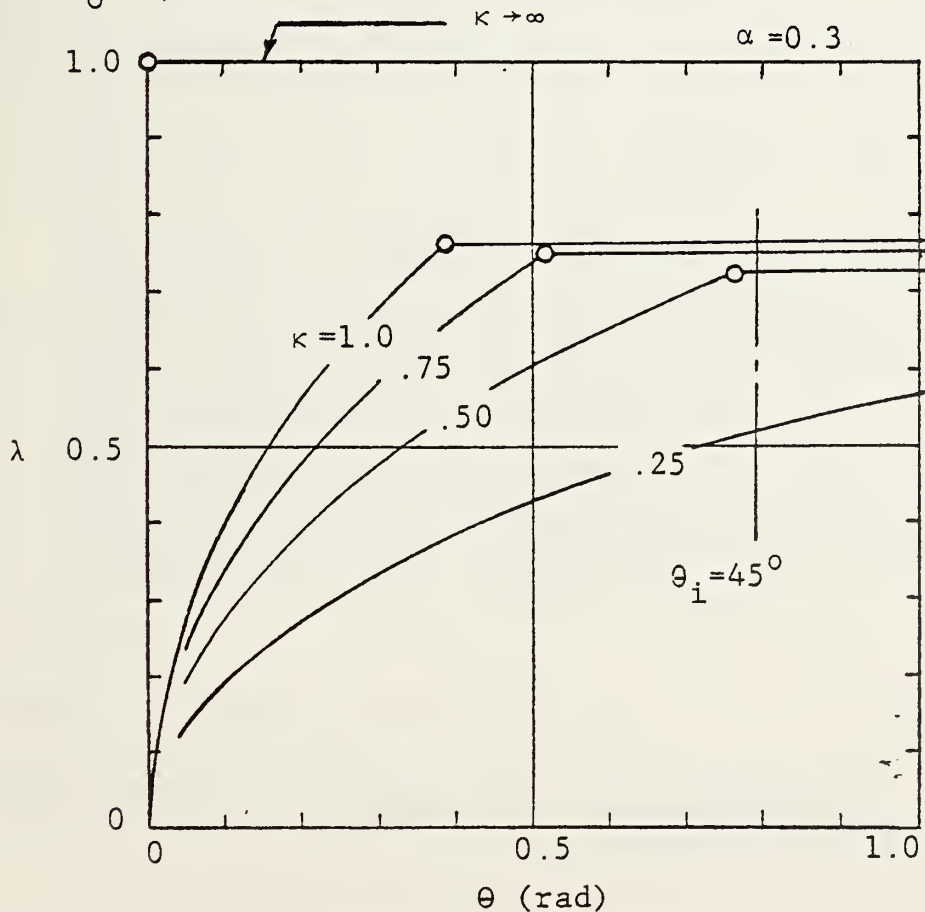


FIGURE 36. ANGULAR VELOCITY - ROTATION RELATIONSHIP FOR PINNED HIP MODEL



This function was evaluated and the results are presented in Figure 37. In particular when  $\tau = \tau_0$  and  $\theta(\tau_0) = \theta_1$

$$T(\theta_1) = \lambda^* \tau_0 = \frac{\lambda^*}{\kappa} \quad (91)$$

the value of  $\lambda_1 = \lambda(\theta_1)$  is then given as

$$\lambda_1 = \lambda^* \sqrt{\sin \theta_1}. \quad (92)$$

The solution for the second phase  $\tau_0 < \tau$  is simply

$$\lambda = \text{constant} = \lambda_1$$

and

$$\tau = \tau_0 + \frac{(\theta - \theta_1)}{\lambda_1}, \quad \tau_0 \leq \tau \quad (93)$$

The complete angular velocity and time details for this case are presented in Figures 36 and 38.

The dimensionless relative horizontal velocity,  $\phi_{zr}$  is identical (see equation (77)) to that for the hip loft model. However, for this model the vertical velocity,  $\phi_y$ , must also be defined, namely

$$\phi_y = \frac{\dot{y}}{V_0} = \lambda \sin \theta \quad (94)$$

These velocity components are presented in Figure 39.

4.5.3 Influence of Slip - The likelihood that a forward facing seated passenger will slide forward in his or her seat before substantial torso rotation will occur, appears to be great. Thus this feature was incorporated into the pinned hip model. It was hoped that such an evaluation would yield a meaningful measure of this effect. The model assumes that the passenger's horizontal motion remains constant at its initial value,  $V_0$ , after the train car deceleration starts ( $t = 0$ ) and until a relative distance,  $s$ , is traversed at  $t = t'$ . This distance represents the knee-to-seat-back clearance which exists and thus it becomes a parameter in the problem. During this period the passenger moves a distance  $z'$  and the train moves a distance  $x'$ .

$$T(\theta) = \int_0^\theta \frac{d\theta}{\sqrt{\sin\theta}}$$

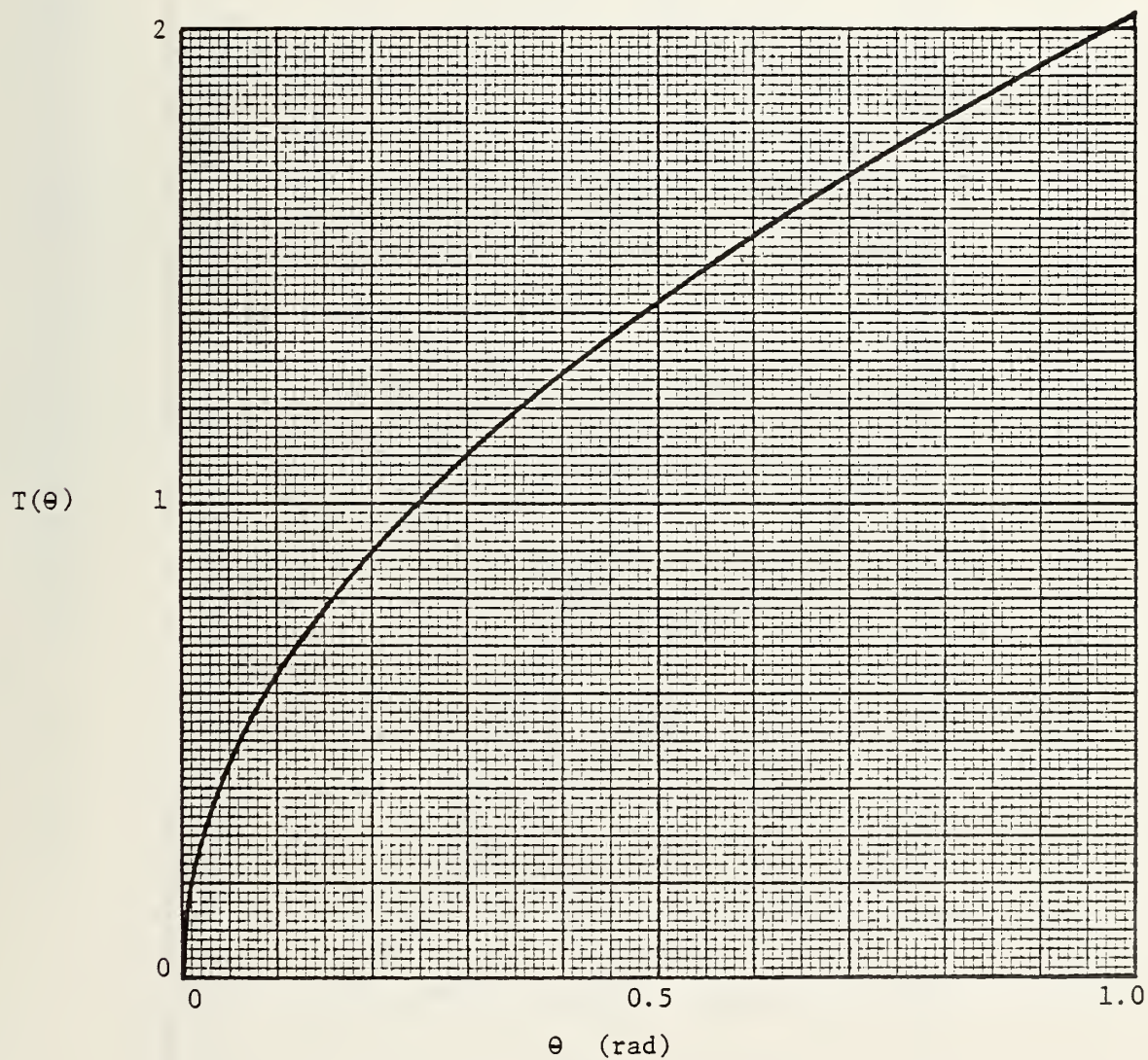


FIGURE 37. TIME FUNCTION

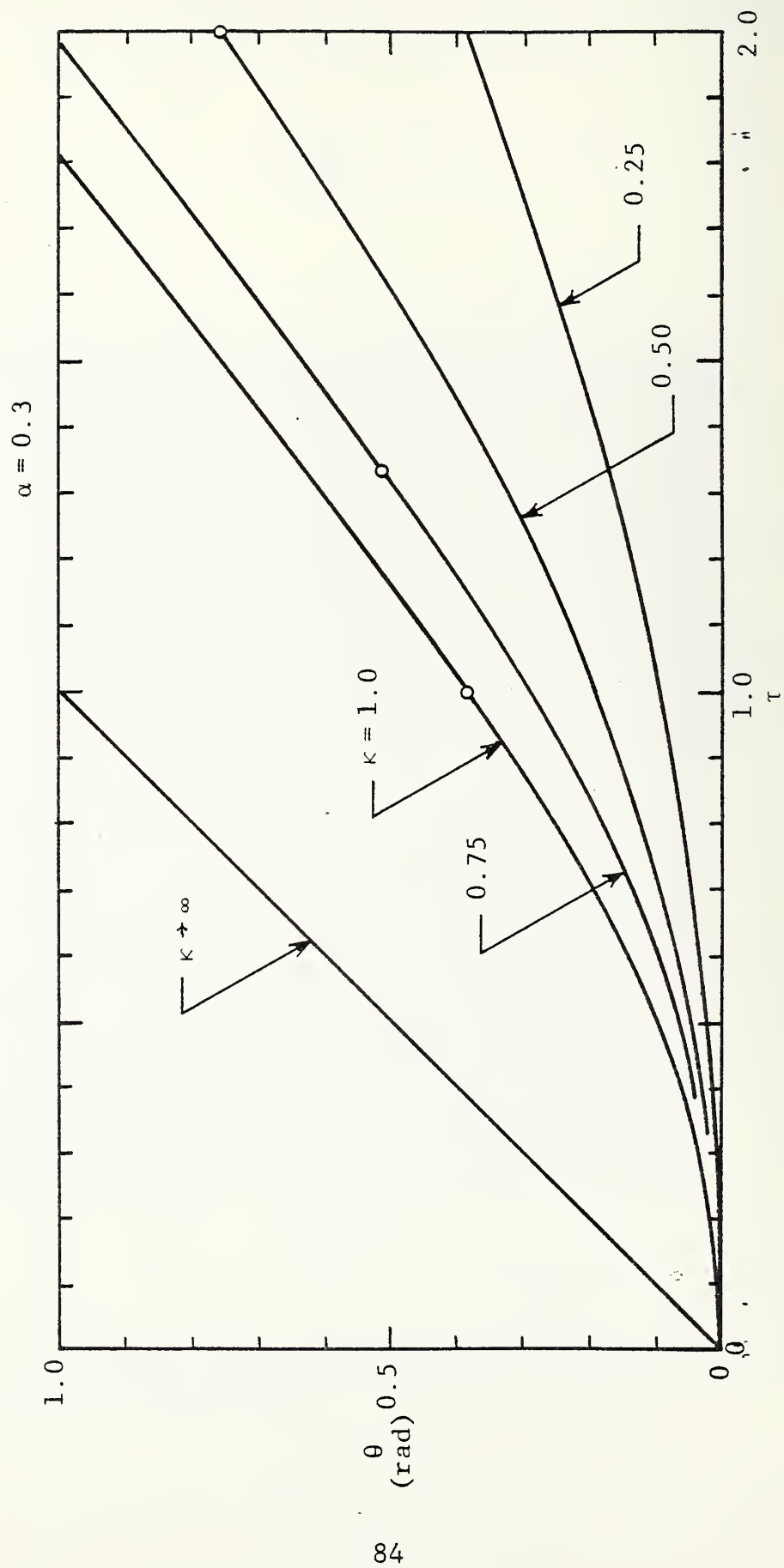


FIGURE 38. ROTATION HISTORY FOR PINNED HIP MODEL

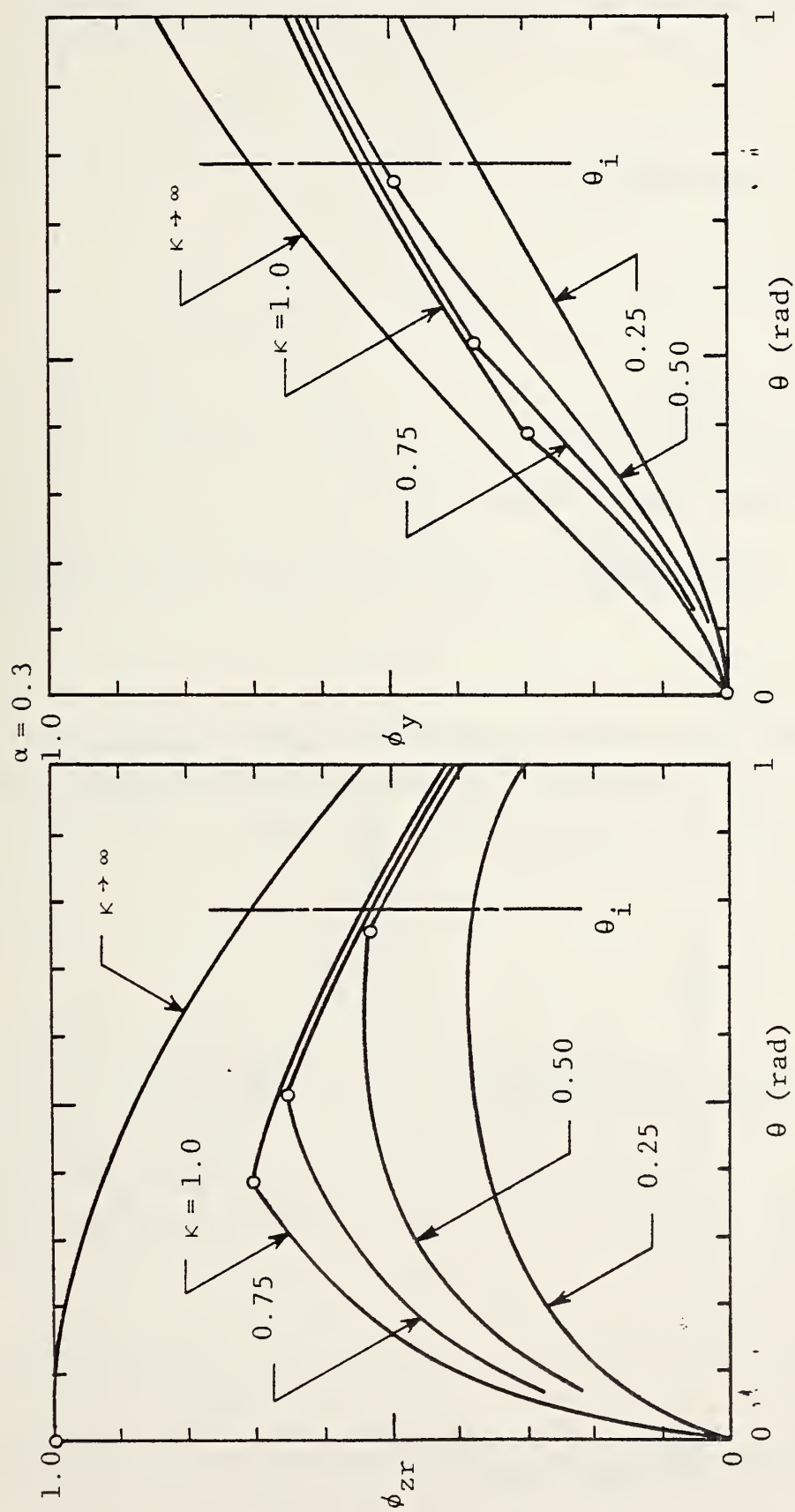


FIGURE 39. CENTER OF GRAVITY VELOCITY COMPONENTS FOR PINNED HIP MODEL

These distances are obtained from the respective acceleration histories as

$$z' = V_0 t \quad (95)$$

and

$$x' = V_0 t - \frac{a_0 t^2}{2} \quad (96)$$

But at  $t = t'$

$$s = z' - x' \quad (97)$$

hence

$$t' = \sqrt{\frac{2s}{a_0}} \quad (98)$$

or in dimensionless terms

$$\tau' = \frac{t'}{t_0} = \sqrt{\frac{2\sigma}{\kappa}} \quad (99)$$

where

$$\sigma = \frac{s}{D} \quad (100)$$

When knee impact occurs the model assumes that the linear momentum is converted instantaneously to angular momentum and rotation of the vertical body bar begins. Thus the new initial conditions for  $t = t'$  are

$$\begin{aligned} \theta(t') &= 0 \\ \omega(t') &= \frac{\Delta V}{D} \end{aligned} \quad (101)$$

where  $\Delta V$  is the instantaneous velocity change that point A experiences at the time of impact (see Figure 40(a)). This velocity change is simply  $a_0 t'$  provided that  $t' \leq t_0$ . This time limitation is usually satisfied since  $s$  will generally be much less than  $x_0$ . In dimensionless terms the second boundary condition becomes

$$\lambda_0 = \tau' \kappa \quad (102)$$

Before the solution is presented it will be appropriate to recognize that due to the forward slippage of the point A the clearance between the passenger and the barrier which was originally  $S$  has been reduced to a value  $S - s$ . Thus the amount of



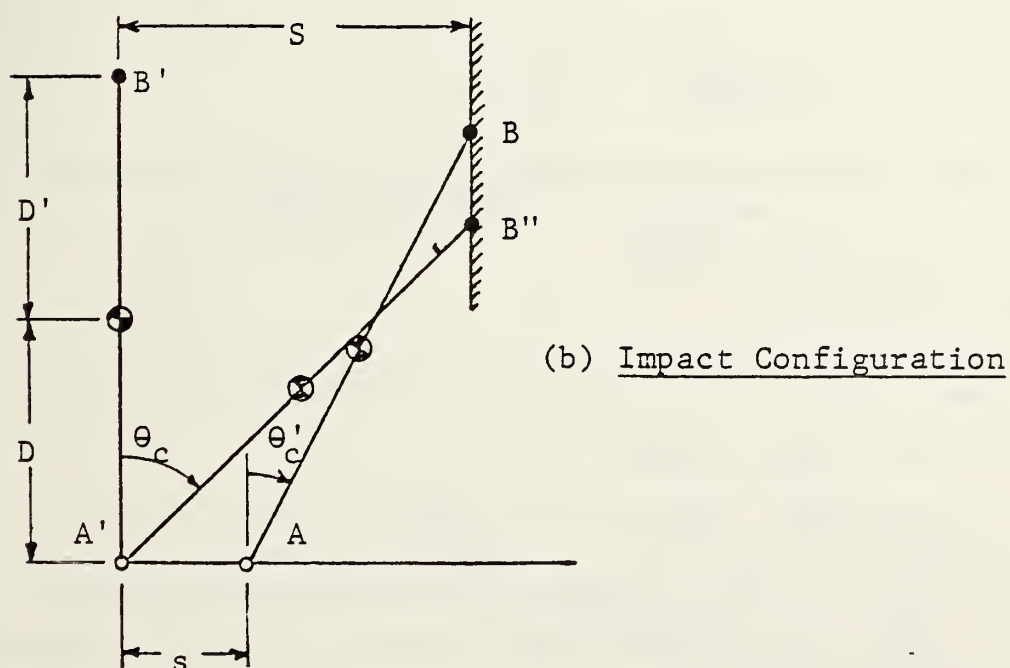
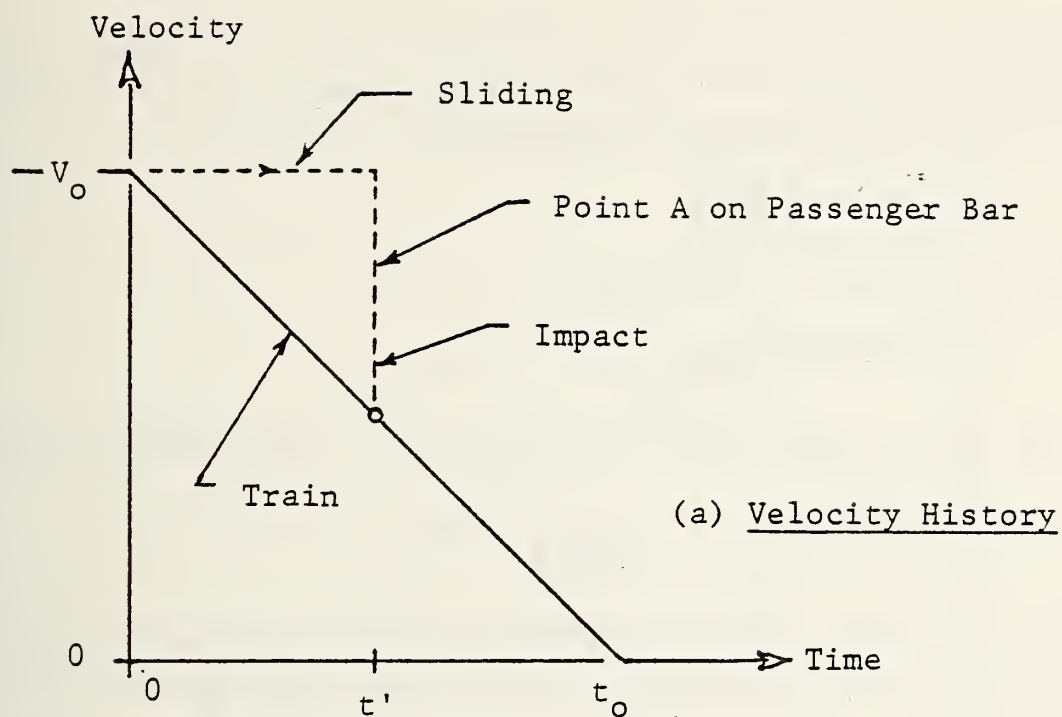


FIGURE 40. HIP SLIP CHARACTERISTICS FOR PINNED HIP MODEL

rotation which would have occurred without slippage,  $\theta_i'$ , has been reduced to  $\theta_i$  with slippage. This effect is illustrated in Figure 40(b). This angle is given as

$$\theta_i' = \arcsin \left[ \frac{S-s}{D+D'} \right] \quad (103)$$

whereas without slippage

$$\theta_i = \arcsin \left[ \frac{S}{D+D'} \right]. \quad (104)$$

Using the conditions  $D' = D$  and  $\theta_i = 45$  degrees requires that  $S = \sqrt{2D}$ , thus

$$\theta_i' = \arcsin \left[ \frac{1}{2} (\sqrt{2-\sigma}) \right]. \quad (105)$$

Since the value of  $D$  is approximately 1 ft values of  $\sigma = 0.25$  and  $0.5$  were selected as being appropriate for this evaluation. These correspond to values of  $\theta_i'$  of 38.4 degrees and 27.2 degrees respectively (or 0.621 and 0.475 rad).

The basic equation (equation 84) can now be integrated to yield

$$\lambda^2 = \lambda_0^2 + \frac{2\kappa \sin\theta}{(1+\alpha)} \quad (106)$$

which with the use of equations (99) and (102) becomes

$$\lambda = \sqrt{2\kappa} \sqrt{\sigma + \frac{\sin\theta}{1+\alpha}}, \quad \tau' \leq \tau \leq \tau_0. \quad (107)$$

Define, as before

$$\lambda_1 = \lambda(\tau_0) \quad (108)$$

then for the second phase

$$\lambda = \text{constant} = \lambda_1 \quad \tau_0 \leq \tau. \quad (109)$$

A representative solution is illustrated in Figure 41. The time details must be evaluated numerically for both phases from the basic definition, viz.

$$\tau = \tau' + \int_0^{\theta} \frac{d\theta}{\lambda(\theta)}. \quad (110)$$

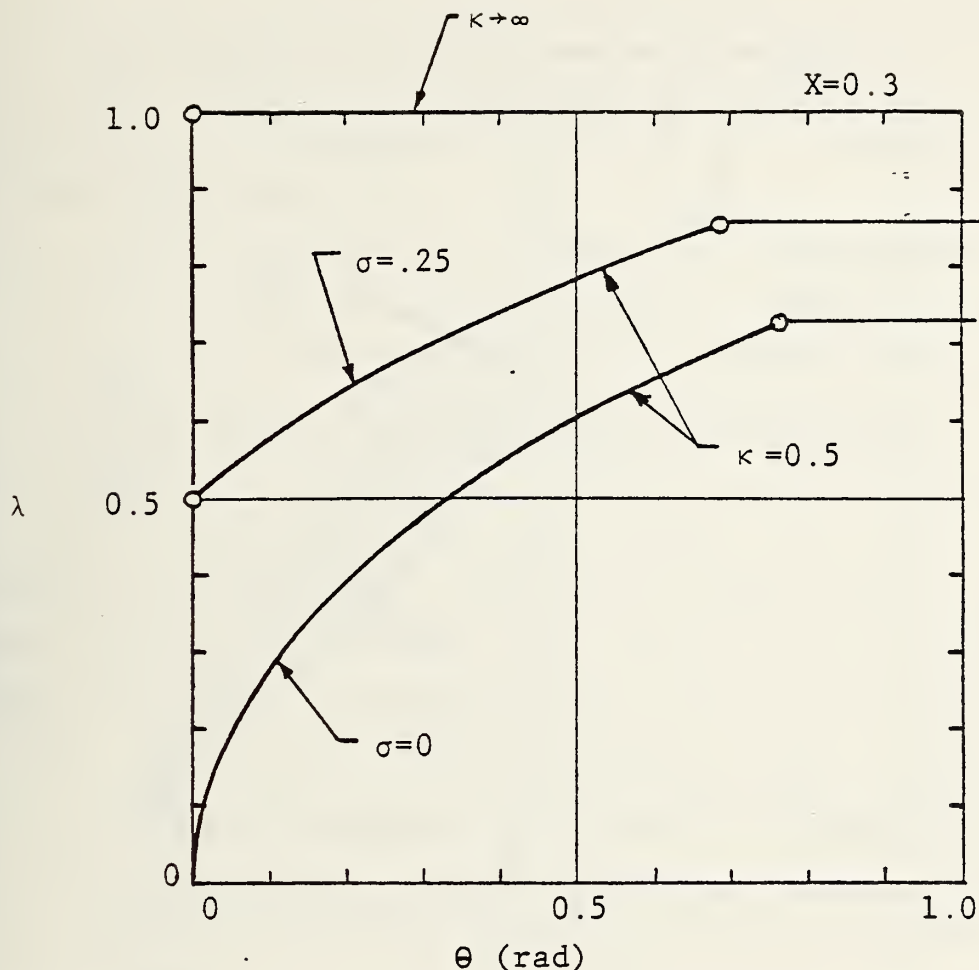


FIGURE 41. INFLUENCE OF SLIP ON ANGULAR VELOCITY - PINNED HIP MODEL

The velocity components are given by the same basic definitions as before, however their values are different. These results are given in Figure 42 for the representative solution.

4.5.4 Variability of Impact Conditions - The previous three subsections have developed results with which to evaluate the impact conditions for the hip loft model, the pinned hip model and to measure the influence of slip for the pinned hip model. For the nonslip condition the body component impact environment should be bounded by the two models. The amount of slip which will occur will be less than that permitted by the above slip conditions used in the slip version of the pinned hip model. The value of  $\sigma$  will vary with

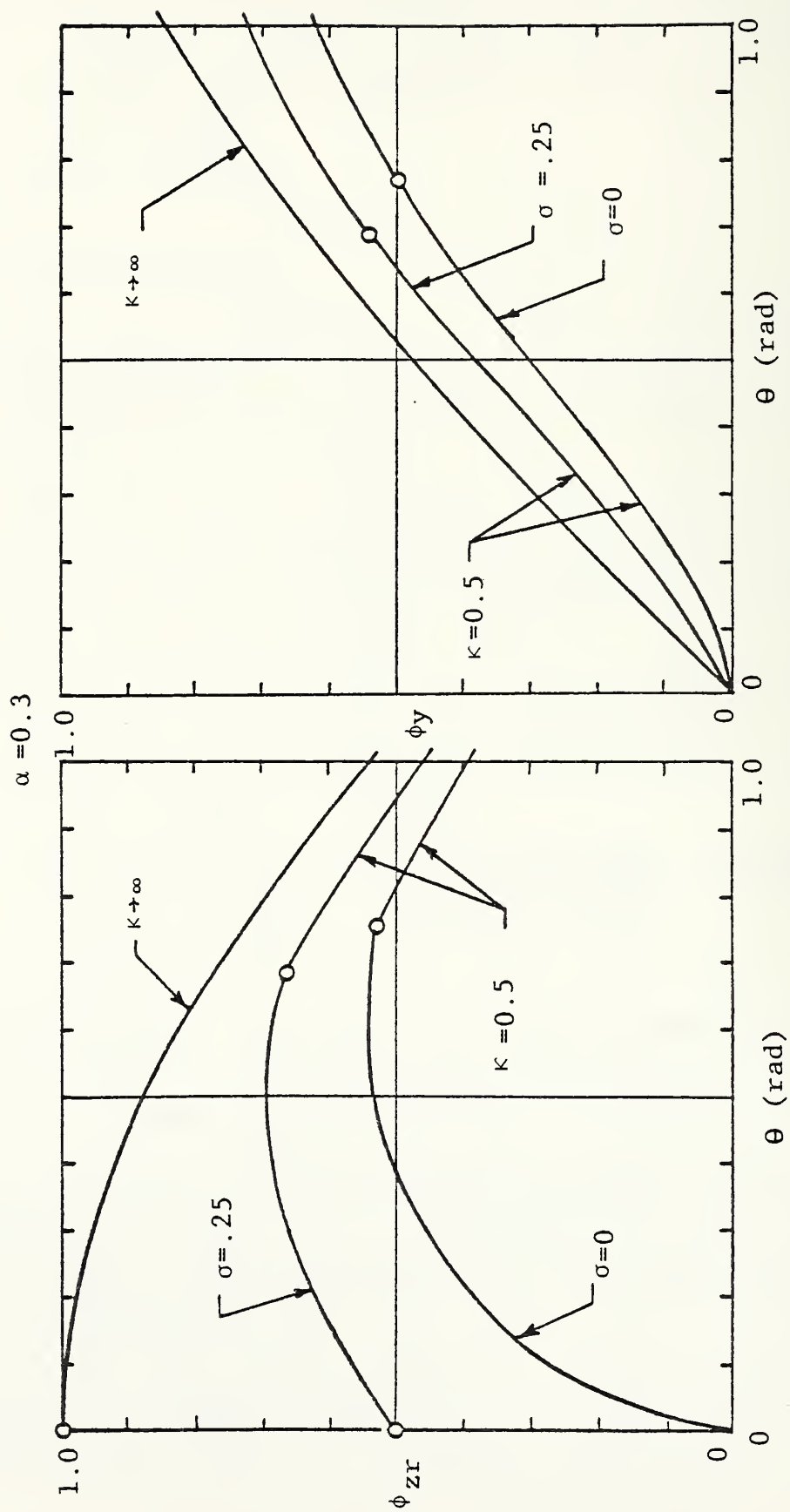


FIGURE 42. INFLUENCE OF SLIP ON CENTER OF GRAVITY VELOCITY COMPONENTS - PINNED HIP MODEL

both car seat design and spacing and anthropometric variances. It is hoped that the two models in addition to the range of  $\sigma$  selected, will represent a narrow enough band of impact conditions such that this collection of information can be used to establish some nominal impact environment.

Figure 43(a) presents, for a given set of conditions, the velocity vectors corresponding to the hip loft model, where  $\phi_{imax}$  was defined in Section 4.5.1. Figure 43(b) presents the velocity vectors corresponding to the pinned hip model without slip ( $\sigma = 0$ ) and the resultant vectors for different slip distances,  $\sigma$ . The vector  $a$  is identical to the resultant vector for the corresponding hip loft model. The magnitude of the impact vector for the two nonslip cases are approximately equal and not much smaller than the magnitudes of those vectors for the various slip distances. It would appear that both the magnitudes and the direction are similar enough to make use of some averaged condition and to treat the calculated variance as just another variance contribution is a situation where many variances will exist. Figures 44 and 45 present the maximum impact velocity dependence on the parameter  $\kappa$  for the cases examined above and for one set of anthropometric and seat spacing values.

4.5.5 Influence of Pulse Shape - The pinned hip model (without slip) was used to evaluate the influence that train car deceleration pulse shape has upon the body component impact environment for the forward facing seated passenger. This model was selected because of its relative simplicity, however no specific derivations are presented. The pulse shape that was selected was the double step pulse (see Section 4.1) with the parameter values  $\delta = 0.5$  and  $\tau_1 = 0.5$ ; thus  $\beta = 0.417$  and  $\gamma = 4/3$  (see Figure 14). Equivalency in this evaluation was based upon conserving both the change in velocity,  $V_0$ , and the stopping distance,  $x_0$ . The conservation of the stopping distance was selected in view of the importance that the parameter  $\kappa$  plays in defining the severity of this impact environment.



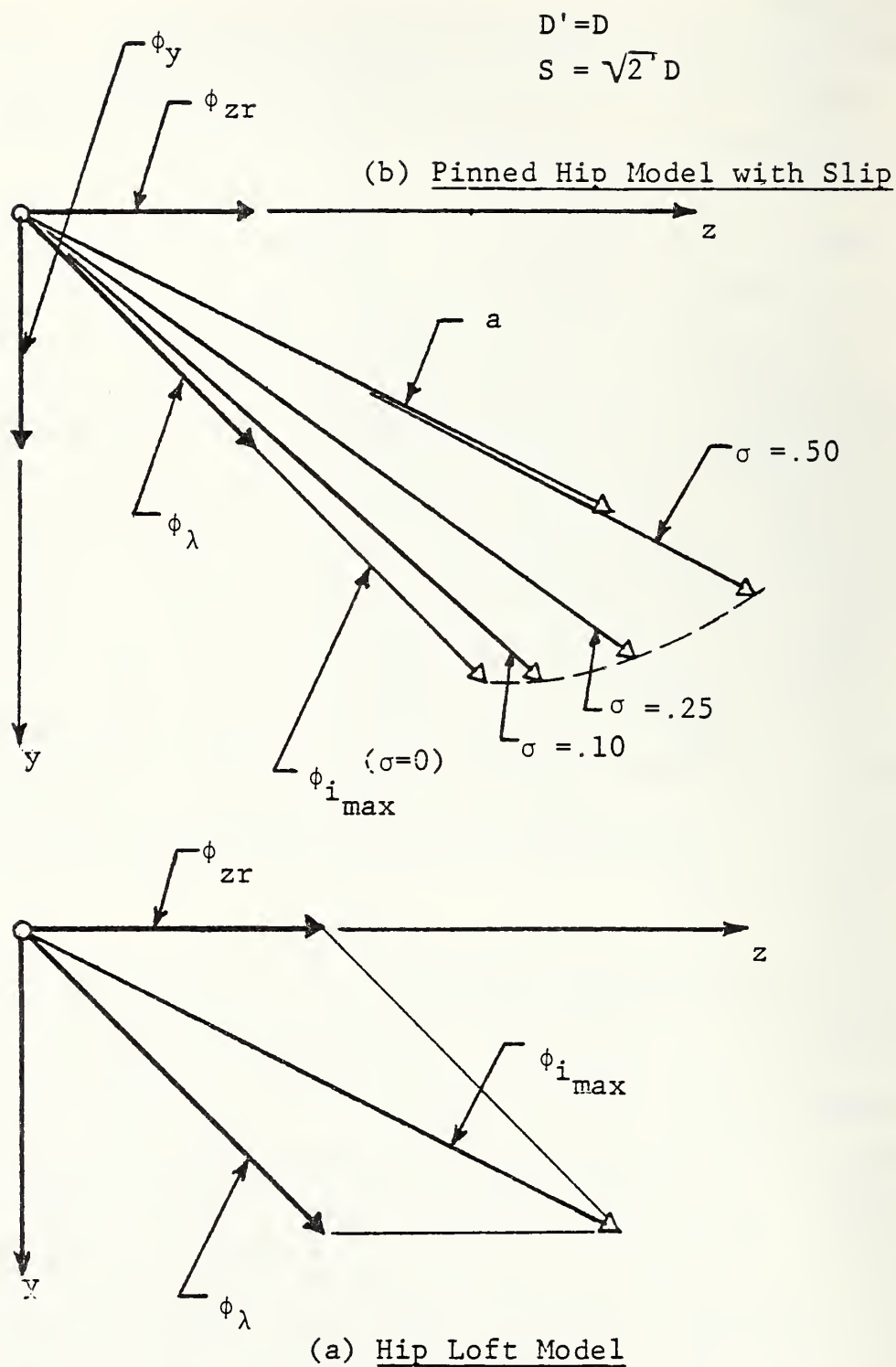


FIGURE 43. VECTOR DIAGRAMS FOR IMPACT VELOCITIES OF SEATED PASSENGER FACING FORWARD

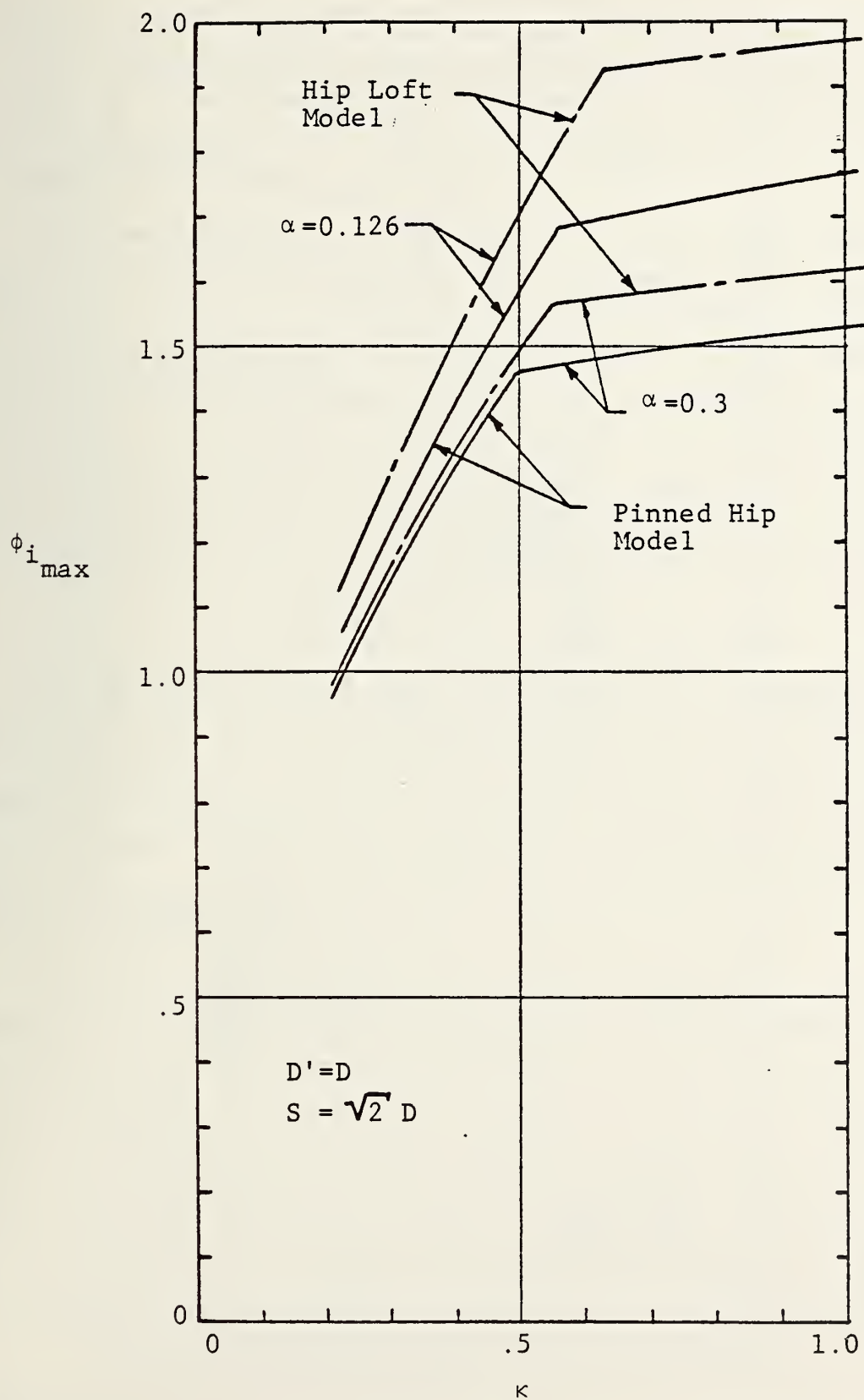


FIGURE 44. IMPACT VELOCITY DEPENDENCE ON MODEL

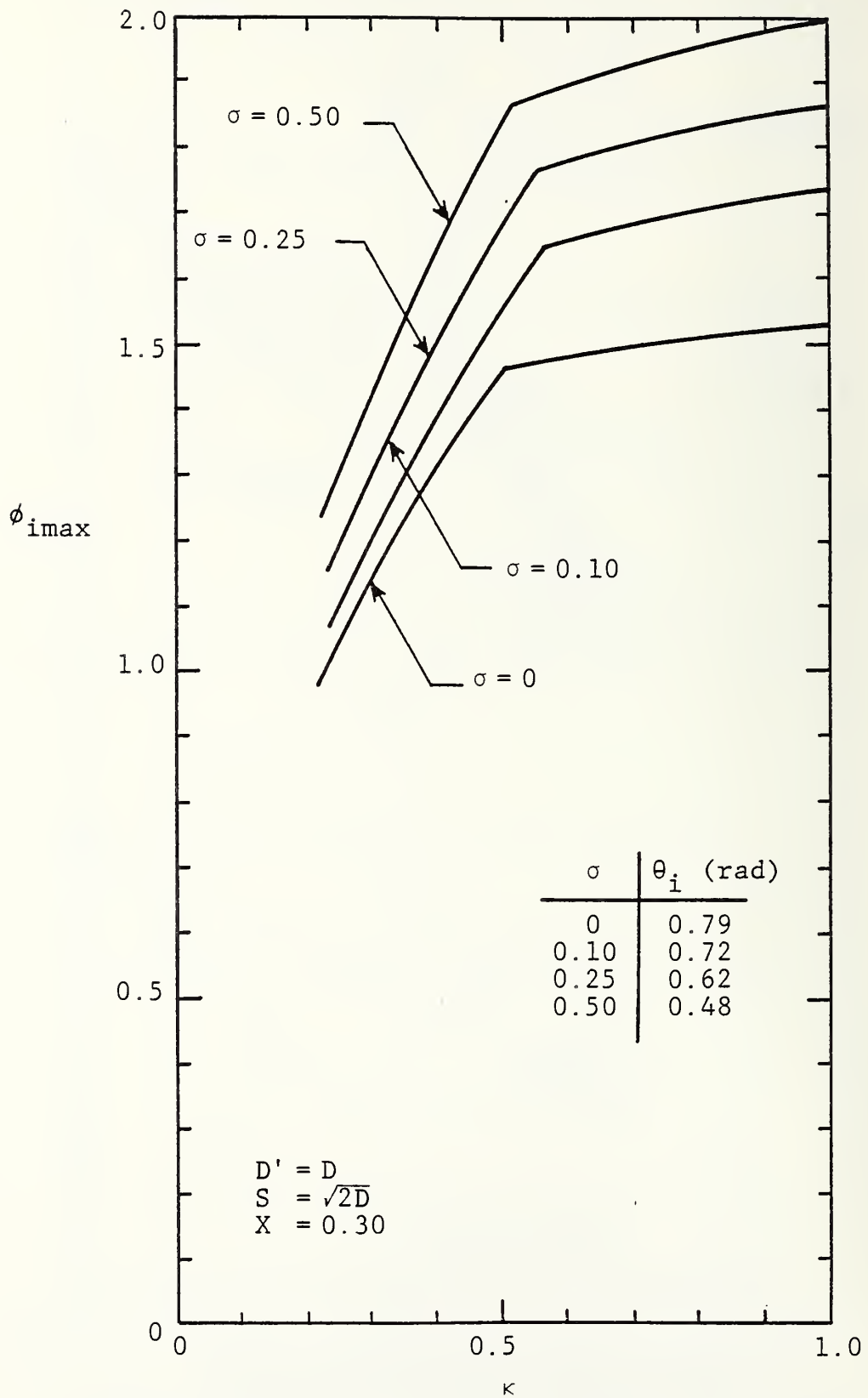


FIGURE 45. IMPACT VELOCITY DEPENDENCE ON SLIP - PINNED HIP MODEL

This equivalency requires that  $\beta t_0 (= x_0/V_0)$  remain constant for the two pulses, thus the pulse duration for the double step pulse must be 1.2 times larger than the reference step pulse duration and the average acceleration must be 1.2 times less than that of the reference step pulse.

The results for the angular velocity for these two equivalent cases are presented in Figure 46 and indicate that in general the differences are not large, in particular if  $\theta_i \approx 0.8$  rad. The influence of the pulse shape is more properly evaluated by examining their influence on the impact velocity  $\dot{\phi}_{imax}$ . This comparison is presented in Figure 47 and clearly demonstrates that the influence of the pulse shape is quite small and generally less than the variations or uncertainties introduced by the degree of hip loft or slip, or by anthropometric uncertainties.

#### 4.6 Backward Facing Seated Passenger

The backward facing seated passenger will be pressed back into his or her seat due to the sudden change in motion brought about by the railcar crash. Therefore, the motion of passengers in this passenger configuration will be generally restrained and no significant impact events are expected. The primary, potentially detrimental, response will be the so-called whiplash or neck flexion response.

Flexion response data<sup>6</sup> for the 50th percentile adult male is presented in Figure 48 and represents the basis for the following analysis. A pinned bar model was used for this analysis where the bar represents the head and the lower pinned end (point A in the previous analysis) represents the neck connection. The neck will offer a resistance to rotation as illustrated in Figure 48 and the onset of injury will occur after the head has rotated approximately 70 to 80 degrees. A linear rotational resistance, B, was assumed for this model and a nominal value of 50 ft lb/rad was selected.

---

<sup>6</sup>"Biomechanics and Its Application to Automotive Design", Society of Automotive Engineers, p 49, 1973.

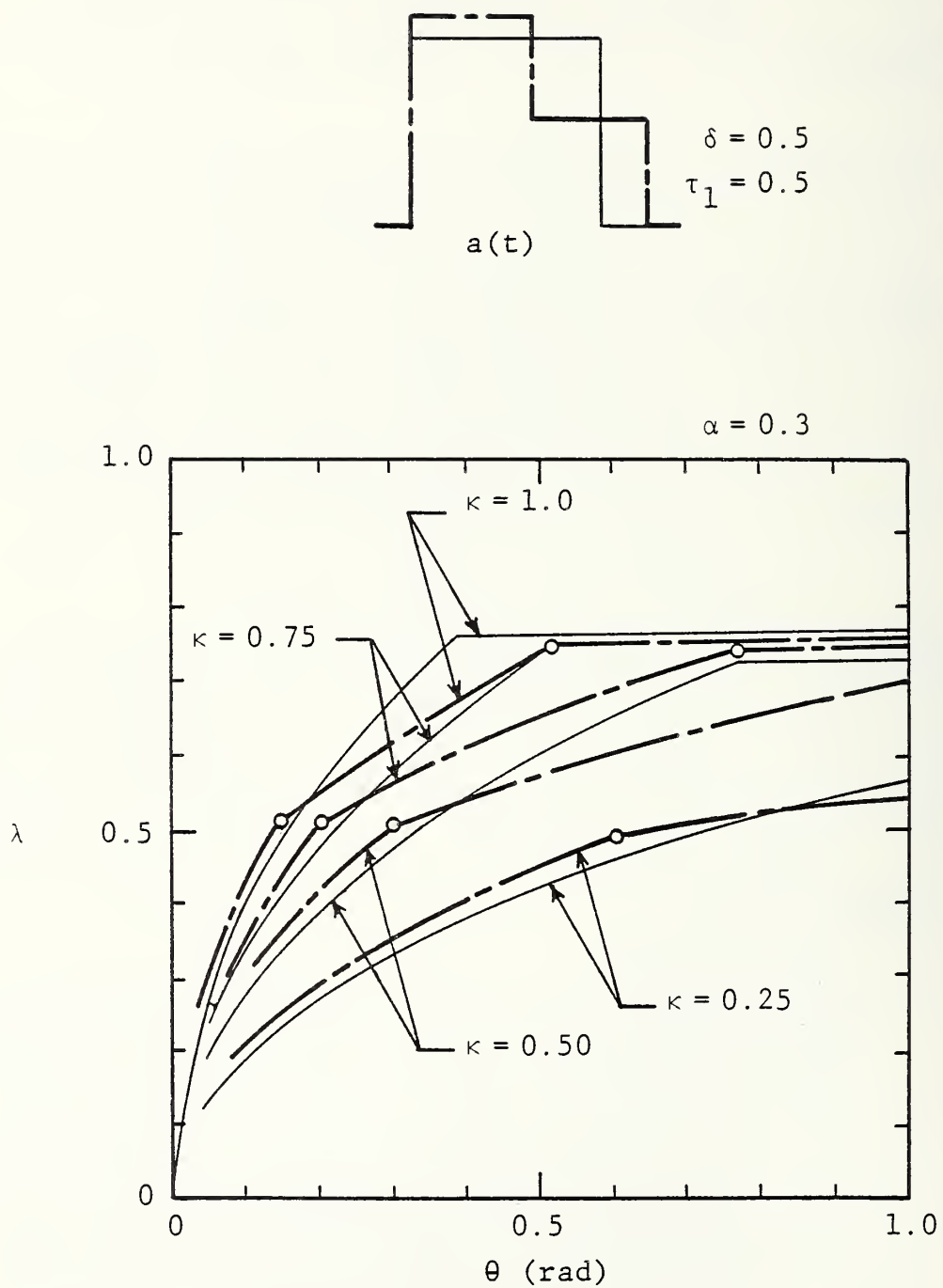


FIGURE 46. INFLUENCE OF PULSE SHAPE UPON ANGULAR VELOCITY  
PINNED HIP MODEL FOR FORWARD FACING SEATED  
PASSENGER



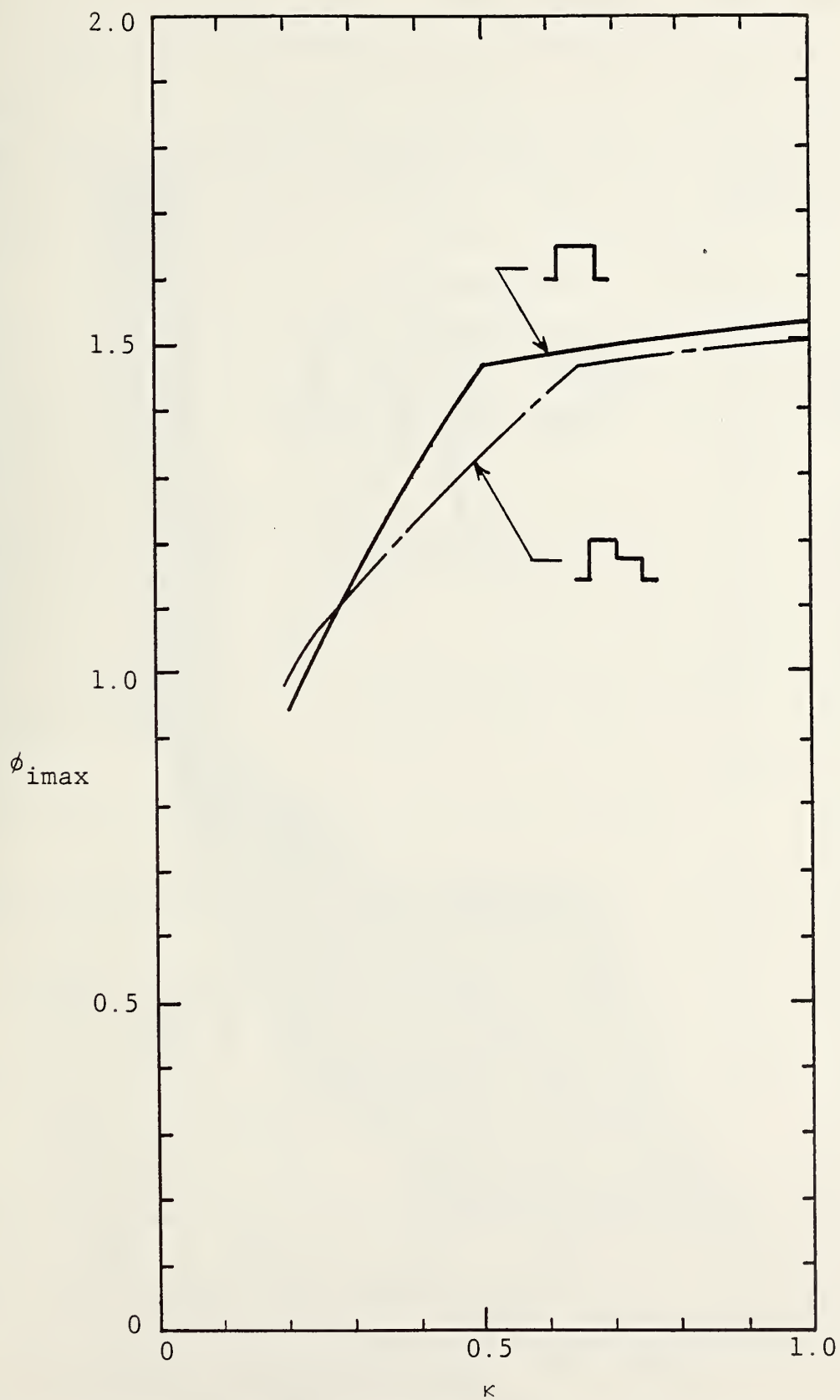


FIGURE 47. INFLUENCE OF PULSE SHAPE ON IMPACT VELOCITY

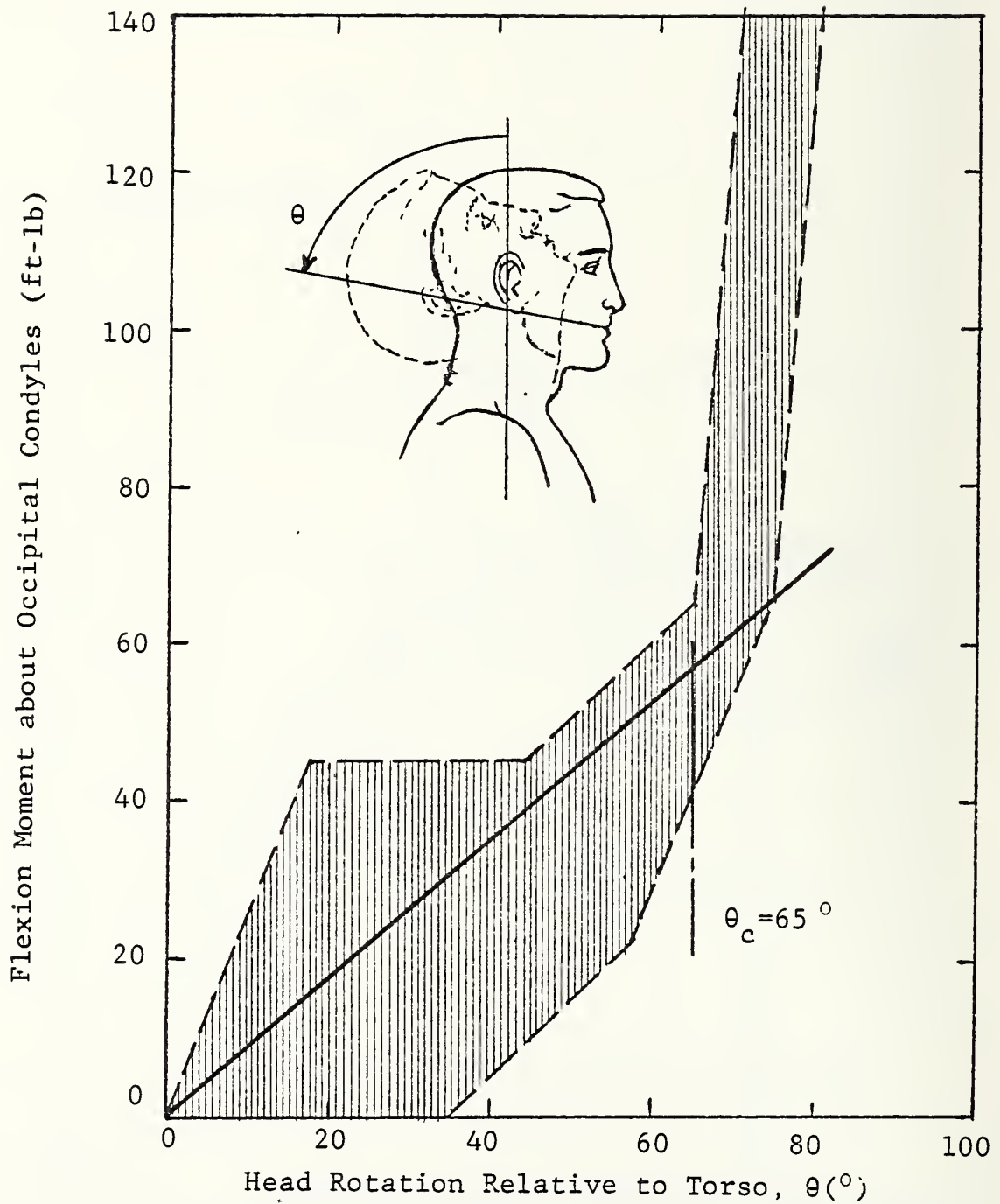


FIGURE 48. FLEXION RESPONSE ENVELOPES  
FOR 50TH PERCENTILE ADULT MALE

No attempt was made to simulate the increased resistance which occurs at large rotations since the energy involved in this additional rotation is not excessive and is small compared to the uncertainty of the rotation resistance at smaller angles of rotation. Furthermore, a conservative critical angle,  $\theta_c$ , of 65 degrees (1.135 rad) was selected as the injury threshold. In this manner the analysis is rather conservative. The other pertinent anthropometric data were presented in Section 4.3.

The basic equation and initial conditions used for the pinned hip model (see Section 4.5.2) apply for this model, except that the moment equation must be expanded to include the rotational resistance term, namely

$$M = G(z-x) - yF - B\theta \quad (111)$$

and the basic differential equation becomes

$$\ddot{\theta}(1+\alpha) = -\frac{\ddot{x}}{D} \cos\theta - \frac{B\theta}{WD^2} \quad (112)$$

which when rewritten in its dimensionless form for the two train motion phases become

$$\lambda \frac{d\lambda}{d\theta} (1+\alpha) = \kappa \cos\theta - 2\kappa\epsilon\theta, \quad 0 \leq \tau \leq \tau_0 \quad (113)$$

and

$$\lambda \frac{d\lambda}{d\theta} (1+\alpha) = 2\kappa\epsilon\theta, \quad \tau_0 \leq \tau \quad (114)$$

where

$$\epsilon = \frac{B}{2WV_0^2\kappa} = \frac{B}{2a_0 WD} \quad (115)$$

Integration of equation (113) yields

$$\lambda = \sqrt{\frac{2\kappa}{1+\alpha}} \sqrt{\sin\theta - \epsilon\theta^2}. \quad (116)$$

Note that the parameter  $\epsilon$  involves the acceleration  $a_0$ . If  $\kappa$  is small, which will be the case for long duration acceleration pulses ( $\tau_0$  large), the maximum neck rotation will occur during the first phase. The maximum value of  $\theta$  can then be obtained simply from

$$\epsilon = \frac{\sin\theta}{\theta^2} \quad (117)$$

or more importantly a critical value of  $\epsilon$ , say  $\epsilon_c$  can be evaluated corresponding to the critical (threshold) value of  $\theta$ , namely  $\theta_c$ . In this manner a critical or limiting value of  $a_o$  can be determined, namely

$$a_{o,c} = \frac{B}{2\epsilon_c W D}, \quad (118)$$

For the anthropometric values used the limiting acceleration is 11.8 g and  $\epsilon_c = 0.705$ . Since most train crash environments are expected to have average decelerations considerably less than this amount it would appear the whiplash injuries will be minimal.

For extremely high train decelerations (i.e., the instantaneous stopping) the limiting solution  $\kappa \rightarrow \infty$  will be of value. As before the second phase equation ( $\tau_o \leq \tau$ ) applies with the special boundary condition ( $\lambda(0) = 1$ )

$$\lambda = \sqrt{1 - \frac{\gamma}{1+\alpha} \theta^2} \quad (119)$$

where

$$\gamma = 2\kappa\epsilon = \frac{B}{WV_o^2}. \quad (120)$$

There exists a corresponding critical value for velocity change  $V_{o,c}$  which will limit  $\theta$  to the critical value  $\theta_c$ , namely

$$V_{o,c} = \sqrt{\frac{\theta_c^2 B}{(1+\alpha)W}}. \quad (121)$$

Since  $\alpha = 0.3$ ,  $\gamma_c = 1.01$  and  $V_o = 12.6$  fps.

Using the general relationship (equation (72)) for the dimensionless time, we can again define

$$\lambda(\tau_o) = \lambda_1 \quad (122)$$

and

$$\theta(\lambda_1) = \theta_1 \quad (123)$$

and integrate the basic equation for the second phase. This results in

$$\lambda = \sqrt{\lambda_1^2 + \left[ \frac{2\epsilon\kappa}{1+\alpha} \right] \left[ \theta_1^2 - \theta^2 \right]}, \quad \tau_0 \leq \tau. \quad (124)$$

Typical results of the angular history of the head are presented in Figure 49. Maximum rotation contours are presented in Figure 50(a) and when compared with  $\theta_c$  permit the mapping of "safe" and "unsafe" domains in the  $\kappa$ - $\epsilon$  plane. These domains are presented in Figure 50(b). The safe region, when mapped in the train crash domain (see Figure 51) provides an immediate impression of the low hazard that backward facing seated passengers are exposed to in typical crash environments.

#### 4.7 Sideward Facing Seated Passenger

The last of the passenger configurations studied is that of the sideward facing seated passenger. The body bar representation was again selected to describe the primary motion characteristics of this passenger configuration to the sudden deceleration of the train car. Figure 52(a) illustrates the passenger motion. The whole body c.g. for this seated condition is just above the apparent point of rotation and since no lofting effect is expected a pinned body bar (at point A) representation was used. The basic equations are identical to those presented in Section 4.5.2 for the forward seated passenger. However, in this configuration the anthropometric variables are numerically different and thus the corresponding parameter values are substantially different. The moment of inertia of the seated whole body is larger and the characteristic dimension D is somewhat smaller; thus  $\alpha \approx 11$  to 17 and the range of  $\kappa$  of interest is approximately 0.02 to 0.10. Furthermore the H/D ratio is larger, approximately 10.

The dimensionless angular velocity is smaller due to the smaller value of D. Typical results for the angular velocity are presented in Figure 53. The dimensionless impact velocity  $\phi_{imax}$  is approximately the same as for the forward facing seated passenger. The results are presented in Figure 54 and a range of  $\alpha$  values and impact rotation angles of  $\theta_i = 0.4, 0.5, \text{ and } 0.6$  rad.



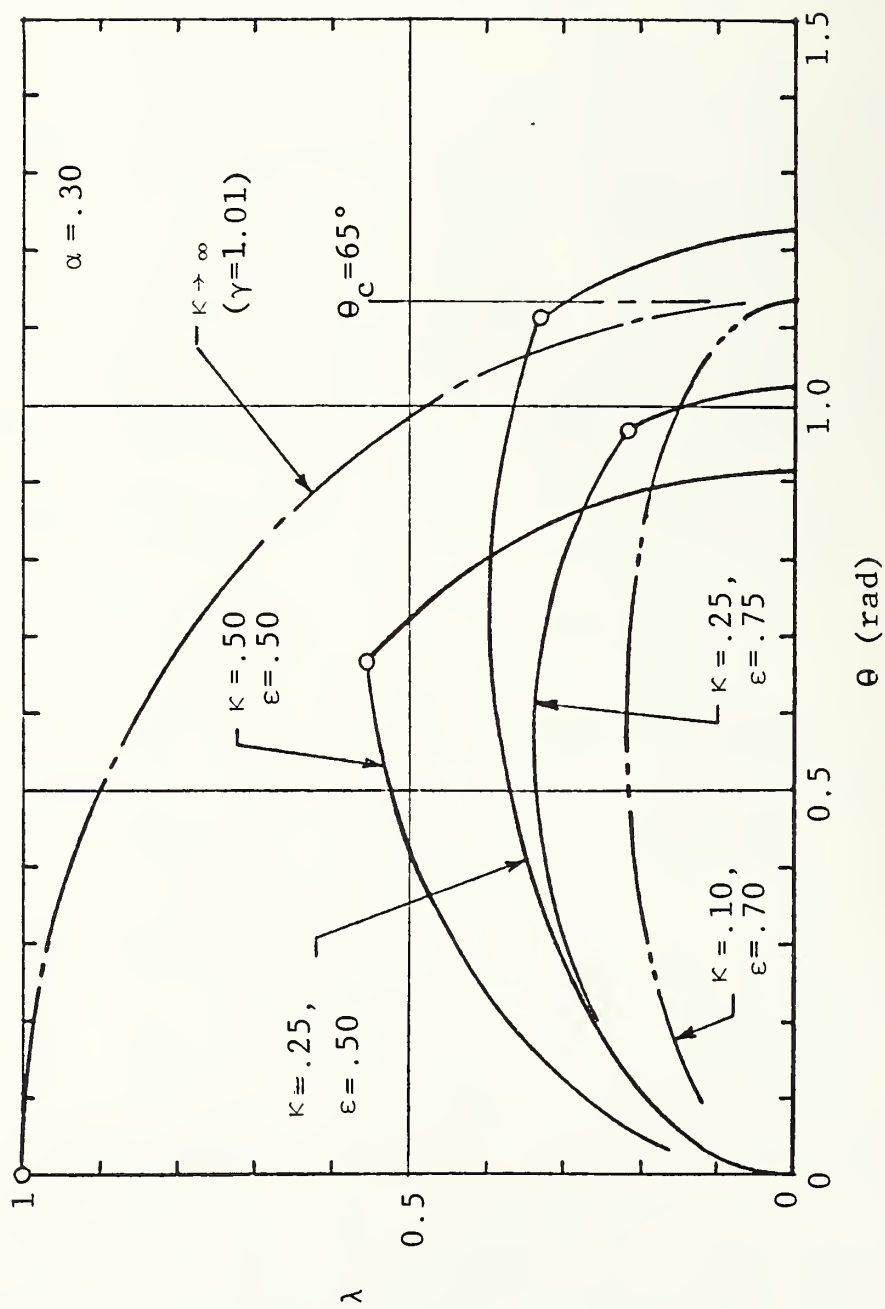


FIGURE 49. ANGULAR VELOCITY HISTORY FOR NECK MODEL

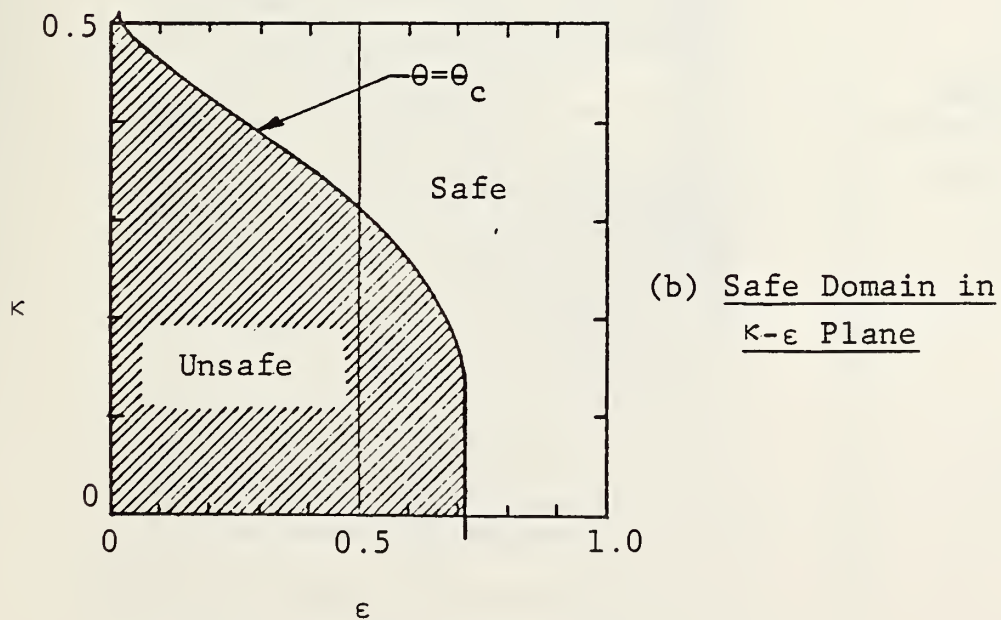
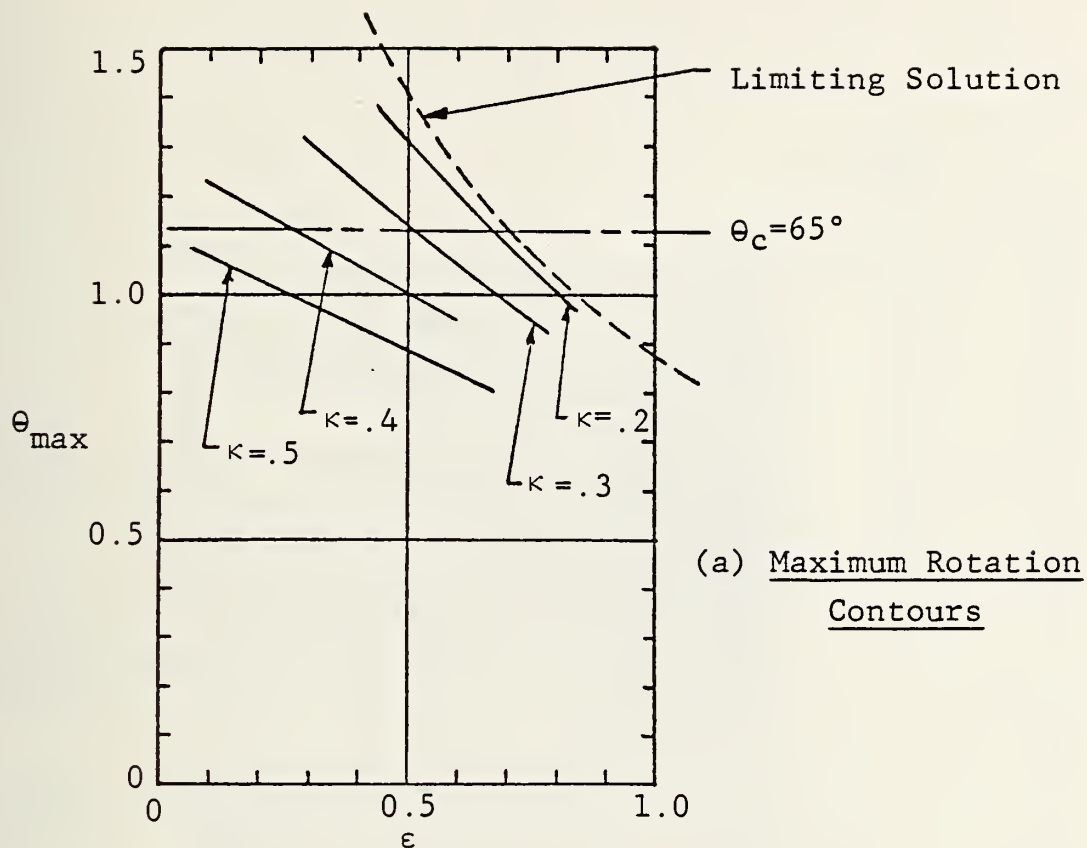


FIGURE 50. RESPONSE CHARACTERISTICS OF NECK MODEL

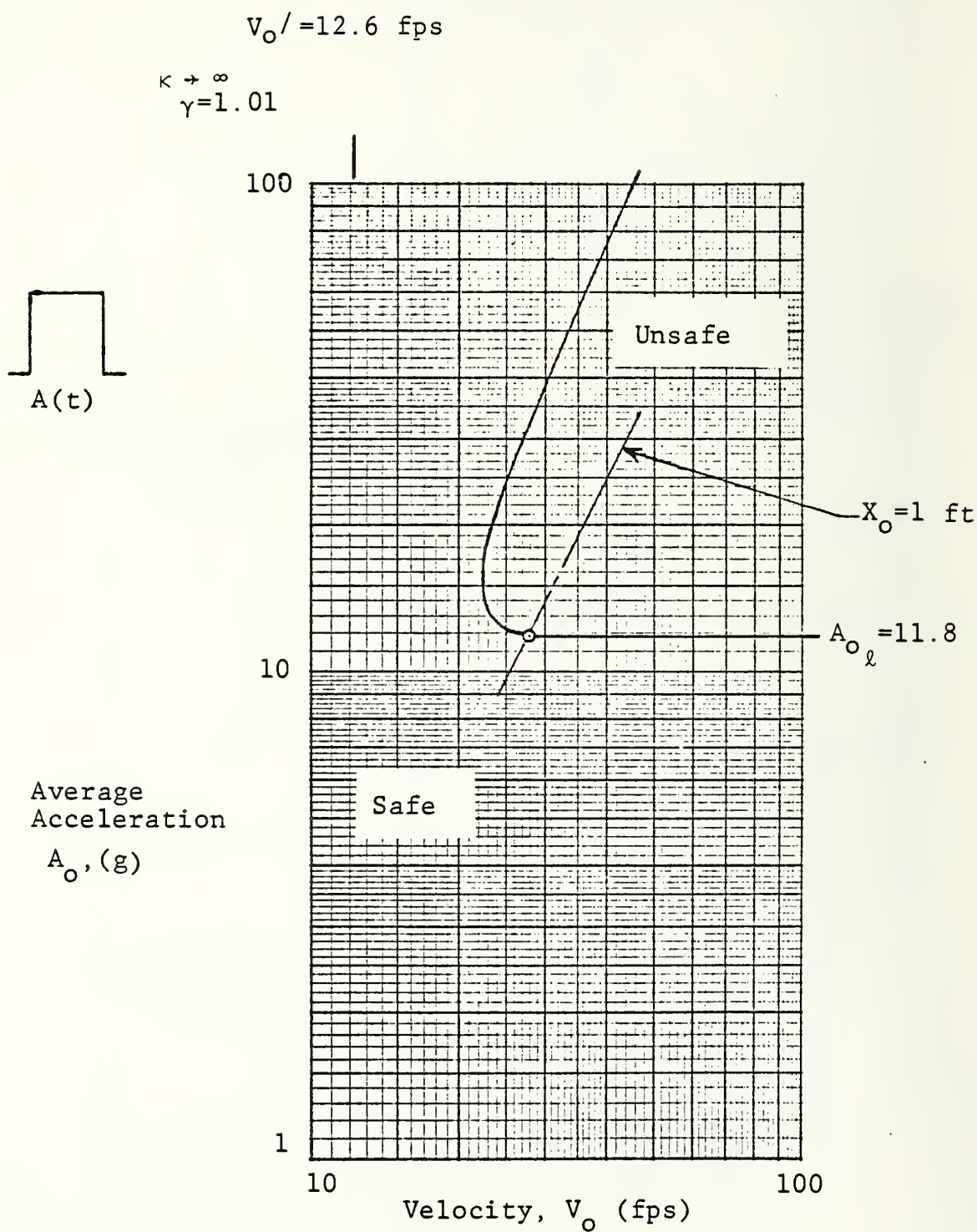
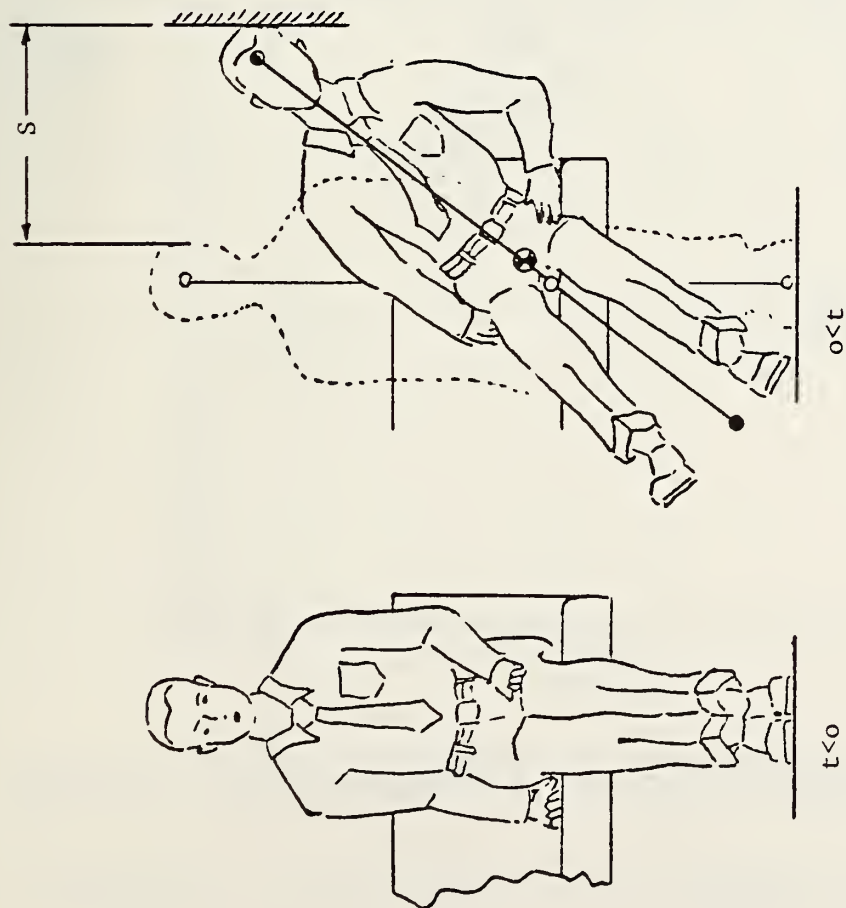
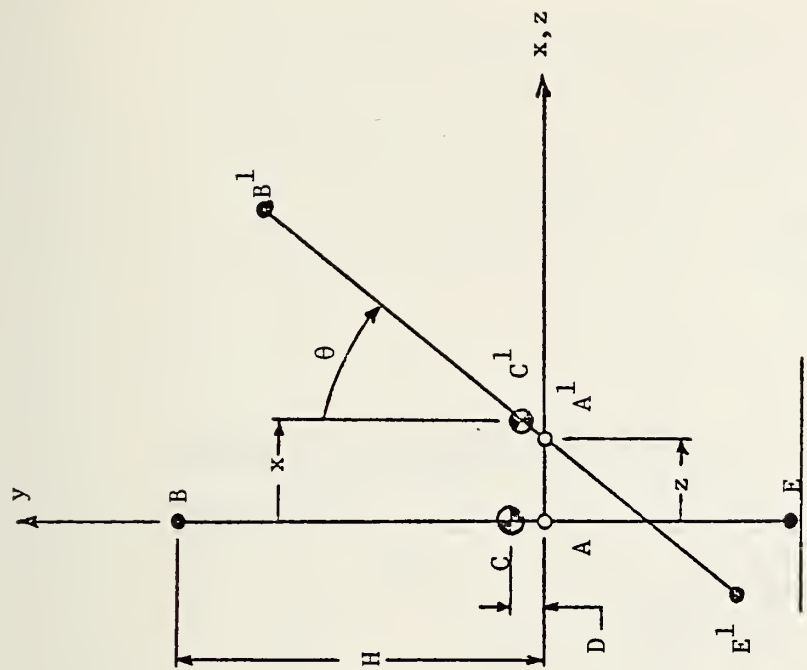


FIGURE 51. SAFE REGION IN TRAIN CRASH DOMAIN  
FOR BACKWARD FACING SEATED PASSENGERS



(a) Physical Configuration



(b) Body Bar Representation

FIGURE 52. PINNED HIP MODEL FOR SIDEWARD FACING SEATED PASSENGER

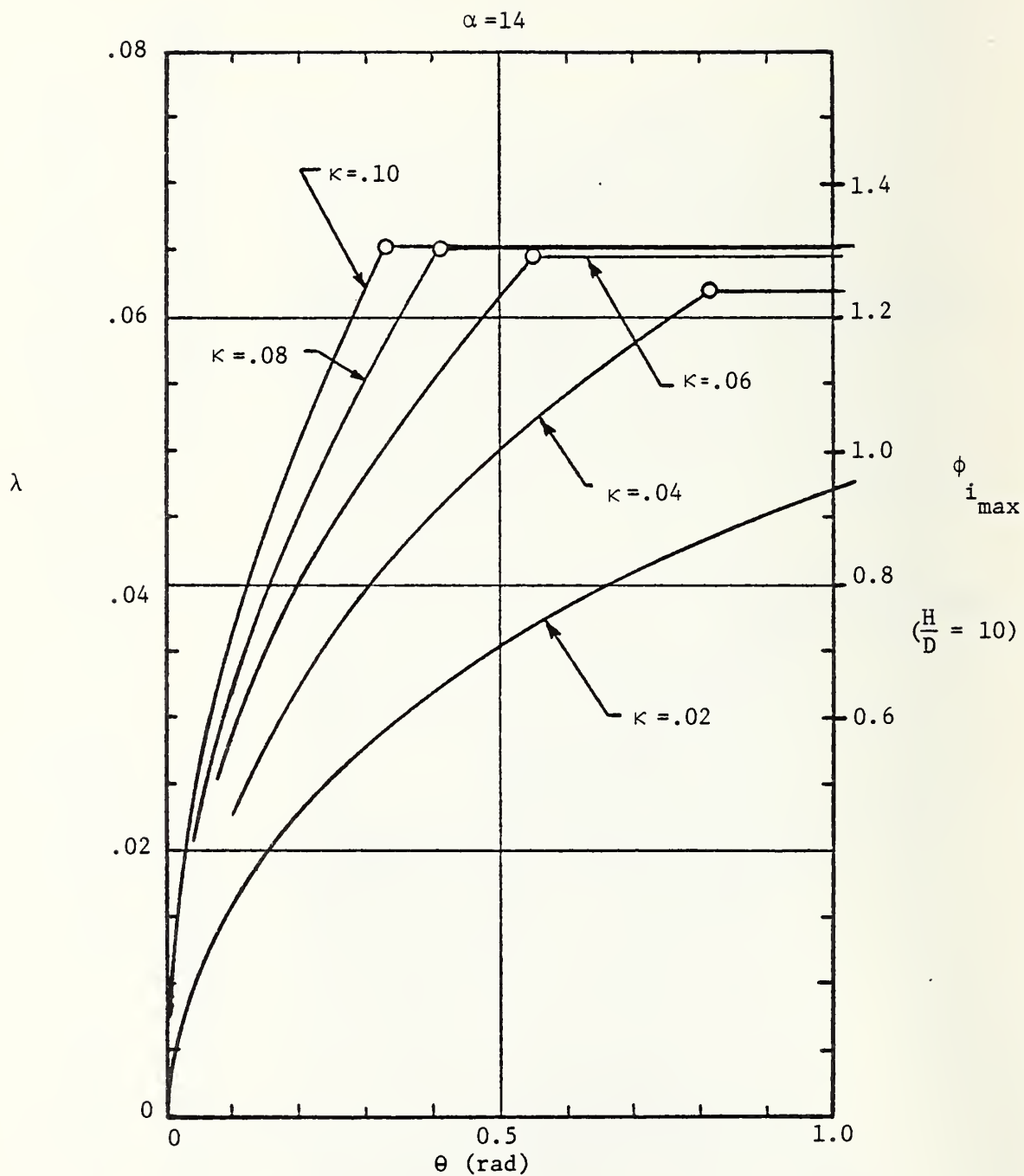


FIGURE 53. ANGULAR VELOCITY FOR SIDEWARD SEATED PASSENGER



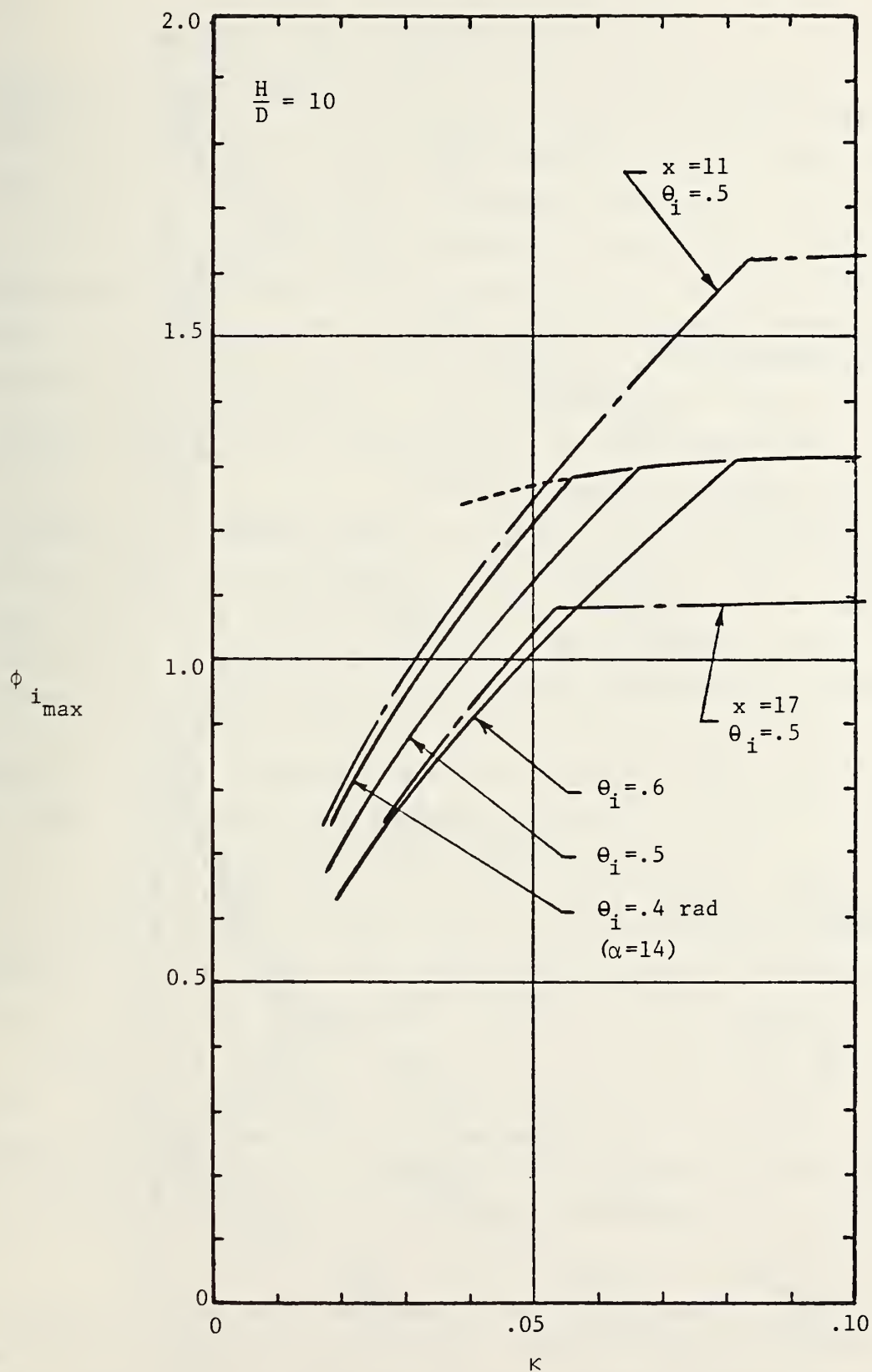


FIGURE 54. IMPACT VELOCITY FOR SIDEWARD SEATED PASSENGER

#### 4.8 Multiple Passenger Interactions

It is quite evident that whenever train cars are crowded, as they frequently are during the peak hours, that standing passengers in particular will bump into each other during a crash exposure. Whereas an isolated passenger may impact a barrier once, interactions with nearby passengers may cause additional impacts, involving the same body component. The secondary passengers who are isolated from the barrier (wall or floor) by another passenger may only experience a crush environment and may not be subjected to any significant impact condition. The concern then is for the primary passenger who is adjacent to the barrier and who may experience multiple impacts.

The approach used herein to attempt to obtain a measure of the increased hazard that passenger interactions may cause to a given passenger is to examine the multiple impact conditions which may result from a short series of multiple passenger interactions and to examine the potential increase that such impact environments may have upon injury criteria, such as the severity index. It is clear, at the onset, that the multiple impact scenario selected is but one of many and that it does not necessarily represent a very severe scenario. It is recognized that these multiple impacts will occur over a time interval for which no injury criteria are directly applicable. When a so-called total severity index is formulated by summing the contribution from individual impacts, it is understood that any interpretation of the final result can only be used as a very rough indication of the effect of multiple impacts. Two barrier types (the perfect absorber and the elastic response barrier) were selected for analysis and the passenger-passenger interaction was assumed to be inelastic such that the masses associated with the passengers remained in contact. The total momentum was conserved.

The path diagram for the first case, the perfect absorber, is illustrated in Figure 55(A). The primary passenger, P1 of weight  $W_1 = W$  impacts the barrier at a velocity  $V_0$ . Thus the severity

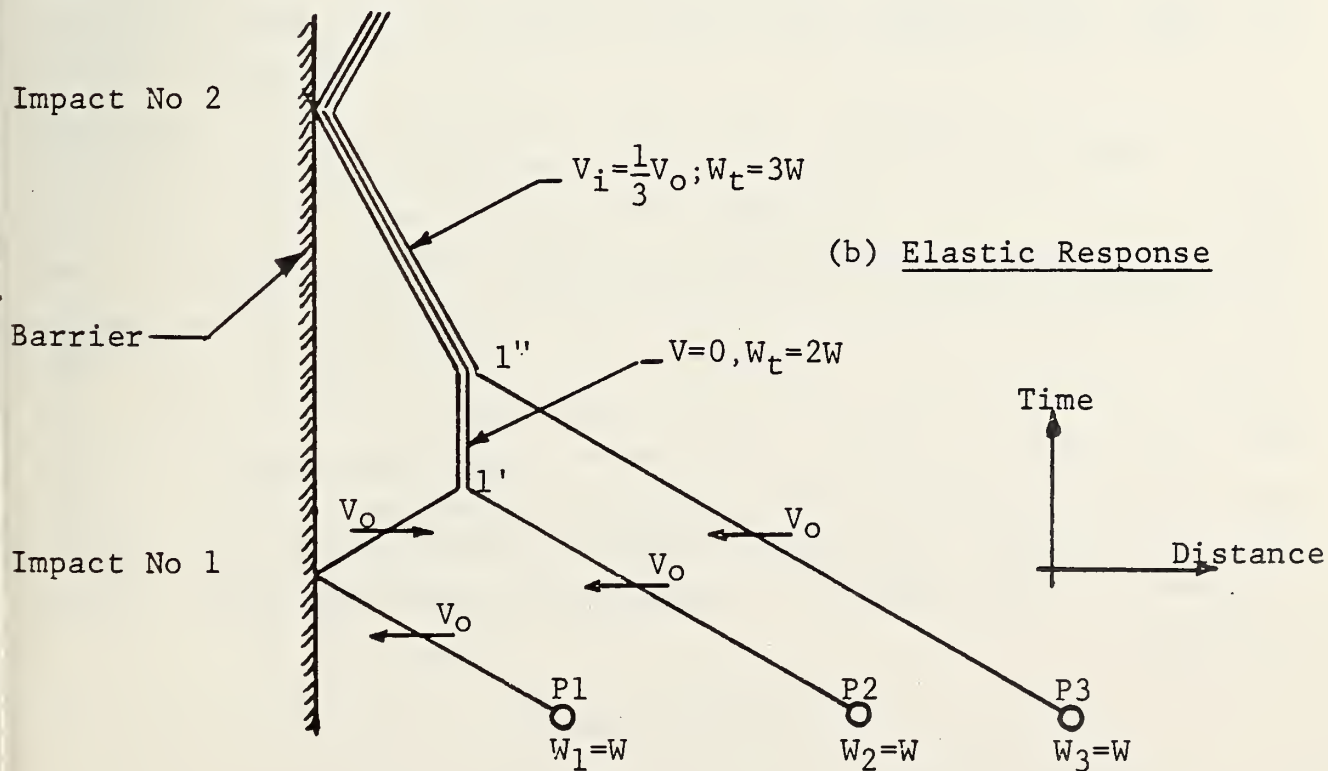
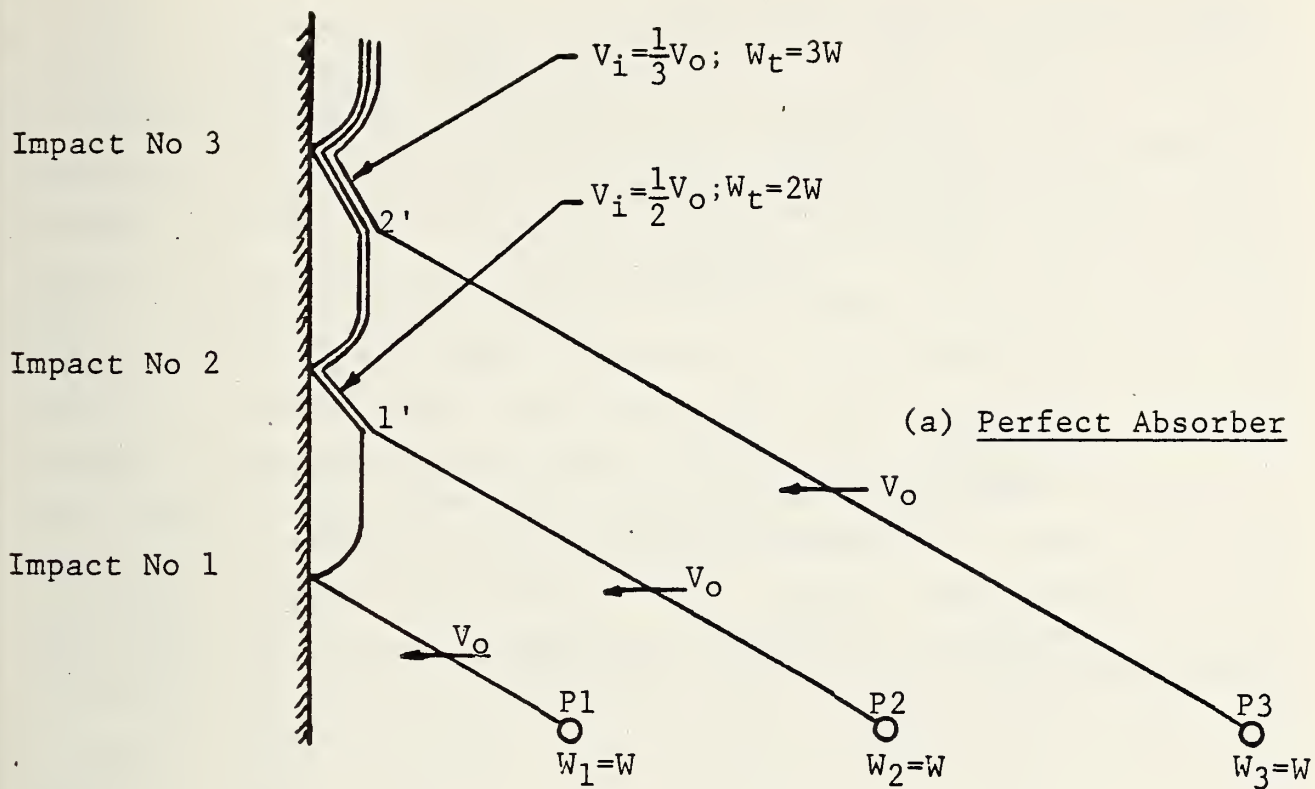


FIGURE 55. PATH DIAGRAMS FOR MULTIPLE IMPACT EVALUATION

index takes on a value  $(SI)_0$  which is proportional to  $V_i = V_0$  and inversely proportional to  $W^{1.5}$ . The remaining parameters of the severity index are assumed to be constant. The body component is assumed to separate slightly from the barrier and come to rest. The second passenger P2 with the weight and velocity indicated, impacts inelastically upon the primary passenger and both move at the velocity  $1/2 V_0$ , the impact velocity for the second impact. Using the increased weight and the decreased velocity, yields a second severity index of  $0.18 (SI)_0$  such that current total severity index is  $1.18 (SI)_0$ . If only the original body component weight  $W$  is involved (such as it might be for the head), the current total severity index is increased at this time to  $1.5 (SI)_0$ . The former value appears small enough to indicate that little additional hazard is produced by multiple passenger interactions (note that five interactions yield a total severity index of only  $1.29 (SI)_0$ ). The latter total severity index (i.e., the head impact) value is sufficiently large to be of some concern. While it may be unlikely that more than two head impacts may occur at one general location of the head, it is difficult to rule out a double head impact event.

A similar evaluation was made using an elastic responding surface (see Figure 55(b)). The body component leaves the barrier with a velocity  $V_0$  after the first impact such that the first passenger-passenger impact results in both passengers being at rest a short distance from the barrier. The collision of a third passenger then causes a barrier impact at a velocity of  $1/3 V_0$ . The current total severity index only increases to  $1.06 (SI)_0$  for the same body component weight. If a larger weight were used such as  $3W$  then the total severity index would be even smaller. In this second case the passenger interaction effect is clearly not significant, at least not with respect to injury due to body component impact phenomena.

#### 4.9 Nomenclature

a	acceleration
$a_0$	average acceleration
$a_0^*$	peak acceleration



$a_1$	specific value of acceleration for double step pulse
$a'$	retarding acceleration
$a_{0,c}$	critical value of acceleration for flexion response
$B$	rotational resistance for head rotation
$D, D'$	characteristic body dimensions
$F$	horizontal force
$G$	vertical force
$H$	body dimension, height of standing passenger
$\bar{H}$	mean height of standing passenger
$I$	moment of inertia
$\bar{I}$	mean value of moment of inertia for standing passenger
$k$	spring constant
$L$	body dimension
$\bar{L}$	mean value of body dimension for standing passenger
$M$	moment
$s$	slip distance
$S$	body dimension, obstacle spacing
$\bar{S}$	mean value of body dimension for standing passenger
$SI, (DI)_0$	severity index
$t$	time
$t_0$	pulse duration
$t_1, t_2$	time parameters for pulse shape
$t'$	time at which slip ceases
$t_i$	time of impact
$V$	velocity
$V_0$	change in velocity
$V_i$	impact velocity
$V_{0,c}$	critical value of velocity for flexion response



$\Delta V$	change in velocity when slip ceases
$\Delta V_x$	velocity perturbation
$V_A, V_B$	velocity contribution due to rotation
$V_A^*, V_B^*$	total velocity
$V_h, V_t$	specific velocity components
$V_{zr}$	relative velocity in horizontal direction
$w$	body dimension, displacement
$\bar{w}$	mean value of body dimension for standing passenger
$W$	whole body or body component weight
$\bar{W}$	mean value of whole body weight for standing passenger
$W_1, W_2, W_3$	weight
$W_T$	total weight
$x$	displacement
$x_o$	stopping distance
$x_b$	barrier distance
$x^*$	passenger location
$\dot{x}_3, \dot{x}_{c.g.}$	velocity components for tumbling block
$x'$	train displacement when slip ceases
$y$	displacement
$z$	displacement
$z'$	passenger displacement when slip ceases
$\alpha$	inertia parameter, acceleration parameter
$\alpha_c$	specific acceleration parameter
$\beta$	stopping distance parameter
$\delta$	acceleration parameter
$\gamma$	acceleration parameter, parameter for flexion response

$\gamma_c$	critical value of parameter
$\epsilon$	acceleration parameter for flexion response
$\epsilon_c$	critical value
$\sigma$	scaling factor, spacing parameter
$\tau$	time
$\tau_0$	pulse duration
$\tau'$	time when slip ceases
$\tau_1, \tau_2$	time parameter for pulse shape
$\lambda$	scaling parameter, angular velocity
$\lambda'$	specific value
$\lambda_0$	specific value when slip ceases
$\lambda^*$	parameter
$\omega$	angular velocity
$\theta$	rotation
$\theta_i, \theta'_i$	rotation at impact
$\theta_1$	specific value
$\theta_c$	critical value
$\zeta$	displacement
$\zeta^*$	passenger location
$\chi$	velocity of train
$\phi_i$	impact velocity
$\phi_{imax}$	maximum impact velocity
$\phi_z, \phi_{zr}, \phi_y$	velocity components

## 5. PASSENGER INJURY PREDICTION METHODOLOGY

### 5.1 General Approach

A computer program based upon the preceding motion and response analyses was prepared to conveniently evaluate injury profiles of passenger groups experiencing an intracity train crash. The objective of the methodology is to evaluate the potential consequences of such a crash as a function of the crash environment, car design, car interior component design and arrangements, and other factors. The computer program "Intra-City Crash Injury Analysis" is presented and documented in the appendix of this volume. The documentation includes a description of the required input data format as well as the output data format. This section presents the overall structure of the code and the general philosophy used in treating each of the four basic passenger configurations. The results of a sample problem are then presented at the end of the section.

The basic structure of the passenger injury prediction methodology is presented in Figure 56 in terms of 11 activities. The activities define, in general, the specific tasks to be performed, data which are to be provided, or conclusions reached. This structure also illustrates the general flow of the calculation procedure and the interrelationships between certain activities.

Activity 1 is a statement of the passenger distribution with respect to the number of passengers. This information is given for each  $k$ th passenger configuration ( $K = 1, 4$ ), in each  $j$ th car in each  $i$ th consist. One or two consists can be specified defining a consist-consist crash or an abutment (or other nonpassenger entity)-consist crash situation.

Activities 2 and 3 deal with an analysis of the gross motion (i.e., car frame motion) of the individual cars of the consists and provides the basic excitation used for the passenger motion analyses. These data include the absolute values of both the change in velocity  $V_{oij}$  and the average acceleration  $a_{oij}$  for each

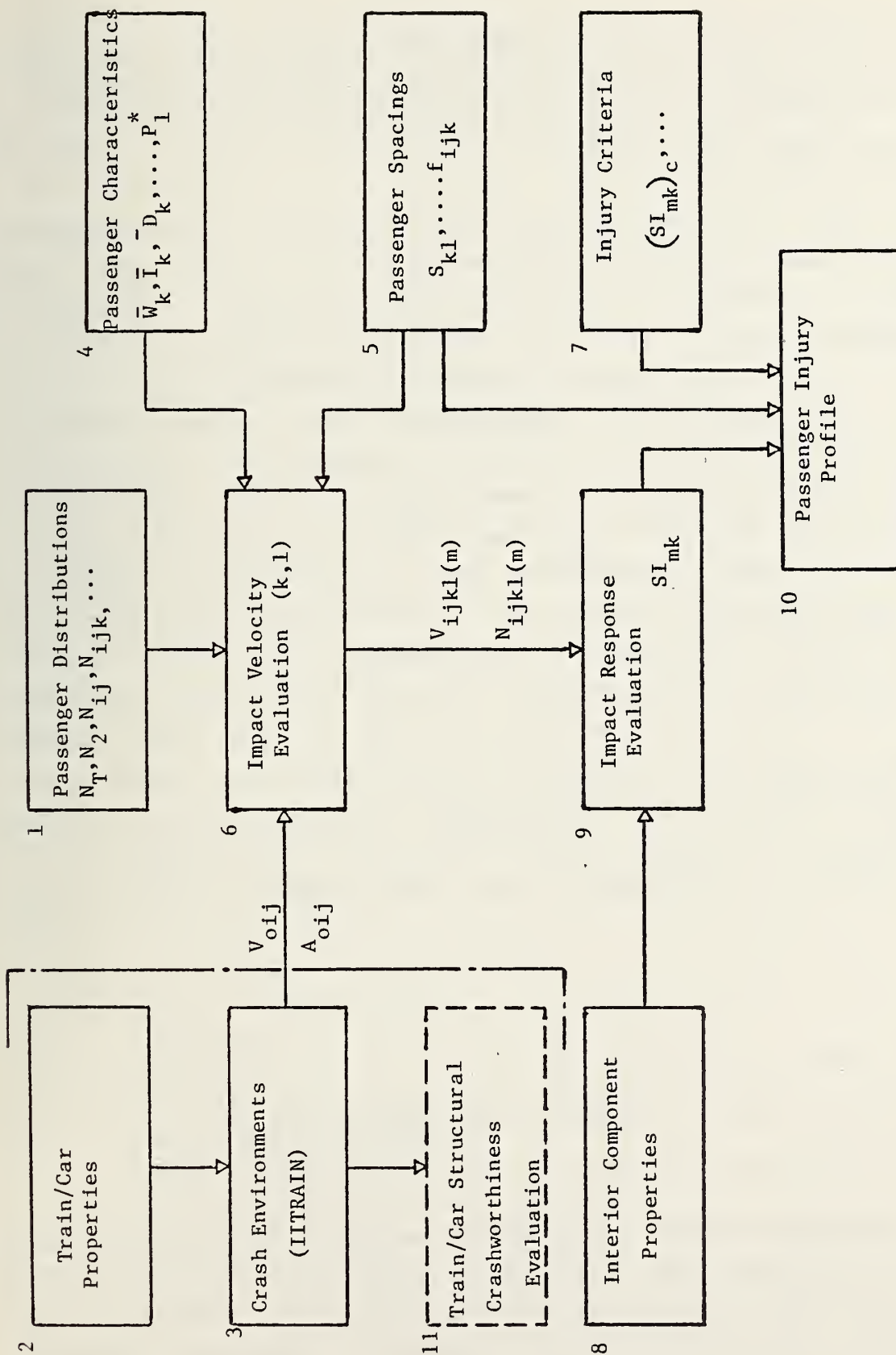


FIGURE 56. PASSENGER INJURY PREDICTION METHODOLOGY

car for each consist. These values correspond to the simple step-pulse form and can be provided in any given case by a crash analysis such as IITRAIN or for parametric studies, the values of  $V_{oij}$  and  $a_{oij}$  can be varied as desired.

Activity 4 represents input data relevant to anthropometric parameter values such as mean weights of a particular body component and related distribution characteristics. The specific values used in each of the basic passenger configurations will be discussed in the appropriate section of this chapter as they are required. In examining the influence that the response characteristics of the surface/structure at the impact point has upon the levels of injury produced it became clear that the value of the impact velocity was significant and that care should be taken to establish the value as accurately as is feasible within the limits of the known details of the event. Furthermore, the analysis of passenger motions indicated that variances in the impact velocity would occur due to anthropometric variances and other uncertainty factors such as slip and passenger alertness. For these reasons the specific passenger population in any basic event (that is the  $i$ th consist,  $j$ th car, and  $k$ th passenger configuration) was further subdivided into 10 equal percentile subpopulation groups and the impact velocity  $V_i$  assigned to each subpopulation group was given as

$$V = V_o \bar{\phi}_i P_{\ell}^* \quad (125)$$

where

$V_o$  = change in velocity of car

$\bar{\phi}_i$  = mean value of dimensionless impact velocity

$P_{\ell}^*$  = distribution factor for  $\ell$ th subpopulation group.

In this manner the value of the impact velocity was allocated in a distributed fashion over the basic population to appropriately reflect the totality of variances which will exist. The anthropometric data, in many instances, appears to follow a "normal" distribution and therefore, the "normal" distribution function was



assumed to apply for all uncertainties in their aggregate. This function is illustrated in Figure 57 as curve A and its integrated or accumulative form as curve B. The unit of standard deviations was used in this representation where the mean (most probable) value corresponds to the value zero. The corresponding incremented form for curve B is shown (as a dotted line) to illustrate the resolution achieved by this number of subpopulation groups and therefore to justify the selection of 10 subdivisions. The general approach used to establish the values of  $P_{\ell}^*$  is illustrated in Figure 58. The standard deviations to mean value ratio ( $\Delta/\bar{\phi}$ ) was estimated for the dimensionless impact velocity functions,  $\bar{\phi}_i$ , for both the forward facing and sideward facing passenger configurations. Since the ratios for each of these configurations were similar a single set of  $P_{\ell}^*$  values were selected for use in the methodology. Furthermore, since the factor is symmetric about the mean value only five specific values needed to be specified. These five are given in the "fixed" data section as PF(1) to PF(5). The remaining values (to PF(10)) are computed in the preliminary calculation section of the code.

Activity 5 represents the introduction of passenger spacing details and other means for dealing with anthropometric variations or the likelihood of reducing or eliminating the injury. These details will be presented in the corresponding section of this chapter for each of the basic passenger configurations.

Activity 6 corresponds to the establishment of the impact velocity  $V_{ijk\ell(m)}$  or its equivalent applicable to the number of passengers  $N_{ijk\ell(m)}$  in the  $\ell$ th subpopulation group involving the  $m$ th body component. Different procedures were used in each of the basic passenger configurations.

Activity 7 consists of the introduction of threshold values SIC separating each of the adjacent injury level categories for the severity index. The values for the head, face and chest as indicated in Figure 3 were used and are included in the "fixed" data section of the code. Whiplash type neck injuries were arbitrarily

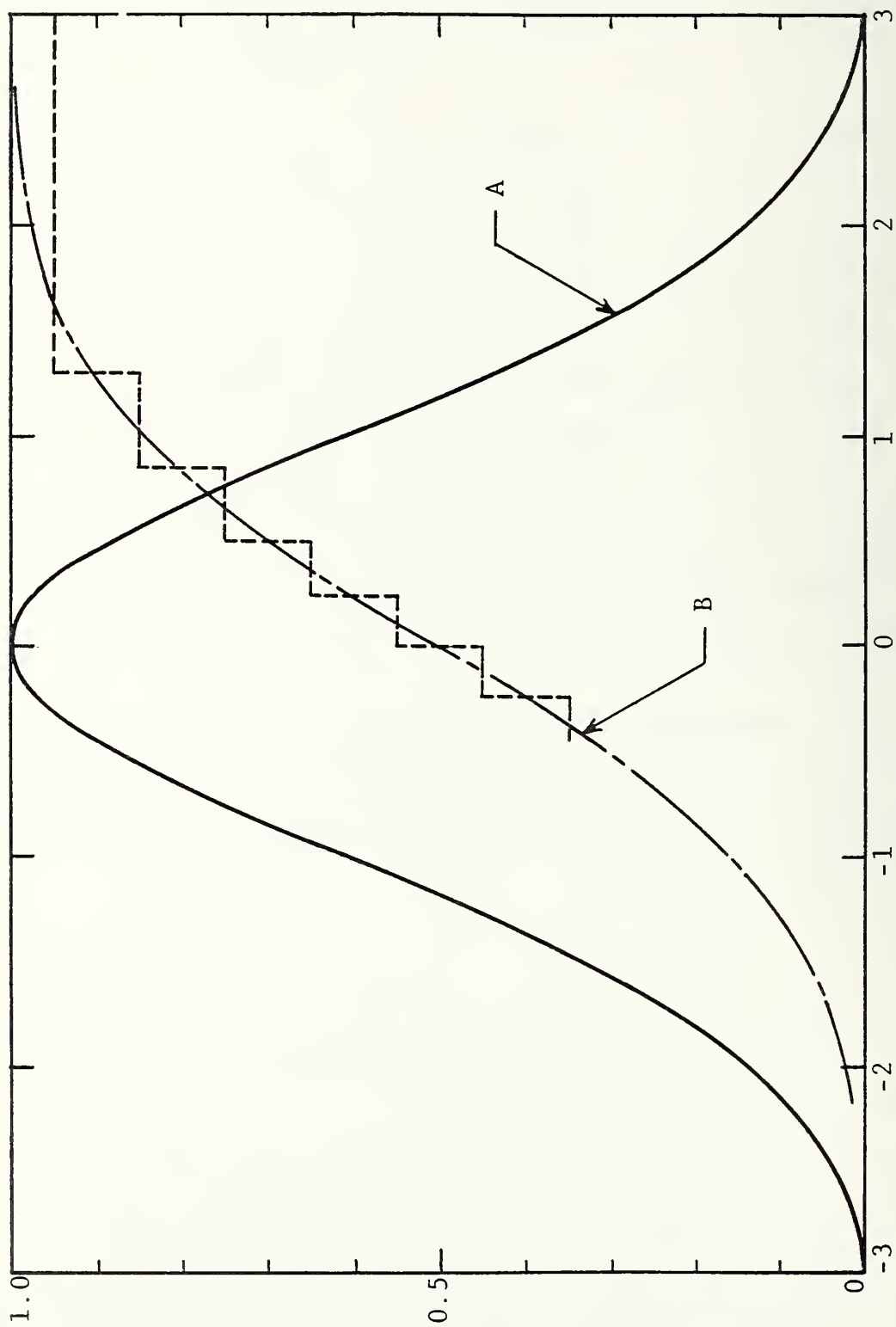


FIGURE 57. NORMAL DISTRIBUTION FUNCTION

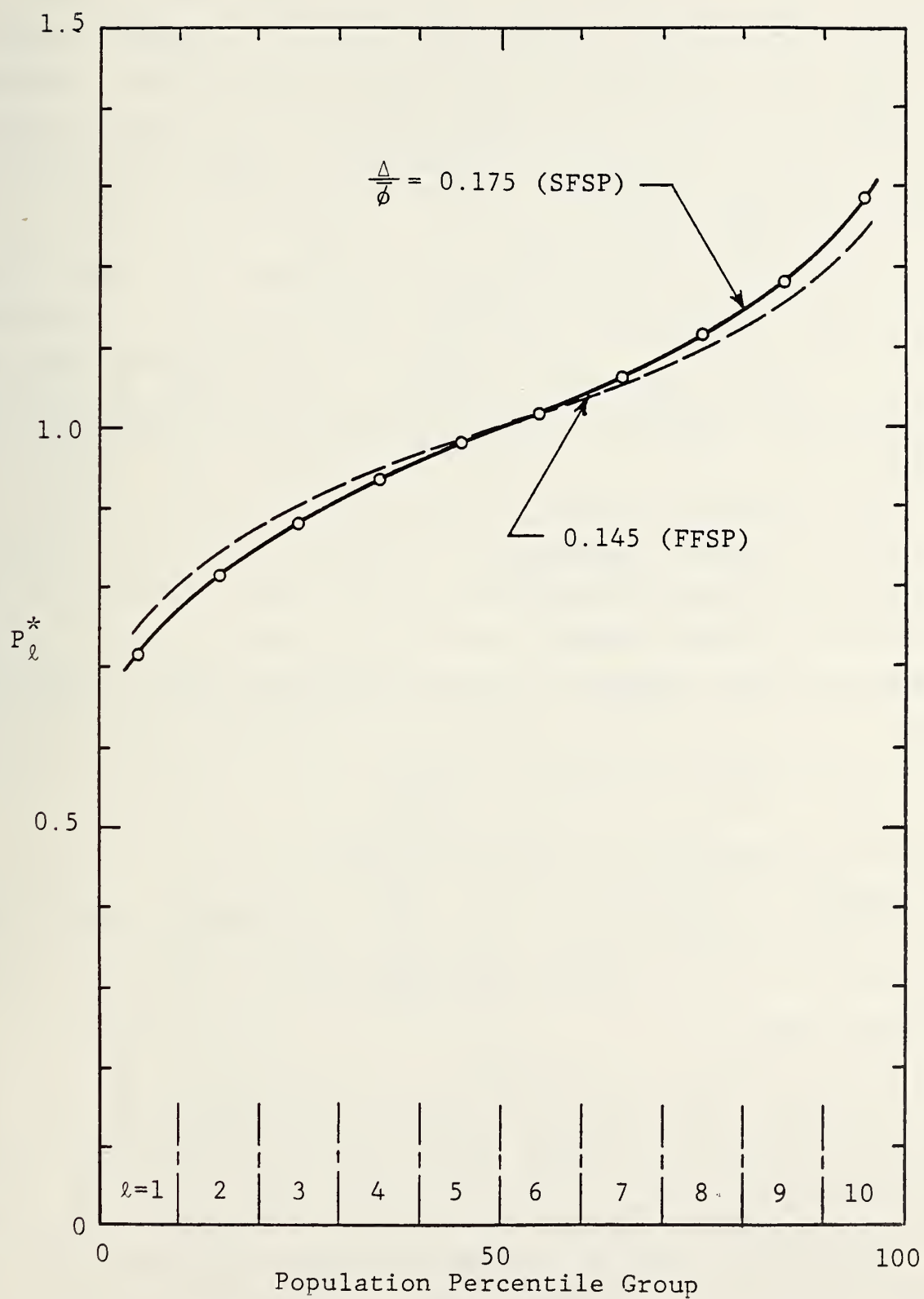


FIGURE 58. DISTRIBUTION FACTOR FOR POPULATION GROUPS

limited to the two lower injury levels of minor and moderate. The critical acceleration (see equation (40)) of 12 g was selected as the threshold value separating "no injury" from "minor injury" and a corresponding value of 20 g was selected for the minor/moderate boundary. An upper limit control value of 100 was used to limit the injury levels to "moderate". These data are also included in the fixed data section of the code.

Activity 8 consists of the introduction of data for the properties of the interior components of the car. It has been assumed that each car in each consist is identical thus this data group is "input" for each consist. Four types of interior components are treated and defined as follows by a component index JR where

- JR = 1 defines a panel
- JR = 2 defines a seatback
- JR = 3 defines a stanchion
- JR = 4 defines a floor

Furthermore, each component type is assigned a response index, IR, where

- IR = 1 defines a perfect absorber
- IR = 2 defines an elastic response
- IR = 3 defines an inelastic response

Two response constants, RC1 and RC2, are needed to define the response of any given impact situation. RC2 is only required for the inelastic response case. These data are user input on a problem to problem basis.

Activity 9 is that activity which computes the value of the severity index corresponding to the sub-subpopulation group for which the stimuli have been determined. A subroutine IMPACT performs this task given the impact value, the structure type, and the corresponding structure parameter values. Two anthropometric constants AH and WH corresponding to the contact area and the weight of the head are used in this subroutine. These constants are introduced into the fixed data section of the code.



Activity 10 is that activity which constructs the passenger injury profiles. A subroutine COMPAR compares the computed severity index SIA for each sub-subpopulation group with the critical values, SIC, for the corresponding mth body component and accumulates the number of passengers which sustain a given level of injury. Since the population group is generally small the number of passengers which appear in any injury level may appear as a decimal quantity. The proper interpretation of this number is the probabilistic interpretation. Thus when the results indicate that 10.8 passengers (out of a total of 631) sustain an injury of "moderate intensity" it means that the probability of sustaining such an injury is 0.017 for the totality of details prescribed by the problem. The passenger injury profiles are represented in terms of the number of passengers sustaining a given level of injury for each kth passenger configuration, in each jth car of each ith consist. These values are totaled twice to yield a breakdown by car and a summary for the entire crash. While it may be of interest to collect and print out more detailed injury profiles, such as by body component, or to express the profiles in terms of percents or probabilities or other entities, such an output format was not implemented at this time.

Activity 11 represents an evaluation of the structural crashworthiness of the cars involved in the crash and is outside the scope of this passenger injury prediction methodology task.

## 5.2 Standing Passenger

The motion details of the standing passenger were developed and evaluated in Section 4.4. A commonalty of behavior was found which indicated that if an impact with the floor occurred as a result of the motion that the impact velocity would be independent for all conditions examined (both car motion and anthropometric parameters). Thus a critical floor impact velocity, VIFC of 22.4 ft, was selected and introduced in the fixed data section of the code for this effect. The commonalty of behavior also



indicated that when impact with a barrier (panel or stanchion) occurred that the impact velocity for those parameters examined is equal to the sum of the initial car velocity  $V_o$  and a velocity increment  $\Delta V_x$ . The latter velocity increment depends upon the "time of flight" of the passenger; the time of flight was approximated by dividing the distance  $x_b$  between the passenger and the barrier by the car velocity  $V_o$ . This ratio, now expressed as

$$ZT = \frac{z_b}{V_o} = Z/VO \quad (126)$$

is used as the independent variable. The results shown in Figure 26 were expressed in an analytical form over two ranges of ZT as shown in Figure 59. These approximations are

$$\begin{aligned} \Delta V_x &= B1 + D1 (ZT), & 0 \leq ZT \leq C1 \\ \text{and} & & \\ \Delta V_x &= A1 - G1 (ZT - C1)^2. & C1 \leq ZT \leq E1 \end{aligned} \quad (127)$$

where

$$B1 = A1 - C1 (D1)$$

and

$$G1 = (F1 - A1)/(E1 - C1)^2.$$

The constants A1, C1, D1, E1, and F1 are incorporated into the fixed data section of the code. If ZT is greater than E1 then impact with the floor will occur at the impact velocity VIFC.

Figure 60 presents the program details for the standing passenger. The value of the index K is 1 for this passenger configuration and these steps are taken for the population group NPG(I,J,1), that is for each ith consist and each jth car. XF is the total number of passengers impacting upon the floor; hence, statement 133 represents an initializing step. The population is divided into 10 subpopulation groups equal to XL in number. These passengers will be distributed equally spacewise between the barrier or stanchion spacing SF (input data) for each ith consist. Statements 135 to 157 are repeated for each of these subpopulation groups. The spacing Z and the associated time ZT are then computed. IF ZT is greater

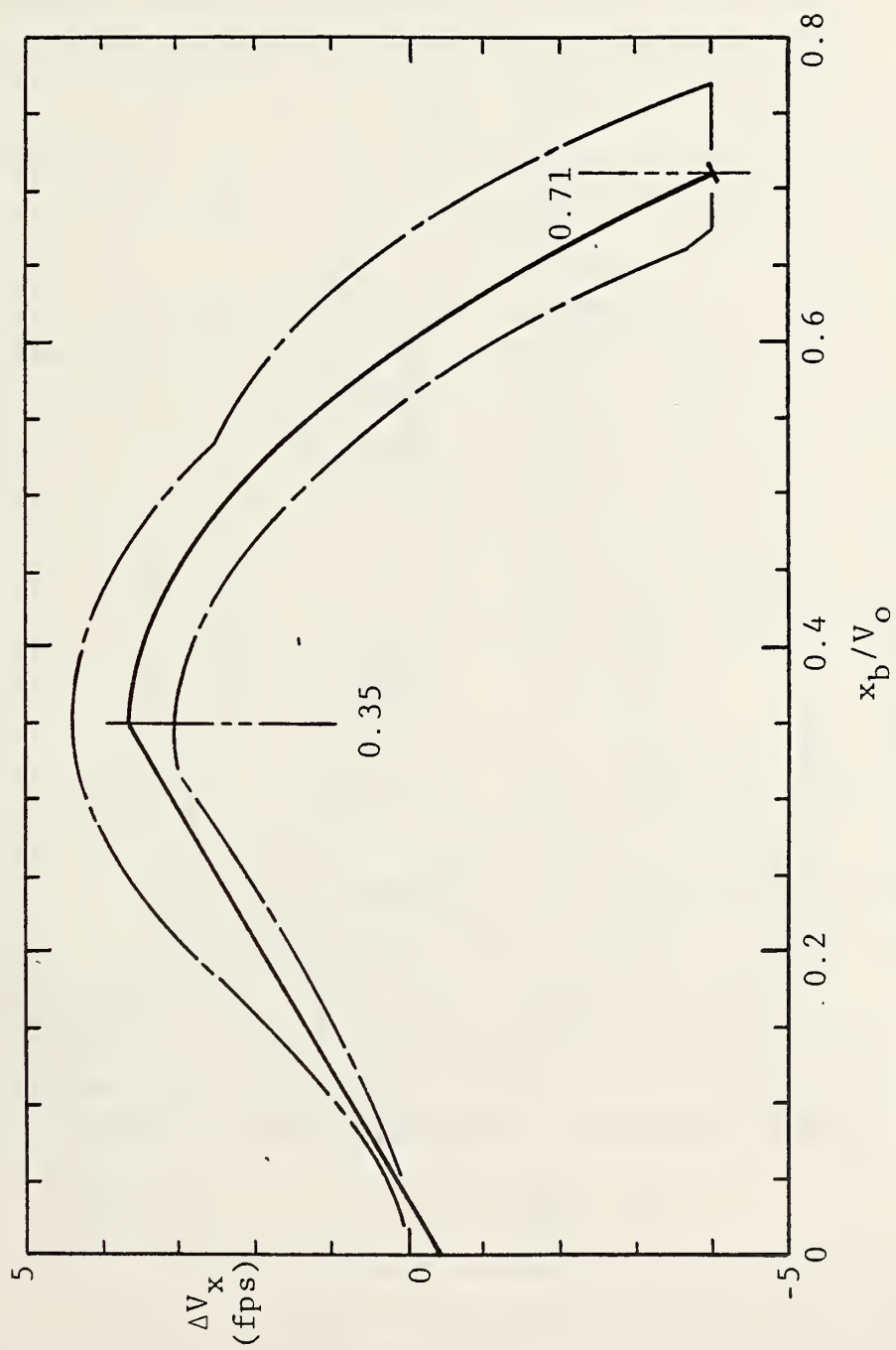


FIGURE 59. VELOCITY INCREMENT FOR STANDING PASSENGER

Statement Number

Statement

```

132*      K = 1
133*      XF = 0.
134*      XL = .1*FLOAT(NPG(I,J,K))
135*      DO 520 L=1,10
136*      Z = .1*SF(I)*FLOAT(L)
137*      ZT = Z/VO(I,J)
138*      IF (ZT.GT. E1)      GO TO 516
139*      IF (ZT.GT. C1)      GO TO 510
140*      VI = VO(I,J)*AMIN1(1.,SQRT(Z/XO(I,J)))+B1+D1*ZT
141*      GO TO 512
142*      VI = VO(I,J)*AMIN1(1.,SQRT(Z/XO(I,J)))+A1+G1*((ZT-C1)**2)
143*      CONTINUE
144*      DO 514      JR=1,3,2
145*      XR = XL*DF(I,J,K)
146*      IF (JR.GT. 1)      XR = .5*XL*(1.-DF(I,J,K))
147*      IF (JR.GT. 1)      XF = XF+XR
148*      XIG(I,J,K,1) = XIG(I,J,K,1)+XR*(1.-PH(1)-PH(2))
149*      CALL IMPACT (JR,SIA)
150*      DO 514      M=1,3,2
151*      XM = PH(1)*XR
152*      IF (M.GT. 1)      XM = PH(2)*XR
153*      CALL COMPAR(SIA,M,IJ)
154*      XIG(I,J,K,IJ) = XIG(I,J,K,IJ)+XM
155*      GO TO 520
156*      XF = XF+XL
157*      CONTINUE
158*      XIG(I,J,K,1) = XIG(I,J,K,1)+XF*(1.-PH(1)-PH(2))
159*      VI = AMIN1(VIFC,VO(I,J))
160*      CALL IMPACT(4,SIA)
161*      CALL COMPAR(SIA,1,IJ)
162*      XIG(I,J,K,IJ) = XIG(I,J,K,IJ)+XF*PH(1)
163*      CALL COMPAR(SIA,3,IJ)
164*      XIG(I,J,K,IJ) = XIG(I,J,K,IJ)+XF*PH(2)

```

FIGURE 60. PROGRAM DETAILS FOR STANDING PASSENGER

than  $E1$ , floor impact will occur and the population group is added to the accumulator  $XF$ . If  $ZT$  is less than  $E1$ , the proper barrier impact velocity  $VI$  is computed. The effect of impact occurring while the barrier is still in motion included by letting the  $VO$  contribution be the minimum between  $VO$  and  $VO \cdot \sqrt{Z/XO}$  where  $XO$  is the appropriate car stopping distance; this follows from equation (51).

A distribution factor  $DF$  is then applied which further subdivides the subpopulation group into two groups reflecting the fraction  $DF$  of the population which is exposed to a panel and the fraction  $(1DF)$  which is exposed to a stanchion. Fifty percent of those exposed to a stanchion are assumed to impact the stanchion; the other half are assumed to miss the adjacent stanchion and are assumed to impact the floor regardless of the closeness of the next stanchion. Finally, to account in some manner for passenger alertness and the fact that each of the above impacts may occur at body positions which are relatively invulnerable to the impact process, such as the arms, the population was split into three segments. The factor  $PH(1)$  suffered head impact, the factor  $PH(2)$  suffered chest impact and the remaining are uninjured.

Statements 144 to 154 performed the appropriate population accounting, calls IMPACT to compute the actual severity index  $SIA$  and then calls COMPAR to evaluate the corresponding level of injury which has occurred for each sub-subpopulation group which impacts a barrier. The code then accumulates the number of passengers sustaining a given level of injury in the array  $XIG(I,J,K,IJ)$ . Statements 158 to 164 then repeat this process for floor impacts. Floor impacts which occur at low speeds (i.e., low values of  $VO$ ) are reduced in magnitude by selecting the minimum between  $VO$  and  $VIFC$ .

### 5.3 Forward Facing Seated Passenger

The motion details of the forward facing seated passenger were developed and evaluated in Section 4.5. That analysis showed that the impact velocity of the passenger with the object immediately forward of the passenger was a function of stopping distance parameter,  $\kappa$ , and that a range of uncertainties occurred as a result of



anthropometric variances and the degree of hip loft and seat slippage which could exist. A mean value curve  $\bar{\sigma}_1$  was constructed as illustrated in Figure 61 and which consisted of two analytical parts. For small values of  $\kappa$  (the symbol C is used in the code) a simple square root dependence is used. For values of  $\kappa$  greater than C2, a linear relationship involving the constants B2 and D2 is used. The intercept value B2 is obtained from A2, C2 and D2 in the preliminary calculation section of the code. A measure of the variance (assumed to be equal to one standard deviation) is shown in this figure.

Figure 62 presents the program details for the forward facing seated passenger. The value of the index K is 2 for this passenger configuration and these steps are applied to the population group NPG(I,J,2). The stopping distance parameter, C, is evaluated using the corresponding body dimension BD (for the c.g. location) and the stopping distance X0. The stopping distance is evaluated at the beginning of the basic calculation section of the code from corresponding velocity change and average acceleration input data. The step-pulse acceleration pulse shape is used. The dimensionless mean value impact velocity FE is then evaluated. Statements 169 to 184 are then repeated for each Lth percentile group. The impact velocity is computed first from equation (125). The subpopulation is then divided into two categories by use of the distribution factor DF. The DF fraction is subjected to impact upon panels; the remainder are subject to impacts upon seatbacks. The subroutine IMPACT is then called to obtain a reference severity index, SI. Statements 176 to 184 are then repeated for each of the three body components (head, face, and chest). If a panel (JR=1) is involved, only head injuries are considered and subroutine COMPAR is called to evaluate the level of injury involved. The final step (statement 183) is the accumulation of the number of passengers involved in the resulting injury level (IJ).

A somewhat more involved procedure is used if a seatback (JR=2) is involved. This is done in an attempt to properly distribute the subpopulation over the body components which could be involved. This procedure is illustrated in Figure 63.



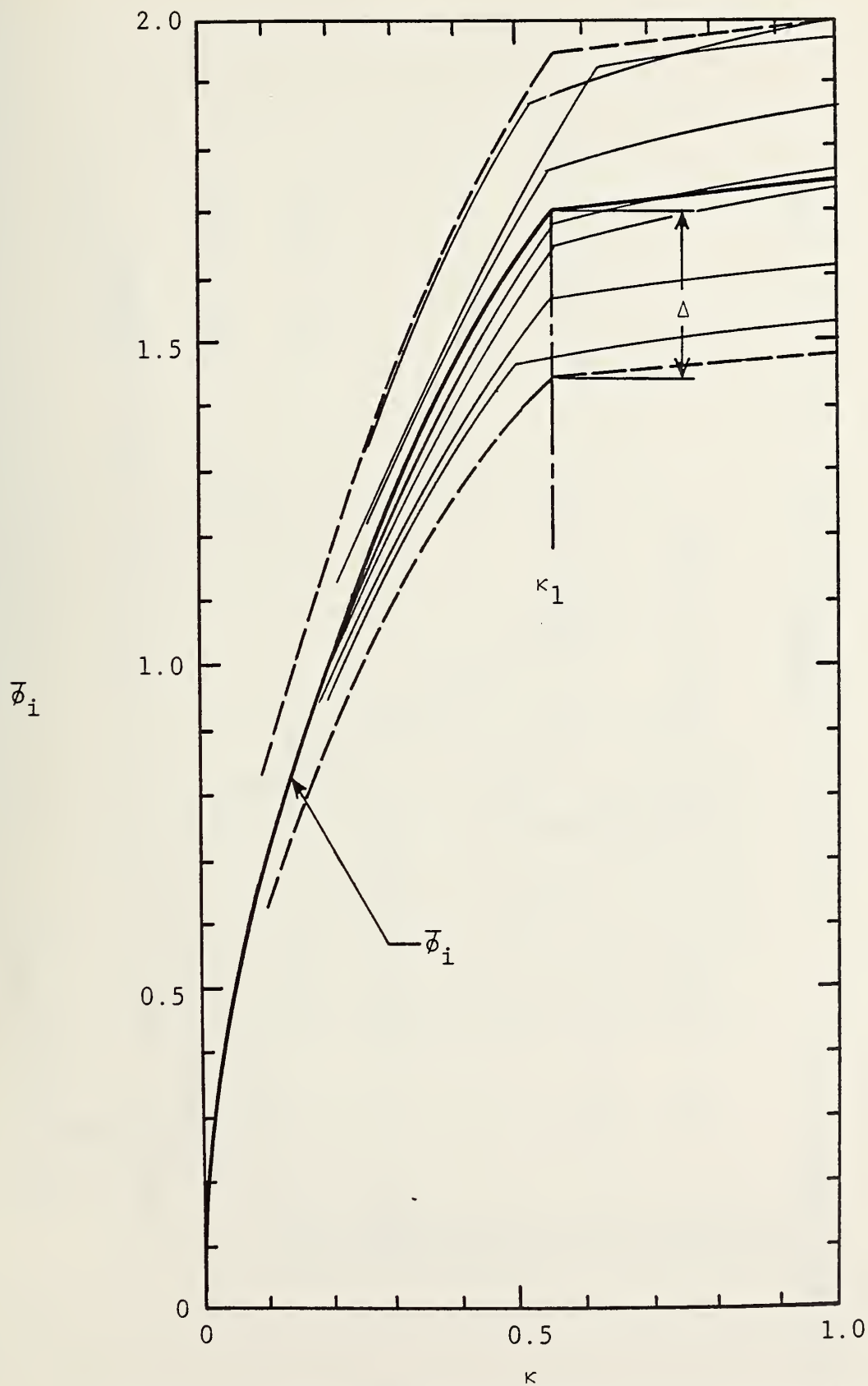


FIGURE 61. MEAN IMPACT VELOCITY FUNCTION FOR FORWARD FACING SEATED PASSENGER

<u>Statement Number</u>	<u>Statement</u>
165*	K = 2
166*	C = .5*RD/XO(I,J)
167*	FE = A2*SQRT(C/C2)
168*	IF (FE .GT. A2) FE = B2 + D2*C
169*	DO 540 L=1,10
170*	VI = VO(I,J)*FE*PF(L)
171*	DO 540 JK=1,2
172*	FD = DF(I,J,K)
173*	IF (JR .EQ. 2) FD = 1.-DF(I,J,K)
174*	XR = .1*FD*FLOAT(NPG(I,J,K))
175*	CALL IMPACT (JR,SI)
176*	DO 540 M=1,3
177*	IF (JR .EQ. 1 .AND. M .GT. 1) GO TO 540
178*	AF = 1.
179*	SIA = AF*SI
180*	XM = PM(I,M)*XR
181*	IF (JR .EQ. 1) XM = XR
182*	CALL COMPAR (SIA,M,IJ)
183*	XIG(I,J,K,IJ) = XIG(I,J,K,IJ)+XM
184*	540 CONTINUE

FIGURE 62. PROGRAM DETAILS FOR FORWARD FACING SEATED PASSENGER

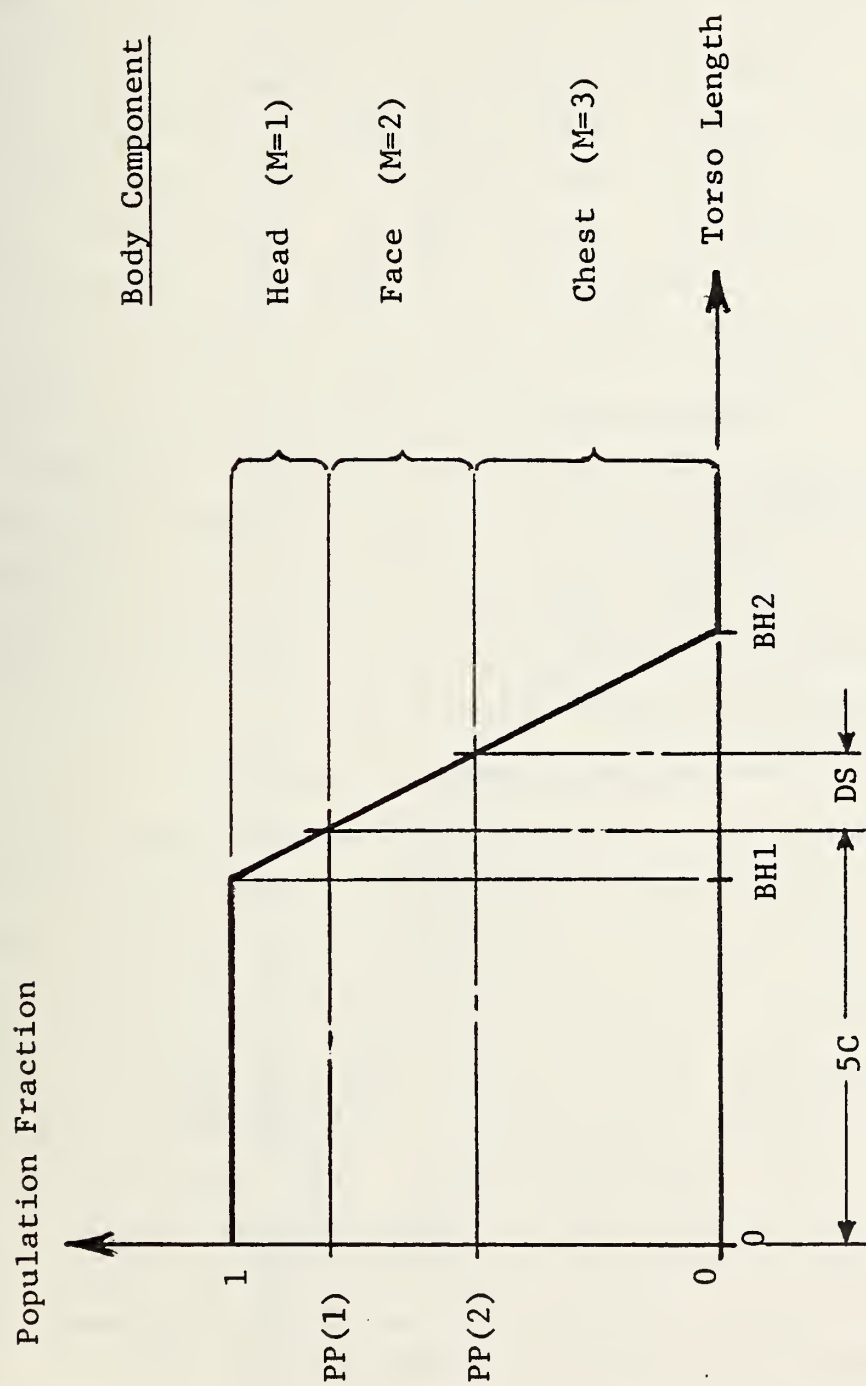


FIGURE 63. DISTRIBUTION OF BODY COMPONENT INVOLVED IN IMPACT

A trilinear torso length distribution curve for the population was selected and is characterized by the two constants BH1 and BH2. A cord length, SC, (evaluated in the preliminary calculation section of the code) was then computed from the seatback height SH (above the hip) and the space SS between the passenger c.g. and the seatback immediately forward of the passenger. The fraction of the population  $(1-PP(1))$  whose torso length is less than the cord length will be exposed to a head impact. The fraction of the population  $(PP(1)-PP(2))$  whose torso is less than the sum of the cord length and the face length, DS, will be exposed to a face impact. The remainder will be exposed to chest impacts. The actual severity index SIA is computed from the reference severity index SI by using a factor AF. This factor was intended to provide some modification of the severity index due to the change in weight of the body component involved. This feature was not incorporated into the current methodology, therefore, a value of AF of unity is used. The parameters A2, C2, D2, BD, DS, BH1 and BH2 are incorporated into the fixed data section of the code.

#### 5.4 Sideward Facing Seated Passenger

The motion details of the sideward facing seated passenger were developed and evaluated in Section 4.7. That analysis showed that the impact velocity of the passenger with the object immediately to his or her side was a function of the stopping distance parameter,  $\kappa$ , and that a range of uncertainty occurred as a result of anthropometric variances and spacing from the adjacent object. A mean value curve  $\bar{\sigma}_i$  was constructed as illustrated in Figure 64 which consisted of two analytical parts. For small values of  $\kappa$  (the symbol C is used in the code) a simple square root dependence is used. For values of  $\kappa$  greater than C3 a constant value A3 was used for the value of  $\bar{\sigma}_i$ . A measure of the variance (assumed to be equal to one standard deviation) is shown in this figure.

Figure 65 presents the program details for the sideward facing seated passenger. The value of the index K is 3 for this passenger configuration and these steps are applied to the population group  $NPG(I,J,3)$ .

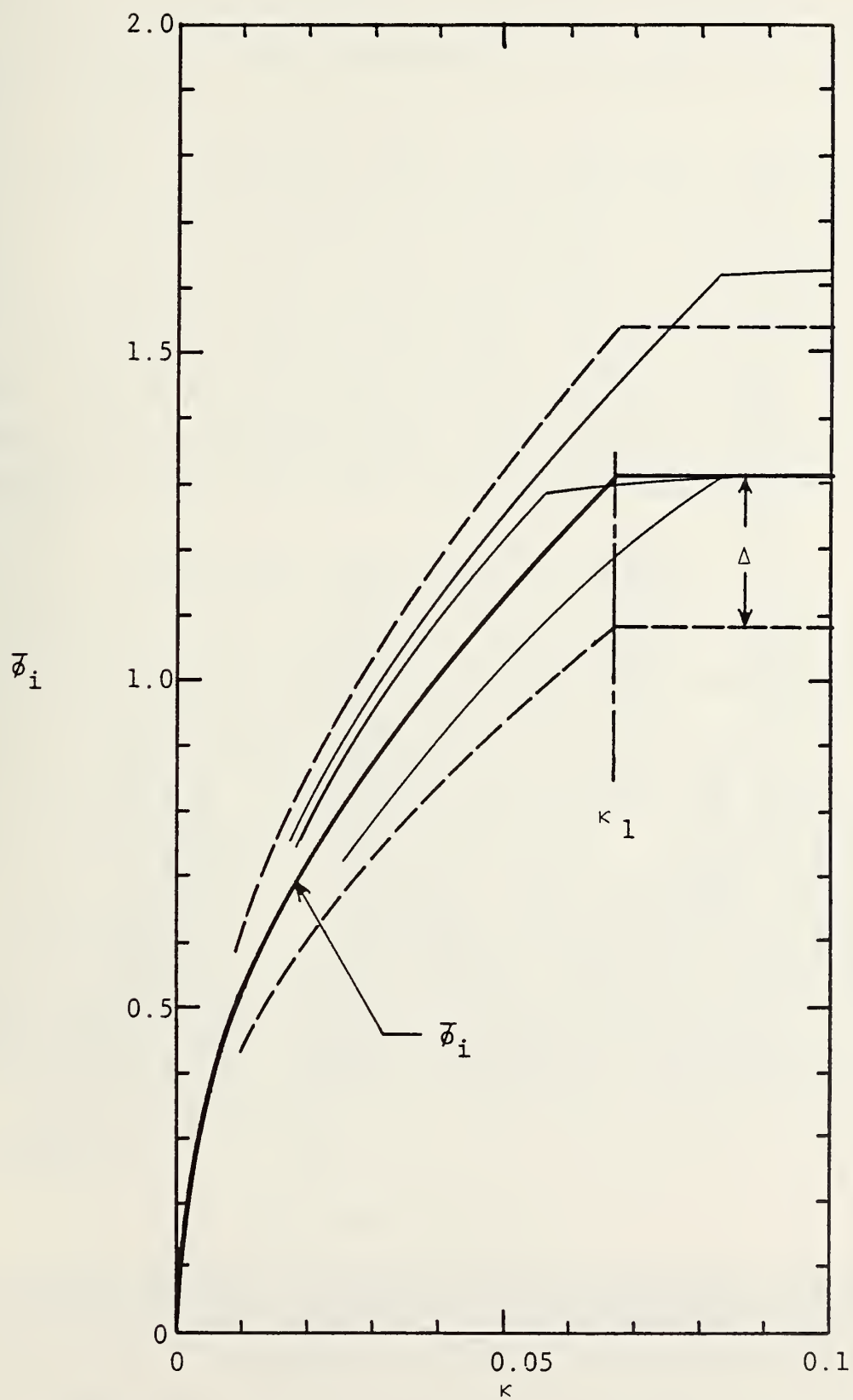


FIGURE 64. MEAN IMPACT VELOCITY FUNCTION FOR SIDEWARD FACING SEATED PASSENGER



Statement Number	Statement
185*	K = 3
186*	C = .5*HE/XU(I,J)
187*	FE = A3*SQR(C/C3)
188*	IF (FE .GT. A3) FE = A3
189*	XL = .1*FLOAT(NPG(I,J,K))*SP(I)
190*	XIG(I,J,K,1) = XIG(I,J,K,1)+(1.-SP(I))*FLOAT(NPG(I,J,K))
191*	DO 550 L=1,10
192*	VI = VU(I,J)*FE*PF(L)
193*	DO 550 JR=1,2
194*	FD = DF(I,J,K)
195*	IF (JR .EQ. 2) FD = 1.-DF(I,J,K)
196*	XR = XL*FD
197*	CALL IMPACT (JR,SI)
198*	DO 550 M=1,3
199*	IF (JR .EQ. 1 .AND. M .GT. 1) GO TO 550
200*	AF = 1.
201*	SIA = AF*SI
202*	XM = PM(I,M)*XR
203*	IF (JR .EQ. 1) XM = XR
204*	CALL COMPAR (SIA,M,IJ)
205*	XIG(I,J,K,IJ) = XIG(I,J,K,IJ)+XM
206*	550 CONTINUE
207*	K = 4
208*	DO 570 L=1,10
209*	SIA = AO(I,J)*PF(L)
210*	XM = .1*FLOAT(NPG(I,J,K))
211*	CALL COMPAR (SIA,4,IJ)
212*	XIG(I,J,K,IJ) = XIG(I,J,K,IJ)+XM
213*	DO 584 IJ=1,6
214*	DO 584 K=1,4
215*	XIC(I,J,IJ) = XIC(I,J,IJ)+XIG(I,J,K,IJ)
216*	DO 588 IJ=1,6
217*	XII(I,IJ) = XII(I,IJ)+XIC(I,J,IJ)
218*	DO 590 IJ=1,6
219*	590 XII(I,IJ) = XII(I,IJ)+XII(I,IJ)

FIGURE 65. PROGRAM DETAILS FOR SIDEWARD AND BACKWARD FACING SEATED PASSENGER

The stopping distance parameter,  $C$ , is evaluated using the corresponding body dimension,  $BE$  (for the c.g. location) and the stopping distance  $XO$ . The dimensionless mean value impact velocity  $FE$  is then evaluated.

The number of passengers who will suffer an impact will be limited to those at the one end of the side bench (or individual seats) that is those adjacent to an obstacle. Thus a reduction factor  $SP$  is used which is equal to one-half (for one end of the bench) divided by the number of passengers on the side bench. This number is obtained by dividing the bench length,  $SB$ , by the body width,  $H3$ . The remaining procedures are similar to those used for the forward facing seated passenger. The values of  $A3$ ,  $C3$ , and  $H3$  are incorporated into the code in the fixed data section of the code.

### 5.5 Backward Facing Seated Passenger

Passengers in this passenger configuration will only be subjected to a "whiplash" type of injury which is largely dependent upon the level of acceleration (see Section 4.6). The program details for this passenger configuration are presented in Figure 65. The index  $K=4$  for this case and the computational steps are applied to the population group  $NPG(I,J,4)$ . The population is divided into 10 percentile subgroups according to the index  $L$  and the car acceleration  $A0$  is adjusted by the factor  $PF$  in each  $L$ th case to obtain some variance due to sensitivity and anthropometric variations. These accelerations are then compared to the criteria values with the aid of subroutine  $COMPAR$  and the accounting procedure with respect to the number of passengers sustaining a given level of injury is followed as was done with the other passenger configurations.

### 5.6 Typical Results

The results of a hypothetical crash situation are presented to demonstrate the nature of the output of the methodology. The crash environments, i.e., the change in velocity  $VO$  and average acceleration  $A0$  for each car of each consist, were selected arbitrarily as

were the car interior component properties, spacing and other factors. Hopefully, these values are somewhat realistic such that the numerical results will be meaningful. The car interior arrangements and the properties of some of the interior components were selected to demonstrate some of the influence that these factors have upon the population of injuries in an intracity train crash situation.

The results are included at the end of this section. A summary is presented of the number of passengers involved in the crash. This is followed by a detailed breakdown of the passengers by number with respect to passenger configuration, car and consist. In this example, consist number 1 did not have any sideward facing seats. The cars of the second consist are more conventional in this respect. The first consist is rather crowded and therefore, there is a larger number of standing passengers than in the second consist.

The injury analysis summary comprises the total number of passengers in each of the six injury categories and a corresponding breakdown by car and consist. The corresponding details with respect to each passenger configuration are also presented. The remaining output, including the "fixed data" for this example, are presented in the appendix.

Most of the fatalities which occur in this example are the result of injuries sustained by standing passengers in consist number 1 who apparently fall to the floor. The floor system for the cars in this consist is quite stiff whereas the stanchions and panels are of nominal stiffness. The distribution of the injuries sustained by standing passengers in consist number 2 is quite different and reflects somewhat stiffer stanchions and panels and a considerably softer floor.

The converse is true for the forward facing seated passenger. The seatback properties in the cars of consist number 2 are stiffer and result in a definite shift in the intensity of the injuries in this configuration. Only a few minor injuries are sustained by passengers in this configuration for consist number 1 even though many more passengers are involved.

No comparison can be made for the sideward seated passengers since none existed in consist number 1. The number of injuries sustained by sideward seated passengers in consist number 2 is quite small and is due in part to the fact that relatively few of these passengers are close to an interior object. Finally, no whiplash injuries occur in the backward facing seated passenger configuration in either consist due to the relatively low acceleration levels involved.

#### INTRA-CITY TRAIN CRASH INJURY ANALYSIS

SPECIFIC COMMENTS - WALL STREET CRASH OF NOVEMBER 1929  
RELATIVE SPEED AT CRASH = 30.0 MPH

TOTAL NUMBER OF PASSENGERS INVOLVED IN CRASH =	631
TOTAL NUMBER OF PASSENGERS IN CONSIST NO. 1 =	464
TOTAL NUMBER OF PASSENGERS IN CONSIST NO. 2 =	167

# PASSENGER DISTRIBUTION BY NUMBER

CONSIST NO.	CAR NO.	TOTAL NUMBER IN CAR	STANDING	SEATED FACING FORWARD	SEATED FACING SIDEWARD	SEATED FACING BACKWARD
1	1	63	10	26	0	27
1	2	62	8	28	0	26
1	3	68	17	28	0	23
1	4	56	4	27	0	25
1	5	56	3	26	0	27
1	6	52	2	23	0	27
1	7	55	7	24	0	24
1	8	52	3	24	0	25
TOTAL IN CONSIST NO. 1			54	206	0	204
2	1	31	8	2	18	3
2	2	30	6	4	14	6
2	3	26	3	7	12	4
2	4	25	5	3	9	8
2	5	27	2	4	16	5
2	6	28	4	6	12	6
TOTAL IN CONSIST NO. 2			28	26	81	32
TOTAL IN CRASH			82	232	81	236



# INJURY ANALYSIS SUMMARY

TOTAL UN-INJURED = 572.1  
 TOTAL MINOR = 24.5  
 TOTAL MODERATE = 14.2  
 TOTAL SERIOUS = 5.2  
 TOTAL CRITICAL = .0  
 TOTAL FATALITIES = 14.9

## INJURY PROFILES BY CAR AND CONSIST

CONSIST NO.	CAR NO.	UN-INJURED	MINOR	MODERATE	INJURY LEVEL	CRITICAL	FATALITIES
					SERIOUS		
1	1	57.57	3.06	.00	.00	.00	2.37
1	2	59.33	.77	.00	.00	.00	1.90
1	3	63.19	.77	.00	.00	.00	4.04
1	4	54.30	.75	.00	.00	.00	.95
1	5	55.29	.00	.00	.00	.00	.71
1	6	51.52	.00	.00	.00	.00	.47
1	7	53.34	.00	.00	.00	.00	1.66
1	8	51.29	.00	.00	.00	.00	.71
TOTAL IN CONSIST NO. 1		445.82	5.35	.00	.00	.00	12.82
2	1	24.38	2.11	2.72	1.62	.01	.17
2	2	23.09	3.27	2.23	1.09	.01	.32
2	3	17.36	4.29	3.24	.55	.01	.56
2	4	19.69	2.77	1.39	.90	.00	.24
2	5	21.66	2.78	1.86	.57	.01	.32
2	6	20.07	3.95	2.78	.73	.01	.48
TOTAL IN CONSIST NO. 2		126.26	19.17	14.21	5.24	.04	2.09

# INJURY PROFILE BY PASSENGER CONFIGURATION

## STANDING PASSENGER

CUNSI ST NU.	CAR NU.	UN-INJURED	MINOR	MODERATE	INJURY LEVEL SERIOUS	CRITICAL	FATALITIES
1	1	7.62	.00	.00	.00	.00	2.57
1	2	6.10	.00	.00	.00	.00	1.90
1	3	12.96	.00	.00	.00	.00	4.04
1	4	3.05	.00	.00	.00	.00	.45
1	5	2.24	.00	.00	.00	.00	.71
1	6	1.52	.00	.00	.00	.00	.47
1	7	5.34	.00	.00	.00	.00	1.66
1	8	2.29	.00	.00	.00	.00	.71
2	1	4.44	.85	1.23	1.47	.00	.00
2	2	3.59	1.33	.00	1.04	.00	.00
2	3	1.80	.66	.00	.54	.00	.00
2	4	2.49	1.10	.00	.90	.00	.00
2	5	1.20	.44	.00	.35	.00	.00
2	6	2.47	.81	.00	.72	.00	.00

FORWARD FACING SEATED PASSENGER

COPIES NO.	CAR NO.	UN-INJURED	MINOR	MODERATE	INJURY LEVEL SERIOUS	CRITICAL	FATALITIES
1	1	22.94	3.06	.00	.00	.00	.00
1	2	27.23	.77	.00	.00	.00	.00
1	3	27.23	.77	.00	.00	.00	.00
1	4	26.25	.75	.00	.00	.00	.00
1	5	26.00	.00	.00	.00	.00	.00
1	6	23.00	.00	.00	.00	.00	.00
1	7	24.00	.00	.00	.00	.00	.00
1	8	24.00	.00	.00	.00	.00	.00
2	1	.00	.55	1.16	.13	.00	.16
2	2	.00	1.47	2.21	.00	.00	.32
2	3	.00	3.22	3.22	.00	.00	.56
2	4	.00	1.38	1.38	.00	.00	.24
2	5	.00	1.84	1.84	.00	.00	.32
2	6	.00	2.76	2.76	.00	.00	.48

# STOWAWAY FACJAC SEATED PASSENGER

CONSIST NU.	CAR NU.	UN-INJURED	MINOR	MODERATE	INJURY LEVEL SERIOUS	CRITICAL	FATALITIES
1	1	.00	.00	.00	.00	.00	.00
1	2	.00	.00	.00	.00	.00	.00
1	3	.00	.00	.00	.00	.00	.00
1	4	.00	.00	.00	.00	.00	.00
1	5	.00	.00	.00	.00	.00	.00
1	6	.00	.00	.00	.00	.00	.00
1	7	.00	.00	.00	.00	.00	.00
1	8	.00	.00	.00	.00	.00	.00
2	1	16.94	.71	.52	.02	.01	.01
2	2	13.49	.47	.02	.01	.01	.00
2	3	11.57	.41	.02	.01	.01	.00
2	4	4.76.	.24	.01	.00	.00	.00
2	5	15.46	.50	.02	.01	.01	.00
2	6	11.60	.34	.02	.01	.01	.00

# HACKERMAN FALING SEATED PASSENGER

CURSI	CAP	UN-INJURED	MINOR	MODERATE	INJURY LEVEL	CRITICAL	FATALITIES
NO.	NO.				SERIOUS		
1	1	27.00	.00	.00	.00	.00	.00
1	2	26.00	.00	.00	.00	.00	.00
1	3	23.00	.00	.00	.00	.00	.00
1	4	25.00	.00	.00	.00	.00	.00
1	5	27.00	.00	.00	.00	.00	.00
1	6	27.00	.00	.00	.00	.00	.00
1	7	24.00	.00	.00	.00	.00	.00
1	8	25.00	.00	.00	.00	.00	.00
2	1	3.00	.00	.00	.00	.00	.00
2	2	6.00	.00	.00	.00	.00	.00
2	3	4.00	.00	.00	.00	.00	.00
2	4	4.00	.00	.00	.00	.00	.00
2	5	5.00	.00	.00	.00	.00	.00
2	6	6.00	.00	.00	.00	.00	.00





## APPENDIX

### COMPUTER CODE DESCRIPTION

A brief description of the computer code used in the injury prediction methodology entitled "Intra-City Crash Injury Analysis" is presented. This code was written in FORTRAN V and has been used on a UNIVAC 1108 computer. It is a relatively small code and has minimal storage requirements. The code is divided into eight sections.

#### 1. Data Section

The multitude of parameter values which are fixed in value are presented. The parameters include distribution values, anthropometric data, injury criteria, etc. Note that as some of these data values are determined more precisely, this section may be modified.

#### 2. Input Section

The introduction of the necessary input data is provided. These data and their corresponding format requirements are presented in Table A-1. The code has a multiple problem solving capability such that any number of problems can be run by adding data card groups as specified in Table A-1.

#### 3. Initialize and Preliminary Calculations

Certain arrays and variables are initialized and a series of preliminary calculations which facilitate the subsequent calculations are performed.

#### 4. Printout - First Phase

This phase prints a title and problem identification along with the precrash speed, a breakdown of the total number of passengers involved in the crash and the total number of passengers involved in each consist. If only one consist is involved, this fact is printed. The passenger number distribution by consist and by car for each of the four passenger configurations treated in the methodology, and the corresponding totals and subtotals are presented.

#### 5. Basic Calculations

All of the basic calculations are performed for each of the four passenger configurations as described in Section 5 of this report. These calculations are

TABLE A-1 INPUT FORMAT

Card (Format)	Variables	Description (units)
Card 1 (18A4)	TITLE	Title
Card 2 (F10.1,4I10)	SPEED	Relative speed of consists at impact (mph)
	IC	Number of consists ( $\leq 2$ )
	NC(1)	Number of cars in Consist 1 ( $\leq 10$ )
	NC(2)	Number of cars in Consist 2 ( $\leq 10$ )
	IPP	Print control index for stored data
Card Group A (one group for each consist I=1,IC)		
Card Group A1 (one subgroup for each kth passenger configuration, K=1,4)		
	K=1	Standing passenger
	K=2	Forward facing seated passenger
	K=3	Sideward facing seated passenger
	K=4	Backward facing seated passenger
Card A1-1 (10I5)	NPG(I,J,K) J=1,NC(I)	Number of passengers in kth configuration of jth car of ith consist
Card A1-2 (10F5.2)	DF(I,J,K) J=1,NC(I)	Distribution factor for kth passenger configuration of jth car of ith consist
NOTE: The last card of this group corresponding to Card A1-2 for K=4 is blank since DF(I,J,4) is not used.		
(End of Card Group A1)		
Card A2 (10F8.2)	A0(I,J) J=1,NC(I)	Acceleration of jth car of ith consist(g)
Card A3 (10F8.2)	VO(I,J) J=1,NC(I)	Velocity change of jth car of ith consist (fps)
Card A4 (4I10)	IR(I,JR) JR=1,4	Response Form Index IR=1 for perfect absorber IR=2 for elastic response IR=3 for inelastic response
Card A5 (4E10.4)	RC1(I,JR) JR=1,4	Response constant Number 1 defined as Yield stress (psi) for IR=1 Spring constant (lb/in.) for IR=2 and 3
Card A6 (4E10.4)	RC2(I,JR) JR=1,4	Response constant Number 2 defined as Critical force (lb) for IR=3 otherwise not used (set=0.)
Card A7 (8F10.2)	SH(I)	Height of seatback above hip (ft)
	SS(I)	Space between forward facing seated pas- senger and object in front of seat (ft)
	SB(I)	Side bench length (ft)
	SF(I)	Floor space length (or stanchion spacing)(ft)
For additional problems repeat entire group (Cards 1 to A7).		

for each car in each consist. Two subroutines are called from this section. The first, subroutine IMPACT, computes the severity index in accordance with the appropriate surface/structure response form. The second, subroutine COMPAR, compares the value of the severity index with the appropriate critical values and determines the level of injury sustained. The number of passengers associated with this injury level are accumulated for each passenger configuration, for each car, and for each consist involved in the crash event.

#### 6. Printout - Second Phase

This phase prints out the injury data. A summary is presented first which lists the total number of passengers assigned to each injury level including uninjured together with a corresponding breakdown by car and consist including appropriate subtotals. This is followed by injury profiles for each of the passenger configurations. These details are given for each car in each consist.

#### 7. Printout - Third Phase

This phase prints out the remaining input data to document the problem appropriately. This includes the interior components data for each consist, that is the response from index (IR) and the two associated response constants RC1 and rC2 for each of the four interior component categories (JR). It includes the car crash environments (velocity change and acceleration) for each car of each consist and a collection of distribution factors and spacing parameter values. The former DF is presented for three of the four passenger consists and for each car of each consist. The latter (SH, SS, SB, and SF) are presented for each consist.

#### 8. Printout - Fourth Phase

This phase is an optional output group controlled by the control index IPP (IPP > 0 provides for the printing of this information). These data are the so-called "fixed data" used in methodology and include probability distribution factors PF(I) (I=1,5) and a collection of constants used to define the results of the motion analyses. These data also include some anthropometric data and the severity index criteria data. The optional form is intended to provide periodic documentation of the fixed values under conditions where some of these values may be updated or modified.

A detailed listing of the code follows together with a listing of the two subroutines IMPACT and COMPAR. A sample problem was run, and the corresponding output data are presented in Section 5 of the report with the exception of the output from Sections 7 and 8 of the code which are presented on the following pages of this appendix and correspond to the sample problem.



C INTRA-CITY TRAIN CRASH INJURY ANALYSIS

C

```

      DIMENSION TITLE(18),AO(2,10),VO(2,10),XO(2,10),NC(2),NPT(2),
1  INPC(2,10),NPG(2,10,4),NPGTC(2,4),NPGIT(4),PF(10),XITUT(6),SP(2),
2  XIT(2,6),XIC(2,10,6),SB(2),DF(2,10,4),SH(2),SS(2),SL(2),PP(2),
3  PH(2,3),XIG(2,10,4,6),PH(2),SF(2)
      COMMON/SUBRT/ I,J,K,VI,AH,WH,IR(2,4),RC1(2,4),RC2(2,4)
1  /SICRIT/ SIC(4,5)

```

C

C DATA SECTION

C

```

      DATA PF(1),PF(2),PF(3),PF(4),PF(5)/.72,.82,.88,.94,.98/
      DATA VIFC,A1,C1,D1,E1,F1,A3,C3,A2,C2,D2,H3/
1  122.4,3.6,.35,11.43,.71,-4.,1.31,.065,1.70,.55,.1,1.75/
      DATA SIC(1,1),SIC(1,2),SIC(1,3),SIC(1,4),SIC(1,5)/
1  650.,1000.,1333.,1667.,2000./
      DATA SIC(2,1),SIC(2,2),SIC(2,3),SIC(2,4),SIC(2,5)/
2  500.,1000.,1500.,2000.,2500./
      DATA SIC(3,1),SIC(3,2),SIC(3,3),SIC(3,4),SIC(3,5)/
3  1000.,1500.,2000.,2500.,3000./
      DATA SIC(4,1),SIC(4,2),SIC(4,3)/12.,20.,100./
      DATA PD,AH,WH,BH1,BH2,DS,BE/1.,10.,10.,1.50,2.50,.75,.27/
      DATA PH(1),PH(2)/.40,.10/

```

C

C INPUT SECTION

C

```

10  READ (5,100,END=999) TITLE,SPEED,IC,NC(1),NC(2),IPP
100  FORMAT (18A4/F10.1,4I10)
      DO 114 I=1,IC
      JC = NC(I)
      DO 102 K=1,4
      READ (5,104) (NPG(I,J,K),J=1,JC)
102  READ (5,105) (DF(I,J,K),J=1,JC)
104  FORMAT (10I5)
105  FORMAT (10F5.2)
      READ (5,108) (AO(I,J),J=1,JC)
106  READ (5,108) (VO(I,J),J=1,JC)
108  FORMAT (10F8.2)
      READ (5,110) (IR(I,JR),JR=1,4)
110  FORMAT (4I10)
      READ (5,112) (RC1(I,JR),JR=1,4)
112  FORMAT (4E10.4)
      READ (5,112) (RC2(I,JR),JR=1,4)
114  READ (5,116) SH(I),SS(I),SB(I),SF(I)
116  FORMAT (8F10.2)

```

C  
 C INITIALIZE AND PRELIMINARY CALCULATIONS  
 C

```

    NPTOT = 0
    DO 200 I=1,IC
      JC = NC(I)
      NPT(I) = 0
      SP(I) = .5*M3/SH(I)
      SC(I) = SQRT(SH(I)*SH(I)+SS(I)*SS(I))
      DO 200 J=1,JC
200    NPC(I,J) = 0
      DO 206 I=1,IC
        JC = NC(I)
        DO 204 J=1,JC
          DO 202 K=1,4
202    NPC(I,J) = NPC(I,J)+NPG(I,J,K)
204    NPT(I) = NPT(I)+NPC(I,J)
206    NPTOT = NPTOT+NPT(I)
      DO 216 K=1,4
        NPGIT(K) = 0
        DO 210 I=1,IC
          JC = NC(I)
          NPGIT(I,K) = 0
          DO 208 J=1,JC
208    NPGIT(I,K) = NPGIT(I,K)+NPG(I,J,K)
210    NPGIT(K) = NPGIT(K)+NPGIT(I,K)
        DO 212 L=0,10
          LL = 11-L
212    PF(L) = 2.-PF(LL)
          K2 = A2-C2*D2
          B1 = A1-C1*D1
          G1 = (F1-A1)/((E1-C1)**2)
          SL = FH2-BH1
          DO 218 IJ=1,0
            XI10T(IJ) = 0.
          DO 218 I=1,IC
            JC = NC(I)
            XI1(I,IJ) = 0.
            DO 214 J=1,JC
              XIC(I,J,IJ) = 0.
              DO 214 K=1,4
214    XIG(I,J,K,IJ) = 0.
            DO 216 M=1,2
              PP(M) = 1.-SL*(SC(I)+FLOAT(M-1)*DS-FH1)
              IF (PP(M) .LT. 0.) PP(M) = 0.
              IF (PP(M) .GT. 1.) PP(M) = 1.
216    CONTINUE
            PM(I,1) = 1.-PP(1)
            PM(I,2) = PP(1)-PP(2)
218    PM(I,3) = PP(2)
  
```

C

C PRINT OUT - FIRST PHASE (NUMBER DISTRIBUTION AND IDENTIFICATION)

C

```

      WRITE (6,600) TITLE,SPEED,NPTOT
600  FORMAT (1H1,2HX,'INTRA-CITY TRAIN CRASH INJURY ANALYSIS'///
110X,'SPECIFIC COMMENTS -',18A4/
210X,'RELATIVE SPEED AT CRASH =',F6.1,' MPH'//
320X,'TOTAL NUMBER OF PASSENGERS INVOLVED IN CRASH =',I5)
      IF (IC .EQ. 1) GO TO 150
      WRITE (6,602) NP1(1),NP1(2)
602  FORMAT (20X,'TOTAL NUMBER OF PASSENGERS IN CONSIST NO. 1 =',I6/
120X,'TOTAL NUMBER OF PASSENGERS IN CONSIST NO. 2 =',I6///)
      GO TO 152
150  WRITE (6,604)
604  FORMAT (20X,'(ONLY ONE CONSIST INVOLVED)'///)
152  WRITE (6,610)
610  FORMAT (///,34X,'PASSENGER DISTRIBUTION BY NUMBER'//
13X,'CONSIST      CAR      TOTAL NUMBER      STANDING      SEATED FACING
2  SEATED FACING      SEATED FACING'/5X,'NO.',7X,'NO.',8X,'IN CAR',22X
3,'FORWARD',8X,'SIDEWARD',8X,'BACKWARD'/)
      DO 156 I=1,IC
      JC = NC(I)
      DO 156 J=1,JC
156  WRITE (6,612) I,J,NPG(I,J),(NPG(I,J,K),K=1,4)
612  FORMAT (17,I10,I13,I15,I13,2I16)
158  WRITE (6,614) I,(NPGTC(I,K),K=1,4)
614  FORMAT (/1X,'TOTAL IN CONSIST NO.',I2,I22,I13,2I16//)
      WRITE (6,616) (NPGTT(K),K=1,4)
616  FORMAT (/1X,'TOTAL IN CRASH',I30,I13,2I16)

```

C

C BASIC CALCULATIONS

C

```

      DO 590 I=1,IC
      JC = NC(1)
      DO 588 J=1,JC
      XO(1,J) = .5*VO(I,J)*VO(I,J)/(AO(I,J)*32.2)
      K = 1
      XF = 0.
      XL = .1*FLOAT(NPG(I,J,K))
      DO 520 L=1,10
      Z = .1*SF(I)*FLOAT(L)
      ZT = Z/VO(1,J)
      IF (ZT .GT. E1) GO TO 516
      IF (ZT .GT. C1) GO TO 510
      VI = VO(I,J)*AMIN1(1.,SQRT(Z/XO(1,J)))+B1+D1*ZT
      GO TO 512
510 VI = VO(I,J)*AMIN1(1.,SQRT(Z/XO(1,J)))+A1+G1*((ZT-C1)**2)
512 CONTINUE
      DO 514 JR=1,3,2
      XR = XL*DF(1,J,K)
      IF (JR .GT. 1) XR = .5*XL*(1.-DF(I,J,K))
      IF (JR .GT. 1) XF = XF+XR
      XIG(I,J,K,1) = XIG(I,J,K,1)+XR*(1.-PH(1)-PH(2))
      CALL IMPACT (JR,SIA)
      DO 514 M=1,3,2
      XM = PH(1)*XR
      IF (M .GT. 1) XM = PH(2)*XR
      CALL COMPAR(SIA,M,IJ)
514 XIG(I,J,K,IJ) = XIG(I,J,K,IJ)+XM
      GO TO 520
516 XF = XF+XL
520 CONTINUE
      XIG(I,J,K,1) = XIG(I,J,K,1)+XF*(1.-PH(1)-PH(2))
      VI = AMIN1(VIFC,VO(1,J))
      CALL IMPACT(4,SIA)
      CALL COMPAR(SIA,1,IJ)
      XIG(I,J,K,IJ) = XIG(I,J,K,IJ)+XF*PH(1)
      CALL COMPAR(SIA,3,IJ)
      XIG(I,J,K,IJ) = XIG(I,J,K,IJ)+XF*PH(2)
      K = 2
      C = .5*RD/XO(I,J)
      FE = A2*SQRT(C/C2)
      IF (FE .GT. A2) FE = B2+D2*C
      DO 540 L=1,10
      VI = VO(I,J)*FE*PF(L)

```

```

DO 540 JR=1,2
FD = DF(I,J,K)
IF (JR .EQ. 2) FD = 1.-DF(I,J,K)
XR = .1*FD*FLOAT(NPG(I,J,K))
CALL IMPACT (JR,SI)
DO 540 M=1,3
IF (JR .EQ. 1 .AND. M .GT. 1) GO TO 540
AF = 1.
SIA = AF*SI
XM = PM(I,M)*XR
IF (JR .EQ. 1) XM = XR
CALL COMPAR (SIA,M,IJ)
XIG(I,J,K,IJ) = XIG(I,J,K,IJ)+XM
540 CONTINUE
K = 3
L = .5*BE/XO(I,J)
FE = A3*SQRT(C/CS)
IF (FF .GT. A3) FE = A3
XL = .1*FLOAT(NPG(I,J,K))*SP(I)
XIG(I,J,K,1) = XIG(I,J,K,1)+(1.-SP(I))*FLOAT(NPG(I,J,K))
DO 550 L=1,10
V1 = VO(I,J)+FE*PF(L)
DO 550 JR=1,2
FD = DF(I,J,K)
IF (JR .EQ. 2) FD = 1.-DF(I,J,K)
XR = XL*FD
CALL IMPACT (JR,SI)
DO 550 M=1,3
IF (JR .EQ. 1 .AND. M .GT. 1) GO TO 550
AF = 1.
SIA = AF*SI
XM = PM(I,M)*XR
IF (JR .EQ. 1) XM = XR
CALL COMPAR (SIA,M,IJ)
XIG(I,J,K,IJ) = XIG(I,J,K,IJ)+XM
550 CONTINUE
K = 4
DO 570 L=1,10
SIA = AO(I,J)*PF(L)
XM = .1*FLOAT(NPG(I,J,K))
CALL COMPAR (SIA,4,IJ)
570 XIG(I,J,K,IJ) = XIG(I,J,K,IJ)+XM
DO 584 IJ=1,6
DO 584 K=1,4
584 XIC(I,J,IJ) = XIC(I,J,IJ)+XIG(I,J,K,IJ)
DO 588 IJ=1,6
588 XI1(I,IJ) = XI1(I,IJ)+XIC(I,J,IJ)
DO 590 IJ=1,6
590 XI1TOT(IJ) = XI1TOT(IJ)+XI1(I,IJ)

```



C

C PRINT OUT - SECOND PHASE (INJURY DATA)

--C--

```

      WRITE (6,800) (XITOT(IJ),IJ=1,6)
800  FORMAT (1H1,45X,'INJURY ANALYSIS SUMMARY'///
146X,'TOTAL UN-INJURED =',F6.1/46X,'TOTAL MINOR      =',F6.1/
146X,'TOTAL MODERATE   =',F6.1/46X,'TOTAL SERIOUS    =',F6.1/
246X,'TOTAL CRITICAL   =',F6.1/46X,'TOTAL FATALITIES =',F6.1//)
      WRITE (6,802)
802  FORMAT (41X,'INJURY PROFILES BY CAR AND CONSIST'//
13X,'CONSIST      CAR',41X,'INJURY LEVEL'/5X,'NO.',7X,'NO.',7X,'UN-
2NJURED',7X,'MINOR',7X,'MODERATE',7X,'SERIOUS',6X,'CRITICAL',5X,'I
3TALITIES'//)
      DO 810  I=1,IC
      JC = NC(I)
      DO 804  J=1,JC
804  WRITE (6,806) I,J,(XIC(I,J,IJ),IJ=1,6)
806  FORMAT (17,I10,F15.2,5F14.2)
      WRITE (6,808) I,(XIT(I,IJ),IJ=1,6)
808  FORMAT (/ 'TOTAL IN CONSIST NO.',I2,F9.2,5F14.2//)
810  CONTINUE
      WRITE (6,812)
812  FORMAT (1H1,35X,'INJURY PROFILE BY PASSENGER CONFIGURATION'//)
      DO 826  K=1,4
      IF (K .EQ. 1)  WRITE (6,814)
      IF (K .EQ. 2)  WRITE (6,816)
      IF (K .EQ. 3)  WRITE (6,818)
      IF (K .EQ. 4)  WRITE (6,820)
814  FORMAT (////20X,'STANDING PASSENGER'//)
816  FORMAT (////20X,'FORWARD FACING SEATED PASSENGER'//)
818  FORMAT (////20X,'SIDEWARD FACING SEATED PASSENGER'//)
820  FORMAT (////20X,'BACKWARD FACING SEATED PASSENGER'//)
      WRITE (6,822)
822  FORMAT (
13X,'CONSIST      CAR',41X,'INJURY LEVEL'/5X,'NO.',7X,'NO.',7X,'UN-
2NJURED',7X,'MINOR',7X,'MODERATE',7X,'SERIOUS',6X,'CRITICAL',5X,'I
3TALITIES'//)
      DO 826  I=1,IC
      JC = NC(I)
      DO 826  J=1,JC
      WRITE (6,824) I,J,(XIG(I,J,K,IJ),IJ=1,6)
824  FORMAT (17,I10,F15.2,5F14.2)
826  CONTINUE

```

```

C
C PRINT OUT - THIRD PHASE (INPUT DATA)
C
      WRITE (6,900)
900  FORMAT (1H1,24X,'INTERIOR COMPONENTS DATA'//)
      DO 904      I=1,IC
      WRITE (6,902) I
902  FORMAT (/5X,'CONSIST NO.',I3//10X,'JR',10X,'IR',15X,'RC1',21X,'RC2
1'//)
      DO 904      JR=1,4
904  WRITE (6,906) JR,IR(I,JR),RC1(I,JR),RC2(I,JR)
906  FORMAT (2I12,2F22.2)
      WRITE (6,907)
907  FORMAT (/3X,'PANEL (JR=1), SEATBACK (JR=2), STANCHION (JR=3), FLU
10R (JR=4)'//3X,'PERFECT ABSORBER (IR=1), ELASTIC RESPONSE (IR=2), I
2NELASTIC RESPONSE (IR=3)'//)
      WRITE (6,908)
908  FORMAT (/33X,'CAR CRASH ENVIRONMENT'//10X,'CONSIST      CAR',15X
1,'VELOCITY CHANGE      ACCELERATION'//12X,'NO.      NO.',18X,'(FT/SE
2C)      (FT/SEC SW)'//)
      DO 910      I=1,IC
      JC = NC(I)
      DO 910      J=1,JC
910  WRITE (6,912) I,J,VC(I,J),AC(I,J)
912  FORMAT (I14,I10,F25.1,F16.2)
      WRITE (6,914)
914  FORMAT (1H1,16X,'DISTRIBUTION FACTORS BY CAR AND CONSIST'//
13X,'CONSIST      CAR      STANDING      SEATED FACING      SEATED FACING'//
25X,'NO.',I7X,'NO.',I9X,'FORWARD',9X,'SIDEWARD'//)
      DO 916      I=1,IC
      JC = NC(I)
      DO 916      J=1,JC
916  WRITE (6,918) I,J,(DF(I,J,K),K=1,3)
918  FORMAT (I7,I10,F11.2,F14.2,F16.2)
      WRITE (6,920)
920  FORMAT (/33X,'SPACING PARAMETERS'//)
      DO 922      I=1,IC
922  WRITE (6,924) I,SH(I),SS(I),SB(I),SF(I)
924  FORMAT (5X,'CONSIST NO.',I3,10X,'SH =',F6.2,5X,'SS =',F6.2,5X,'SB
2=',F6.2,5X,'SF =',F6.2//)

```

```

C
C PRINT OUT - FOURTH PHASE (OPTIONAL PRINT OUT OF FIXED DATA)
C
      IF (IPP.EQ. 0) GO TO 998
      WRITE (6,950)
950  FORMAT (1H1,35X,'PARAMETER VALUES USED IN INJURY ANALYSIS - FIXED
DATA'//)
      WRITE (6,952) PF(1),A1,A3,BD,BH1,PF(2),C1,C3,AH,BH2,PF(3),D1,A2,
1WH,PH(1),PF(4),E1,C2,DS,PH(2),PF(5),F1,D2,H3,VIFC,BE
952  FORMAT (
110X,'PF(1)=' ,F4.2,10X,'A1  =',F5.1,10X,'A3  =',F5.2,
210X,'BD  =',F5.2,10X,'BH1  =',F5.2/,
310X,'PF(2)=' ,F4.2,10X,'C1  =',F5.2,10X,'C3  =',F5.3/,
410X,'AH  =',F5.2,10X,'BH2  =',F5.2/,
510X,'PF(3)=' ,F4.2,10X,'D1  =',F5.2,10X,'A2  =',F5.2,
610X,'HW  =',F5.2,10X,'PH(1)=' ,F5.2/,
710X,'PF(4)=' ,F4.2,10X,'E1  =',F5.1,10X,'C2  =',F5.2,
810X,'DS  =',F5.2,10X,'PH(2)=' ,F5.2/,
910X,'PF(5)=' ,F4.2,10X,'F1  =',F5.1,10X,'D2  =',F5.2,
110X,'H3  =',F5.2,10X,'VIFC =' ,F5.1/50X,'BE  =',F5.2/)
      WRITE (6,954)
954  FORMAT (///50X,'SEVERITY INDEX CRITERIA'//5X,'THRESHOLD LEVEL',1,
1,'HEAD',21X,'FACE',21X,'CHEST'//)
      DO 956 IB=1,5
956  WRITE (6,958) IB,(SIC(M,IB),M=1,3)
958  FORMAT (115,3F25.0)
      WRITE (6,960) SIC(4,1),SIC(4,2),SIC(4,3)
960  FORMAT (//20X,'NECK INJURY CRITERIA',10X,'MINOR INJURY THRESHOLD
1 SIC =' ,F5.0/50X,'MODERATE INJURY THRESHOLD , SIC =' ,F5.0/
250X,'UPPER LIMIT CONTROL, SIC =' ,F5.0/)
998  GO TO 10
999  CONTINUE
      STOP
      END

```

```

1*      SUBROUTINE IMPACT(JR,SI)
2*      COMMON/SUBRT/ I,J,K,VI,AH,WH,IR(2,4),RC1(2,4),RC2(2,4)
3*      IF (IR(I,K)=2) 1,2,3
4*      C PERFECT ABSORBER
5*      1 SI = ((RC1(I,JR)*AH/WH)**1.5)*VI/32.2
6*      GO TO 4
7*      C ELASTIC RESPONSE
8*      2 SI = 1.42*((RC1(I,JR)*386./WH)**.75)*((VI/32.2)**2.5)
9*      GO TO 4
10*     C INELASTIC RESPONSE
11*     3 FN = RC2(I,JR)/(VI*SQRT(RC1(I,JR)*WH*.373))
12*     IF (FN .LT. .1 .OR. FN .GT. 5.) GO TO 10
13*     F = (10.**((.314*((1.+ALOG10(FN))**2.524)-.15)))
14*     GO TO 20
15*     10 IF (FN .LE. .1) F = .71
16*     IF (FN .GE. 5.) F = FN**1.5
17*     20 SI = F*((RC1(I,JR)*386./WH)**.75)*((VI/32.2)**2.5)
18*     4 RETURN
19*     END

```

```

1*      SUBROUTINE COMPAR(SIA,M,IJ)
2*      COMMON/SICRIT/ SIC(4,5)
3*      IJ = 0
4*      10 IJ = IJ+1
5*      IF (IJ .EQ. 6) GO TO 20
6*      IF (SIA .GT. SIC(M,IJ)) GO TO 10
7*      20 RETURN
8*      END

```

# INTERIOR COMPONENTS DATA

## CONSIST NO. 1

JR	IR	RC1	RC2
1	3	20.00	98.00
2	3	98.00	307.00
3	3	114.00	218.00
4	2	8000.00	.00

## CONSIST NO. 2

JR	IR	RC1	RC2
1	3	200.00	300.00
2	1	100.00	.00
3	3	200.00	20.00
4	2	2200.00	.00

PANEL (JR=1), SEATBACK (JR=2), STANCHION (JR=3), FLOOR (JR=4)  
 PERFECT ABSORBER (IR=1), ELASTIC RESPONSE (IR=2), INELASTIC RESPONSE (IR=

# CAR CRASH ENVIRONMENT

CONSIST NO.	CAR NO.	VELOCITY CHANGE (FT/SEC)	ACCELERATION (FT/SEC SQ)
1	1	25.2	5.32
1	2	23.4	4.37
1	3	22.9	4.28
1	4	22.8	4.09
1	5	22.5	4.08
1	6	22.2	3.99
1	7	22.1	3.98
1	8	22.0	3.97
2	1	41.3	7.82
2	2	35.2	6.41
2	3	34.0	6.32
2	4	33.7	6.28
2	5	33.5	6.24
2	6	32.8	6.20



# DISTRIBUTION FACTORS BY CAR AND CONSIST

CONSIST NO.	CAR NO.	STANDING	SEATED FACING FORWARD	SEATED FACING SIDEWARD
1	1	.05	.10	.00
1	2	.05	.10	.00
1	3	.05	.10	.00
1	4	.05	.10	.00
1	5	.05	.10	.00
1	6	.05	.10	.00
1	7	.05	.10	.00
1	8	.05	.10	.00
2	1	.10	.08	.05
2	2	.10	.08	.05
2	3	.10	.08	.05
2	4	.10	.08	.05
2	5	.10	.08	.05
2	6	.10	.08	.05

## SPACING PARAMETERS

CONSIST NO. 1	SH = 1.60	SS = 1.50	SB = 1.00	SF = 6.00
CONSIST NO. 2	SH = 1.60	SS = 1.50	SB = 10.00	SF = 10.00

# PARAMETER VALUES USED IN INJURY ANALYSIS - FIXED DATA

PF(1)= .72	A1 = 3.6	A3 = 1.31	HD = 1.00	BH1 = 1.50
PF(2)= .82	C1 = .35	C3 = .065	AH = 10.00	BH2 = 2.50
PF(3)= .88	D1 = 11.43	A2 = 1.70	HW = 10.00	PH(1)= .40
PF(4)= .94	E1 = .7	C2 = .55	DS = .75	PH(2)= .10
PF(5)= .98	F1 = -4.0	D2 = .10	H3 = 1.75	VIFC = 22.4
		RF = .27		

## SEVERITY INDEX CRITERIA

THRESHOLD LEVEL	HEAD	FACE	CHEST
1	650.	500.	1000.
2	1000.	1000.	1500.
3	1333.	1500.	2000.
4	1667.	2000.	2500.
5	2000.	2500.	3000.

## NECK INJURY CRITERIA

MTNOK INJURY THRESHOLD , SIC = 12.  
 MODERATE INJURY THRESHOLD , SIC = 20.  
 UPPER LIMIT CONTROL , SIC = 100.

HE18.5.A37  
UMTA- 80-1

Increased re  
vehicle cr

Form DOT F 17  
FORMERLY FORM D

DOT LIBRARY



00009972

**U.S. DEPARTMENT OF TRANSPORTATION  
RESEARCH AND SPECIAL PROGRAMS ADMINISTRATION**

**TRANSPORTATION SYSTEMS CENTER  
KENDALL SQUARE, CAMBRIDGE, MA. 02142**

**OFFICIAL BUSINESS  
PENALTY FOR PRIVATE USE, \$300**

**POSTAGE AND FEES PAID**

**U.S. DEPARTMENT OF TRANSPORTATION**

**613**

